EVALUATION OF NEW BRIDGE IMPACTS: SAND MIGRATION STUDY

U.S. 50 BRIDGE, OCEAN CITY, MARYLAND

FOR

THE MARYLAND STATE HIGHWAY ADMINISTRATION

BY

OFFSHORE & COASTAL TECHNOLOGIES, INC.

P.O. BOX 1368, CHADDS FORD, PA 19317

PERFORMED UNDER SUBCONTRACT TO:

JOHNSON, MIRIMAN AND THOMPSON, INC.

CONTRACT 04-0556(BCS 05-05J)

APRIL 1, 2008

TABLE OF CONTENTS

EXECUTIVE SUMMARY **1**

1 INTRODUCTION **5**

1.1 PROJECT DESCRIPTION 5
1.2 STUDY COMPONENTS 6
1.3 PROJECT ALTERNATIVES 7

2 FIELD DATA COLLECTION **10**

2.1 HYDROGRAPHIC SURVEY 10
2.1.1 Survey Area *10*
2.1.2 Survey Control & Calibration *12*
2.1.3 Data Processing Routines & QA/QC Information *16*
2.1.4 Graphical Summary of Deliverables *18*
2.2 HYDRODYNAMIC MEASUREMENTS 23

3 FLOOD SHOAL PROCESSES **28**

4 NUMERICAL MODELING **37**

4.1 INTRODUCTION 37
4.2 MODEL DESCRIPTION 37
4.3 OVERVIEW OF MODELING FOR U.S. 50 BRIDGE 39
4.4 HISTORICAL MODEL 41
4.5 2007 MODEL OF EXISTING CONDITION AND ALTERNATIVES 48

5 SUMMARY AND CONCLUSIONS **74**

6 REFERENCES **79**

LIST OF FIGURES

Figure 1-1. Skimmer Island and U.S. 50 Bridge.....5

Figure 1-2. Project site including survey coverage area. 6

Figure 1-3. Alternative 4 bridge location and alignment. 8

Figure 1-4. Alternative 5 bridge location and alignment. 8

Figure 1-5. Alternatives 5A and 5B bridge location and alignment. 9

Figure 2-1. Map illustrating the final survey design. 11

Figure 2-2. Southern site calibration from Base J 104. 13

Figure 2-3. Northern site calibration from Base *Reedy 2 AZ MK*.....14

Figure 2-4. Map showing the cross-check error analysis which determines the deviation between along- and across-line survey data. 17

Figure 2-5. Map showing all hydrographic and topographic data collected during the April 2007 surveys.....18

Figure 2-6. Map showing hydrographic and topographic data collected in the area of interest. 19

Figure 2-7. Map showing hydrographic and topographic data collected in the Assawoman Bay area. 20

Figure 2-8. Map illustrating the final 30' DEM with contours. 21

Figure 2-9. Map illustrating the final 30' DEM with contours for the area of interest (note different color scale). 22

Figure 2-10. Map showing 3D illuminated and rendered multibeam data collected in the vicinity of the Rt.50 Bridge. View is looking to the south. 23

Figure 2-11. Field gauging locations, April and May, 2007.....24

Figure 2-12. Time history of water levels north and south of U.S. 50 bridge, April and May, 2007 25

Figure 2-13. Time history of water levels north and south of U.S. 50 bridge, April 25-May 5, 2007 25

Figure 2-14. Water level at the NOAA (USCG Inlet) gauge, water level at Chicago Avenue, and current speed in the east channel at 2nd Street (dots), April 18-20, 2007. 26

Figure 2-15. Locations of current measurements and example flow vectors, April 19, 2007 27

Figure 2-16. Current speeds (symbols) along the bridge during a tidal cycle on April 19, 2007. Concurrent water levels north and south of the bridge are shown as curves 27

Figure 3-1. Aerial photograph of Ocean City Inlet and Isle of Wight Bay dated May 7, 1938 28

Figure 3-2. Aerial photograph of Ocean City Inlet and Isle of Wight Bay dated October 31, 1944. 29

Figure 3-3. Aerial photograph of Ocean City Inlet and Isle of Wight Bay dated March 14, 1955. 30

Figure 3-4. Aerial photograph of Ocean City Inlet and Isle of Wight Bay dated March 24, 1976. 31

Figure 3-5. Aerial photograph of Ocean City Inlet and Isle of Wight Bay dated 1989. 32

Figure 3-6. Aerial photograph of Ocean City Inlet and Isle of Wight Bay dated 1998. 33

Figure 3-7. Comparison of flood tide currents in 1987 (left) and 2007 (right), with yellow and red colors indicating strong currents and blues indicating weak currents. 34

Figure 3-8. Shoreline surveys 2004-2007 on a 2004 photograph (MD DNR, 2007). 35

Figure 3-9. Aerial photograph of Ocean City Inlet and Isle of Wight Bay dated 2005. 36

Figure 4-1. Regional model for historical simulation, computational grid (left) and bathymetry (right) 41

Figure 4-2. Local model for historical simulation, computational grid (left) and bathymetry (right) 42

Figure 4-3. Water-surface elevation at Ocean City Fishing Pier, January through March 1985 43

Figure 4-4. Water level and current vectors for the regional model at high and low tides....44

Figure 4-5. Peak ebb current for navigation chart bathymetry 45

Figure 4-6. Peak flood current for navigation chart bathymetry 46

Figure 4-7. Skimmer Island historical shorelines and recent aerial photograph showing shoal extent 46

Figure 4-8. Calculated morphologic evolution at 7-year intervals. 47

Figure 4-9. Local model with 2007 bathymetry 49

Figure 4-10. Computational grid for super-fine resolution model 50

Figure 4-11. Grids for SFR models of existing condition and alternatives 51

Figure 4-12. Predicted tide at Ocean City Fishing Pier for the April-May 2007 calibration period 52

Figure 4-13. Comparison of measured and calculated water level at the gauge located 600 ft south of the U.S. 50 Bridge....53

Figure 4-14. Comparison of measured and calculated water level at the gauge located 600 ft north of the U.S. 50 Bridge 53

Figure 4-15. Comparison of predicted and calculated water level and the NOAA Inlet Gauge....54

Figure 4-16. Comparison of measured and calculated current speed....55

Figure 4-17. Predicted tide at Ocean City Fishing Pier, January through March 2007....55

Figure 4-18. Peak flood current for existing condition calculated by SFR model 56

Figure 4-19. Peak flood current for Alt 4 calculated by SFR model 57

Figure 4-20. Peak flood current for Alt 5 calculated by SFR model 57

Figure 4-21. Peak flood current for Alt 5A calculated by SFR model 58

Figure 4-22. Peak flood current for Alt 5B calculated by SFR model 58

Figure 4-23. Peak ebb current for the existing condition calculated by SFR model 59

Figure 4-24. Peak ebb current for Alt 4 calculated by SFR model 60

Figure 4-25. Peak ebb current for Alt 5 calculated by SFR model 60

Figure 4-26. Peak ebb current for Alt 5A calculated by SFR model 61

Figure 4-27. Peak ebb current for Alt 5B calculated by SFR model 61

Figure 4-28. Difference in current speed between Alt 4 and the existing U.S. 50 Bridge at peak flood 62

Figure 4-29. Difference in current speed between Alt 5 and the existing U.S. 50 Bridge at peak flood 63

Figure 4-30. Difference in current speed between Alt 5A and the existing U.S. 50 Bridge at peak flood 63

Figure 4-31. Difference in current speed between Alt 5B and the existing U.S. 50 Bridge at peak flood 64

Figure 4-32. Difference in current speed between Alt 4 and the existing Rotue 50 bridge at peak ebb 65

Figure 4-33. Difference in current speed between Alt 5 and the existing U.S. 50 Bridge at peak ebb 65

Figure 4-34. Difference in current speed between Alt 5A and the existing U.S. 50 Bridge at peak ebb 66

Figure 4-35. Difference in current speed between Alt 5B and the existing U.S. 50 Bridge at peak ebb 66

Figure 4-36. Initial (2007) bathymetry for evaluation of morphology change for alternatives 67

Figure 4-37. Calculated bathymetry after 5 yr, existing condition 68

Figure 4-38. Calculated bathymetry after 5 yr, Alt 4 68

Figure 4-39. Calculated bathymetry after 5 yr, Alt 5 69

Figure 4-40. Calculated bathymetry after 5 yr, Alt 5A 69

Figure 4-41. Calculated bathymetry after 5 yr, Alt 5B 70

Figure 4-42. Calculated depth change over 5 years, existing condition 71

Figure 4-43. Calculated depth change over 5 years, Alt 4.....71

Figure 4-44. Calculated depth change over 5 years, Alt 5.....72

Figure 4-45. Calculated depth change over 5 years, Alt 5A.....72

Figure 4-46. Calculated depth change over 5 years, Alt 5B.....73

Figure 5-1. Estimated long term impacts of new bridge alternatives.....78

LIST OF TABLES

Table 2-1. Overall calibration results from the southern and northern basestations 15

Table 2-2. Comparison of elevation values for benchmarks checked from both RTK-GPS basestations (overlap MB checks) 15

Table 4-1. Modeling Elements and Purpose 40

Table 5-1. Possible Impacts Due to Alternative Bridges 76

EXECUTIVE SUMMARY

The Maryland State Highway Administration is evaluating alternatives to replace the existing U.S. 50 Bridge that links the mainland to Fenwick Island, at Ocean City, MD. Alternatives under evaluation are the existing U.S. 50 Bridge with no changes, and four action alternatives that involve construction of a new bridge with each action alternative based upon a specific location and bridge alignment. The five alternatives are:

1. Existing condition: Existing U.S. 50 Bridge with no changes.

2. Alternative 4: Construction of new bridge located north of and at an angle to existing U.S. 50 Bridge.

3. Alternative 5: Construction of new bridge located south of and parallel to existing U.S. 50 Bridge.

4. Alternative 5A: Construction of new bridge located north of and parallel to existing U.S. 50 Bridge.

5. Alternative 5B: Construction of new bridge at same location and alignment as Alternative 5A and with removal of existing U.S. 50 Bridge.

Concerns for the bridge replacement effort include the migration and growth of Skimmer Island and the response of currents and morphology change to construction of a new bridge. Goals of the present study are: to evaluate the processes that have controlled the growth and migration of Skimmer Island by using historical information and assess its present stability; and to project changes to the currents, channels, shoal features including Skimmer Island, for each of the proposed alternatives. To achieve these goals, the present study has been conducted by three tasks. These tasks are:

1. Field data collection: Hydrographic survey to update known information about the study area and to provide accurate bathymetry for the numerical model. Water level and current measurements to provide data for numerical model calibration.

2. Evaluation of historical flood shoal processes: Examine the development and changes to the flood shoal and Skimmer Island using historical data to determine the response of these features to tidal currents and human activities.

3. Numerical modeling: Conduct hydrodynamic and morphologic change modeling to determine the response of the currents, channels, and shoal features to construction of bridge alternatives.

A hydrographic survey was conducted in April 2007 that extended from the vicinity of the U.S. 50 Bridge to the northern area of Assawoman Bay. The survey was laid out as transects spaced at 300 ft intervals. Survey instrumentation was calibrated and collected data subjected to a QA/QC procedure to minimize error. Survey data were then rectified and applied to produce a 30 ft gridded DEM. This data was subsequently implemented in the numerical modeling component of the study to provide up-to-date model bathymetry.

Hydrodynamic measurements were made during April and May 2007 in the local vicinity of the existing bridge. Water surface elevation data were taken over approximately a one-month period north and south of the bridge and current speed data were collected in the main navigation channel and along the bridge alignment. The measurements were made to better-understand the tidal and flow properties in the bridge area and to provide a source of validation for the numerical model study.

An analysis of the formation, growth, and movement of the flood shoal and Skimmer Island was conducted using historical aerial photographs, prior studies, and information on engineering activities. Following development of the flood shoal since initial formation of Ocean City Inlet during a 1933 hurricane, and evaluating the control exerted by tidal processes and human activities, the present analysis concludes that hydrodynamic and sedimentation processes in the flood shoals at Ocean City have been largely a function of engineering projects. Changes to the area that led to the formation and migration of Skimmer Island have included the early dredging of navigation channels, the construction of the U.S. 50 Bridge, the stabilization of the north end of Assateague Island, the installation of the U.S. 50 Bridge scour protection, and the rehabilitation of the south jetty at Ocean City Inlet

A numerical modeling effort was conducted to predict the future changes to the flood shoals and channels for each of the proposed alternatives. It should be noted that numerical modeling is a useful tool in gaining insight into physical processes; however, the results should be used with other engineering analyses and judgments in the project decision-making process. The two-dimensional hydrodynamic and sediment transport model CMS-FLOW was selected for this effort because its capabilities are well-suited for the project scale and required analysis. The modeling effort consisted of development of models on three scales in which the larger-scale models provided input to the smaller scale models in such a way that tidal phase information was preserved. The regional-scale model extended from the ocean in the vicinity of Chincoteague Inlet to the northern extent of Assawoman Bay and included the Atlantic Ocean in the vicinity of Ocean City Inlet. The two smaller-scale models focused on the study area and included Ocean City Inlet and ebb shoal, Isle of Wight Bay, and a small area linking Ocean City Inlet to Chincoteague Bay. The difference between the smaller-scale models is resolution, with the "local

scale" model having constant resolution of 25 m, and the super-fine resolution (SFR) model having minimum resolution of 4.7 m.

The modeling system was calibrated and verified for sediment transport by long-term simulation of hydrodynamics and morphology change starting from 1985 bathymetry obtained from navigation charts. This 21-year simulation reproduced the gross movements of the flood shoals and changes to the navigation channel, thereby providing confidence for calculation of changes owing to new bridge construction.

Following the historical simulation, the model bathymetry was updated to include the 2007 survey as well as the 2001 south jetty rehabilitation and scour protection. Water-level and current measurements obtained during April 2007 were then applied to verify the hydrodynamic calculations. The local and super-fine resolution models were then modified to represent each of the proposed action alternatives. Hydrodynamic simulations were conducted at the super-fine scale to determine local current patterns in the vicinity of the bridge piers. Combined hydrodynamic and sediment transport simulations on a local scale were conducted for a 7.5-yr period to predict the morphologic response of each alternative.

Results of the SFR model provide details of flow fields in the vicinity of the bridge, as well as their influence to the south of the existing U.S. 50 Bridge and in the Skimmer Island area. During flood current, the primary flow from the inlet enters on the west side south of the existing U.S. 50 Bridge. The current spreads and decelerates in the vicinity of the bridge. North of the bridge, the primary current shifts to the navigation channel on the east. All of the proposed alternatives show narrow patterns of strong and weak velocity near the bridge piers, which indicate acceleration between the piers and sheltering behind them. During ebb, general flow patterns are consistent among the existing condition and alternative simulations with the strongest ebb current flow being in the east navigation channel, both north and south of the location of the existing U.S. 50 Bridge. The proposed alternatives show some variation in the flow field owing to the presence and location of the bridge piers. Alternatives 4, 5A, and 5B show reductions in current speed in their central areas on the south side of the piers. Alternative 5 shows greater current speed between piers

All of the 7.5-yr simulations show similar patterns of morphologic change with differences being primarily in the amount and localized trends for erosion or deposition. In all cases, the navigation channel widens and deepens, indicating that it will remain self-sustaining for all proposed alternatives. Alternatives 4 and 5A have calculated depth change that is similar to the existing condition in magnitude and pattern. Alternative 5 was calculated to have areas of stronger erosion and of stronger deposition north of the present U.S. 50 Bridge as compared to the existing condition and Alts 4 and 5A. That is, the areas of accretion in Alt 5 are higher and

areas of erosion are lower in elevation than those of the existing condition and Alts 4 and 5A, which will promote faster development of channels and shoals in Alt 5. Alternative 5B was calculated to have the greatest amount of shoaling north of the bridge, particularly in the western area of the bay just north of the proposed Alt 5B bridge location. Removal of the existing bridge allows for stronger current at the present bridge site, which will transport more material northward during flood tide.

A conclusion of the historic evolution of the flood tide delta, including Skimmer Island, is that Skimmer Island is expected to migrate in a west-southwest direction at a rate of about 5-10 ft/yr. Pressure on Skimmer Island is expected to continue on its east and northeast sides from a widening and deepening east channel. Stronger flood tide currents, presumably due to the rehabilitation of the south jetty at Ocean City Inlet, have slowed and possibly stopped the southerly migration of the Island. The primary conclusion of the modeling is that the existing rock scour protection provides a primary control over the hydraulics and sedimentation processes in the area. The existing bridge pilings also play a significant role in controlling hydraulics and sedimentation. These processes would change if the rock scour protection or the existing bridge were removed. The new bridge alternatives will affect the hydraulics and sedimentation in the very local vicinity (a few city blocks) of those structures, but the far-field conditions will continue and evolve in a manner similar to the first, no-action, alternative with slight increases in current speed. The impacts seen in the model results agree with the historic processes analysis, i.e. that Skimmer Island is expected to slowly migrate to the west-southwest, as discussed above, with a continued widening and deepening on its east and northeast side.

Model findings also indicate that the new bridge piers have a very local effect on currents, primarily confined to flow acceleration between the piers and a wake region to the north and south on flood tide and ebb tide, respectively. The effects are mainly confined to a few hundred feet to the north and south of new bridge pier locations. Bridge pier alignment should be considered to minimize impacts on currents, especially near and in the navigation channel.

It is recommended that a monitoring plan be developed to continue to assess these results before, during and after a bridge is constructed because conditions change in this environment constantly change due to man-made and natural effects.

1 Introduction

1.1 Project Description

The Maryland State Highway Administration (Maryland SHA) is undertaking an analysis of proposed alternatives for replacement of the U.S. 50 Bridge that links the mainland to Fenwick Island. The primary area of interest is in the vicinity of the present U.S. 50 Bridge and Skimmer Island (Figure 1-1). The U.S. 50 Bridge and Skimmer Island are located between Ocean City Inlet and Assawoman Bay (Figure 1-2). Skimmer Island developed after Ocean City Inlet formed in 1933 during a hurricane-induced breach. Since initial development of Skimmer Island, it has changed shape and migrated toward the U.S. 50 Bridge. A goal for the present study is to determine whether Skimmer Island will continue to migrate or if its location will be stable in the presence of the proposed alternatives.

Figure 1-1. Skimmer Island and U.S. 50 Bridge.

Figure 1-2. Project site including survey coverage area.

Evaluation of the stability of Skimmer Island must be conducted within the context of historical changes in the island and the larger flood shoal. Thus, understanding of how the island and flood shoal have responded to tidal currents and to engineering activities is necessary to evaluate future response.

1.2 Study Components

This study comprises three components that are necessary to provide sufficient information for alternative selection and anticipation of the response to construction of the selected alternative. These components are:

1. Description and analysis of historical changes in morphology and their relationship to natural processes (tides) and engineering activities (dredging, construction of structures).

2. Field data collection for model setup and verification.

3. Numerical modeling of hydrodynamics and morphology change for both the historical movement of Skimmer Island and for predicted changes for the proposed alternatives.

Historical changes in Skimmer Island and the flood shoal were examined using aerial photographs and historical surveys and profiles. These data sources were combined with information on construction and other human activities to sort out the natural processes from those induced by man-made changes.

Field data collection was conducted to support the numerical modeling effort. A bathymetric survey was conducted to provide up-to-date bottom topography to enter into the model. Accurate bathymetric information is critical for achieving a reliable numerical solution. Measurements of water levels and currents were also obtained and these were used to calibrate and verify the hydrodynamic component of the numerical model.

Evaluation of alternatives was conducted by developing numerical models of the system. These models were verified to reproduce historical morphologic change and then were applied to compute detailed current fields and sediment transport for each proposed alternative. Comparisons of solutions between each proposed action alternative and the present condition (existing U.S. 50 Bridge with no other changes) provide information on the spatial response of the morphology over time as well as changes to the currents.

1.3 Project Alternatives

Five project alternatives were developed and provided by the Maryland SHA analysis. The alternatives are:

1. Existing condition: Existing U.S. 50 Bridge with no changes.

2. Alternative 4: Construction of new bridge located north of and at an angle to existing U.S. 50 Bridge (Figure 1-3).

3. Alternative 5: Construction of new bridge located south of and parallel to existing U.S. 50 Bridge (Figure 1-4).

4. Alternative 5A: Construction of new bridge located north of and parallel to existing U.S. 50 Bridge (Figure 1-5).

5. Alternative 5B: Construction of new bridge at same location and alignment as Alternative 5A and with removal of existing U.S. 50 Bridge (Figure 1-5).

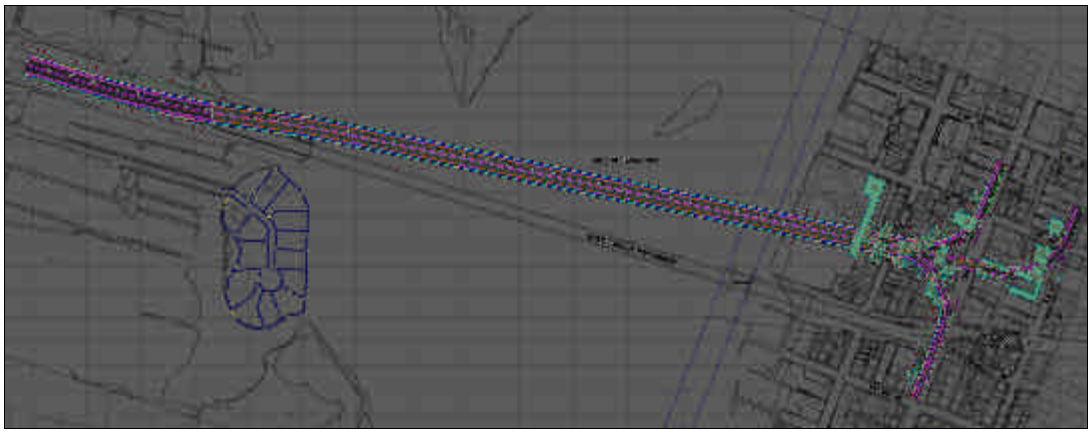

Figure 1-3. Alternative 4 bridge location and alignment.

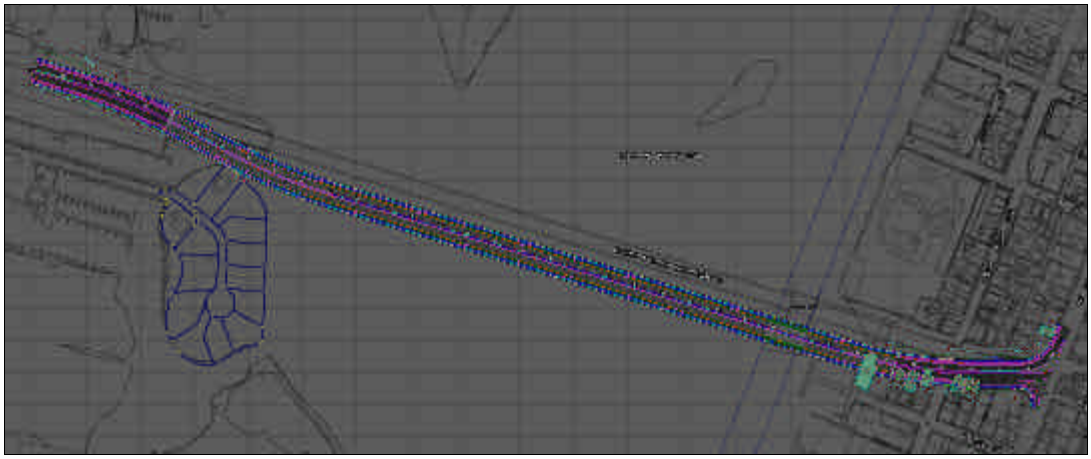

Figure 1-4. Alternative 5 bridge location and alignment.

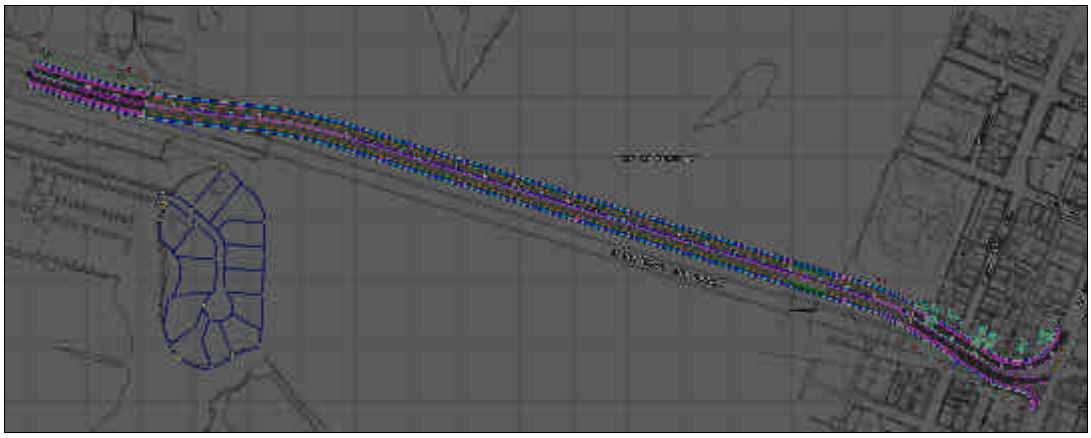

Figure 1-5. Alternatives 5A and 5B bridge location and alignment.

2 Field Data Collection

Field data collection for this project consisted of a hydrographic survey from which a digital elevation model (DEM) was developed, and measurements of water-surface elevation and currents which were applied to calibrate the hydrodynamic model.

2.1 Hydrographic Survey

In order to perform the most accurate hydrodynamic and sediment transport modeling, an accurate bathymetric survey was obtained of Isle of Wight Bay and Assawoman Bay. Although there is navigation chart-based bathymetry available from NOAA, it is based on disparate sources that are decades old. To assess present-day conditions and to model future responses of bridge design alternatives, contemporary survey data were required that describe the hydrography (also termed bathymetry) and intertidal topography. Such a survey was performed in April 2007, producing a seamless topographic/bathymetric digital elevation model (DEM). State-of-the-art survey tools, techniques and designs were employed to provide maximum efficiency and accuracy.

The hydrographic portion of the surveys employed an Odom CV100 survey-grade digital echosounder. The system is integrated with a Trimble 5700 RTK-GPS system for precise heading, supplemental heave calculations, cm-scale positioning and real-time tidal corrections. The sonar system runs at 200 kHz and is compensated for motion with a TSS DMS-10 motion reference unit and sound velocity is calculated with an Applied Microsystems SV probe. The singlebeam sonar and all ancillary sensors are mounted on the *RV Shoals*; a 20' skiff specifically designed for extremely shallow water bathymetric mapping applications.

The Trimble RTK-GPS system used for both topographic and hydrographic operations uses a land-based station coupled with a 25-watt radio and a Maxrad 5 dB high-gain antenna, to broadcast computed real-time horizontal and vertical corrections at 20 Hz to the survey vessel. To compute centimeter-scale position and elevation information, determine the relationship between WGS-84 and local grid coordinates, and to evaluate the local geoid-spheroid separation, we first performed a detailed site calibration in early April of 2007.

2.1.1 Survey Area

The survey encompassed portions of Ocean City Inlet, Isle of Wight Bay, and Assawoman Bay. The survey was divided into two main sections; the area of interest (U.S. 50 Bridge to Bahia Marina) and the Assawoman Bay section (from Bahia marina to the MD-DE line area). The area of interest was comprised of 104 survey lines in a

cross-hatch line scheme that totaled 40.7 line miles of data. Survey lines were spaced at 300' allowing for the creation of a 30' gridded surface. The Assawoman Bay section was comprised of 102 survey lines trending in a generally E-W direction and totaling 145.6 line miles of data. Altogether over 14 square miles of data were collected and merged with existing data to provide a 30' resolution DEM encompassing 16.27 square miles. Figure 2-1 illustrates the final survey design.

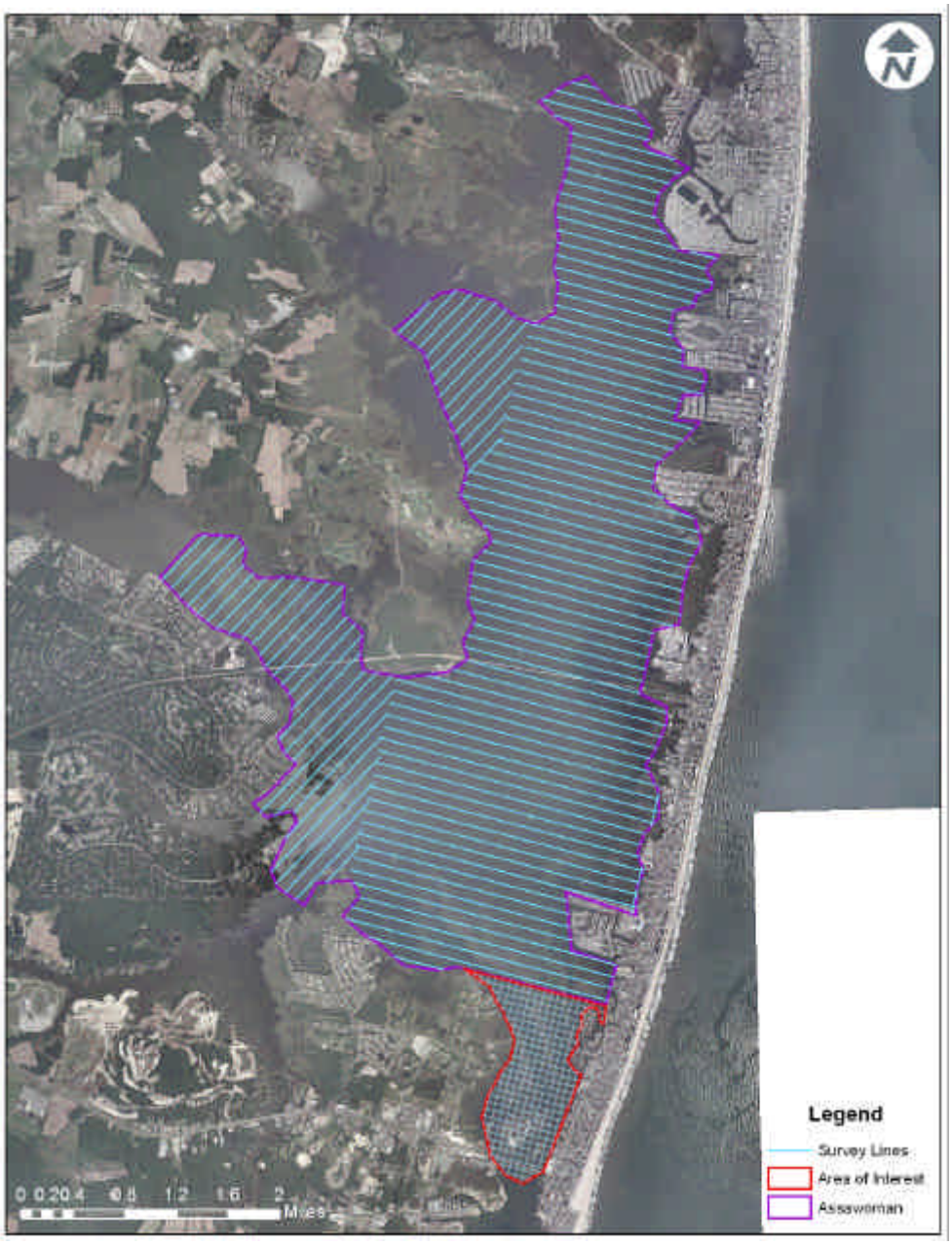

Figure 2-1. Map illustrating the final survey design.

2.1.2 Survey Control & Calibration

A detailed geodetic GPS site calibration was performed over the course of several days starting in mid April 2007 and prior to the start of the hydrographic and topographic data acquisition phases. The site calibration is used to determine the basestation quality and analyze any potential spatial separations between the local geoid heights (GEOID 03) and ellipsoidal values (WGS-84) that may influence the resultant orthometric elevations. The calibration entails selecting the control to be used for the RTK-GPS basestation receiver and radio broadcast system and checking several known geodetic benchmarks of exceptional horizontal and vertical quality within and even outside the survey boundaries. The benchmarks are occupied in "site calibration mode" over 300 epochs or approximately 3 to 5 minutes.

Ultimately the survey had to be broken into two separate RTK-GPS broadcasting zones to limit baseline distance and increase overall vertical accuracy because of the large survey extents. The southern portion (OC Inlet to Bahia Marina) of the survey utilized a station at the Ocean City Airport (Figure 2-2). Extensive calibration had already been completed on the NGS J 104 base; however, further analysis was completed on this mark to test the northern range, accuracy up to the Route 90 Bridge and to include many overlapping marks that were checked with the northern base setup. The northern zone utilized NGS mark Reedy 2 AZ MK3 as the base location to achieve range from Route 90 to the Delaware line (Figure 2-3). Table 2-2 illustrates the overall calibration values from both base stations, while Table 2-2 shows the elevation difference in overlapping benchmarks to quantify accuracy between the two base stations.

A number of hydrographic calibration procedures were performed, including the collection of sound velocity profiles spatially across the survey area, crosscheck error analysis and calibration check of the singlebeam sounder. The calibration check is a standard singlebeam calibration procedure in which the sonar depth measurement is adjusted to read that of a calibrated bar placed under the sonar transducer. This calibration check is necessary to determine and/or verify the index associated with the singlebeam sounder and transducer. Since accurate sound velocity profiles are acquired throughout the survey, the sounder is set to a standard specified initial sound velocity (4921 ft/s) and traditional bar checks at depth intervals are not necessary.

To go a step further, a singlebeam calibration technique for the *RV Shoals* was developed that uses a direct seafloor elevation measurement derived from an RTK-GPS rover. The sonar is held steady in approximately 0.5 ft to 6 ft of water with a flat sandy bottom. A rod man takes a measurement directly under the transducer to get an accurate seafloor elevation. If necessary, the sonar system is then adjusted to read the measured elevation. This procedure serves to verify the index calibration check and confirmed that RTK-GPS topo data is in complete agreement with the singlebeam data.

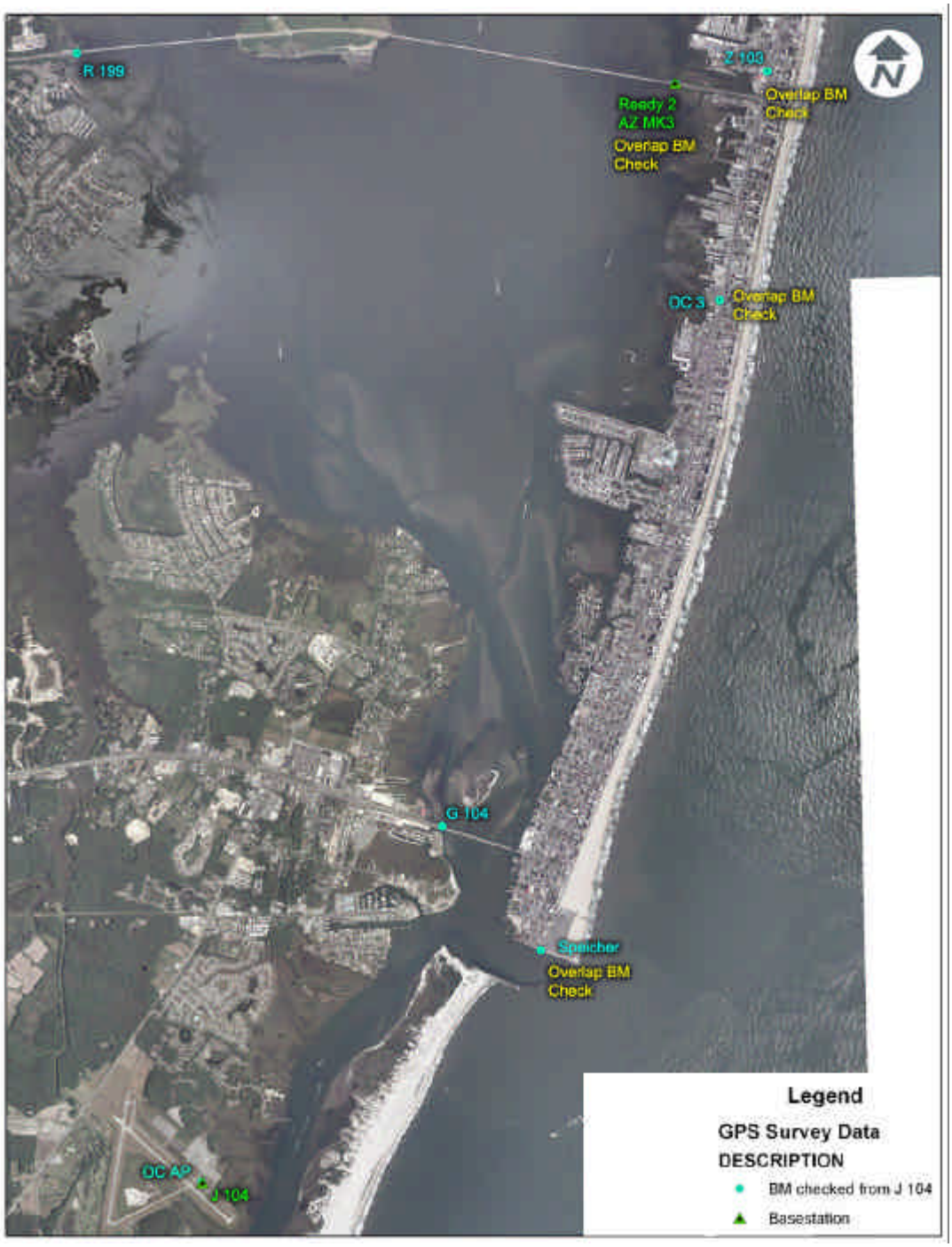

Figure 2-2. Southern site calibration from Base J 104.

Figure 2-3. Northern site calibration from Base *Reedy 2 AZ MK*.

Table 2-1. Overall calibration results from the southern and northern basestations

BM checks from J 104			BM checks from Reedy 2 AZ MK		
Vertical			*Vertical*		
0.050	ft	Absolute Value Average	0.083	ft	Absolute Value Average
0.066	ft	St. Dev	0.088	ft	St. Dev
Horizontal			*Horizontal*		
N			N		
0.102	ft	Absolute Value Average	0.190	ft	Absolute Value Average
0.131	ft	St. Dev	0.269	ft	St. Dev
E			E		
0.031	ft	Absolute Value Average	0.058	ft	Absolute Value Average
0.045	ft	St. Dev	0.072	ft	St. Dev

Table 2-2. Comparison of elevation values for benchmarks checked from both RTK-GPS basestations (overlap MB checks)

BM	Published	Ck from J 104	Ck from Reedy	Diff in Cks
Z 103	7.228	7.239	7.189	0.050
Speicher	9.767	9.748	9.831	-0.083
OC 3	4.393	4.520	4.569	-0.049
Reedy	9.865	9.808	n/a	n/a

2.1.3 Data Processing Routines & QA/QC Information

A typical singlebeam survey design will consist of a series of cross sectional profiles used to describe the two-dimensional morphology at a single point. In order to generate an accurate three-dimensional surface with singlebeam requires a design which incorporates alongshore profiles to create a grid of singlebeam data (see Figure 2-1 for survey design).

To meet accuracy and resolution standards for measured depths specified in the USACE Hydrographic Surveying Manual and the NOS Hydrographic Surveys, Specifications and Deliverables Manual, and SOW, measured echosounder depths were corrected for all departures from true depths attributable to the method of sounding or to faults in the measuring apparatus. These corrections are subdivided into four categories, and are listed below in the sequence in which they were applied to the data.

1. Instrument error corrections: account for the sources of error related to the sounding equipment itself.

2. Vessel offsets: were added to the observed soundings to account for the sensor and antenna locations.

3. Velocity of sound correctors: were applied to the soundings to compensate for the fact that echosounders may only display depths based on an assumed sound velocity profile while the true velocity may vary in time and space.

4. Tide: is integrated with soundings from RTK-GPS to commonly reference data in a vertical datum (NGVD29 for this project).

In order to assess the accuracy in soundings and topographic data between the across- and along-inlet / bay survey lines a detailed cross check analysis was performed in Hypack. A map of the cross check analysis is shown in Figure 2-4. Overlapping data were selected at a maximum search radius of 50 ft and elevations compared as close to each crossing as possible. The average cross check error was 0.11 ft.

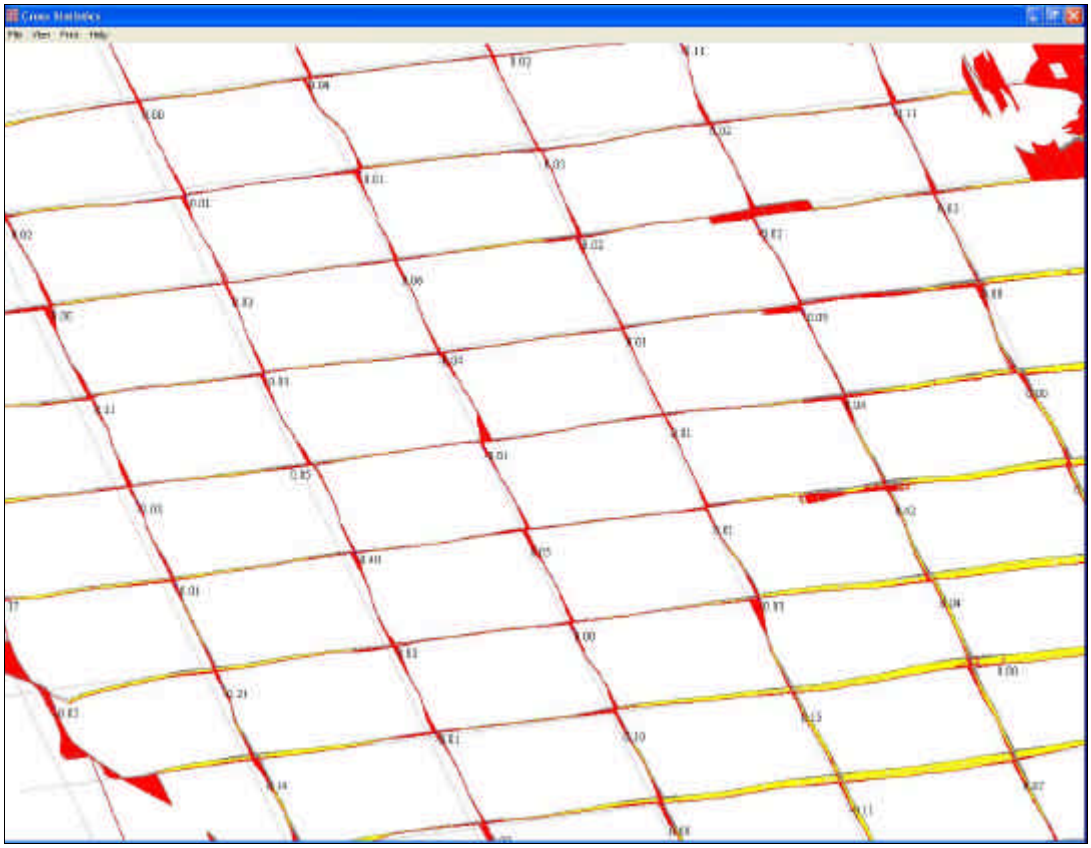

Figure 2-4. Map showing the cross-check error analysis which determines the deviation between along- and across-line survey data.

A comprehensive multibeam sonar survey of the Ocean City Inlet was performed for the U.S. Army Corps of Engineers, Baltimore District, in August 2006. Data from this survey was merged into the singlebeam and topographic data in order to create the most inclusive DEM for the project area. In order to assess the alignment and accuracy to which the multibeam and singlebeam data merge together a visual and semi-quantitative exercise was performed. Soundings from a section of singlebeam data collected in the April 2007 survey were compared to multibeam grid soundings that neighbored the singlebeam data. The average deviation noted through this process was 0.20 ft.

2.1.4 Graphical Summary of Deliverables

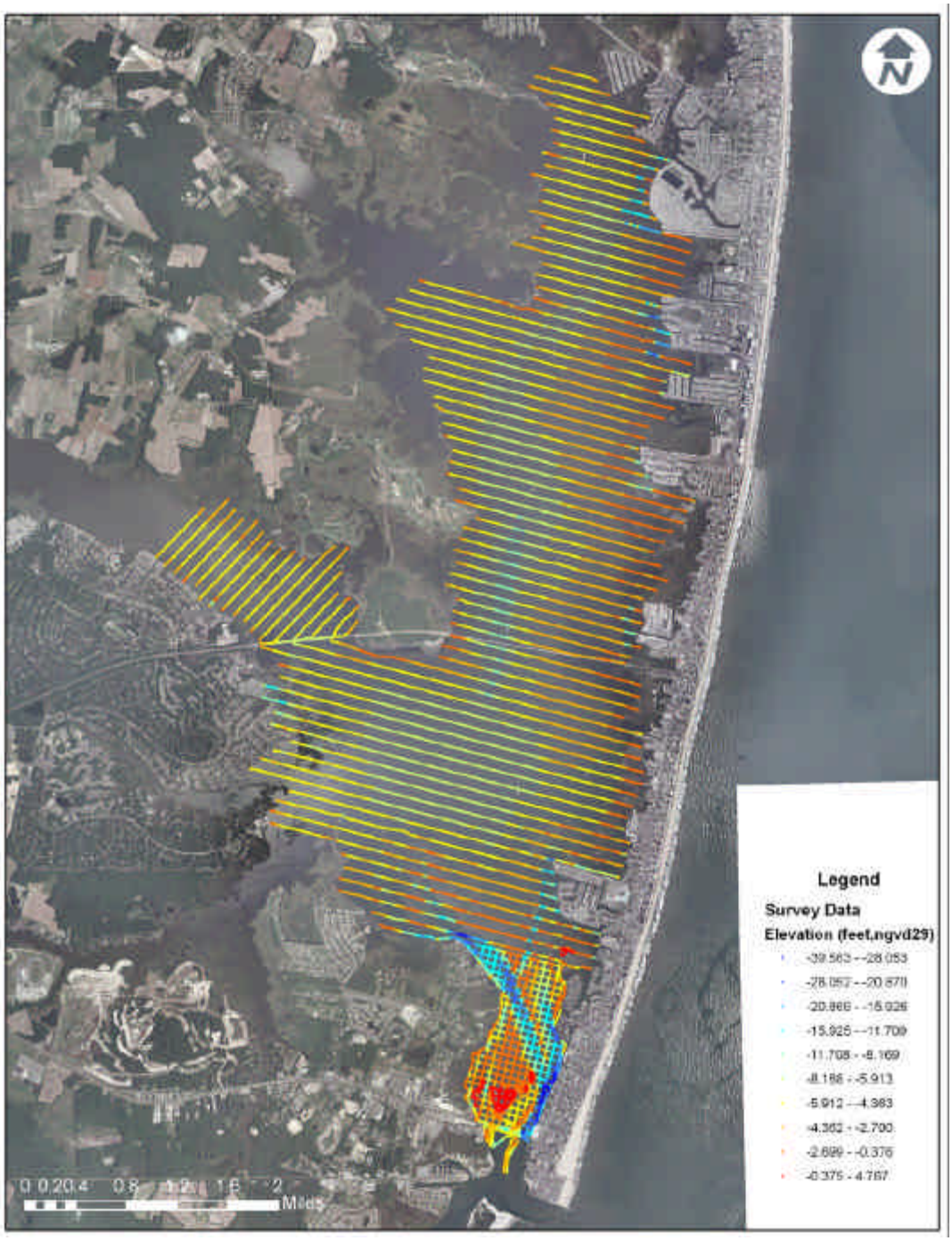

Figure 2-5. Map showing all hydrographic and topographic data collected during the April 2007 surveys.

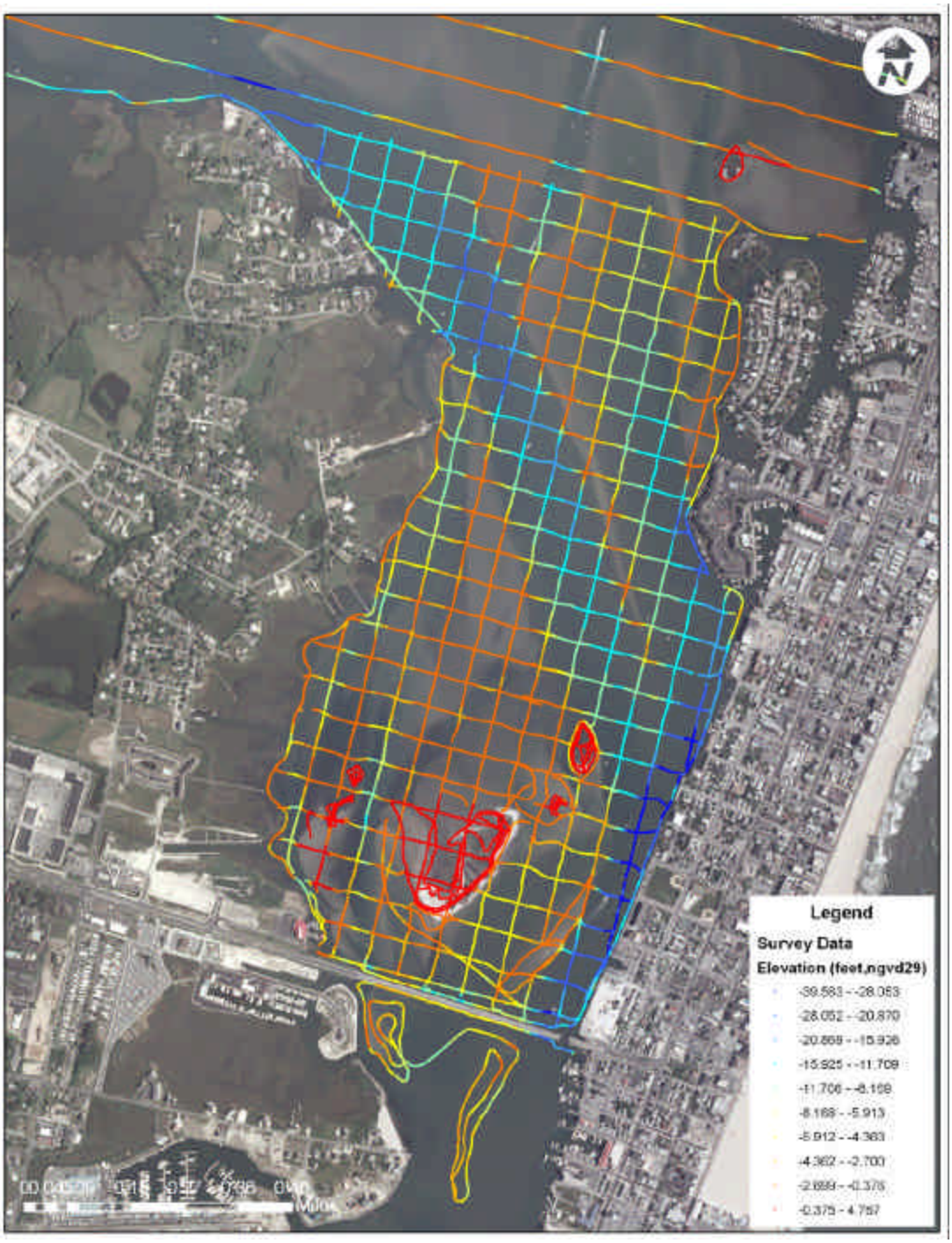

Figure 2-6. Map showing hydrographic and topographic data collected in the area of interest.

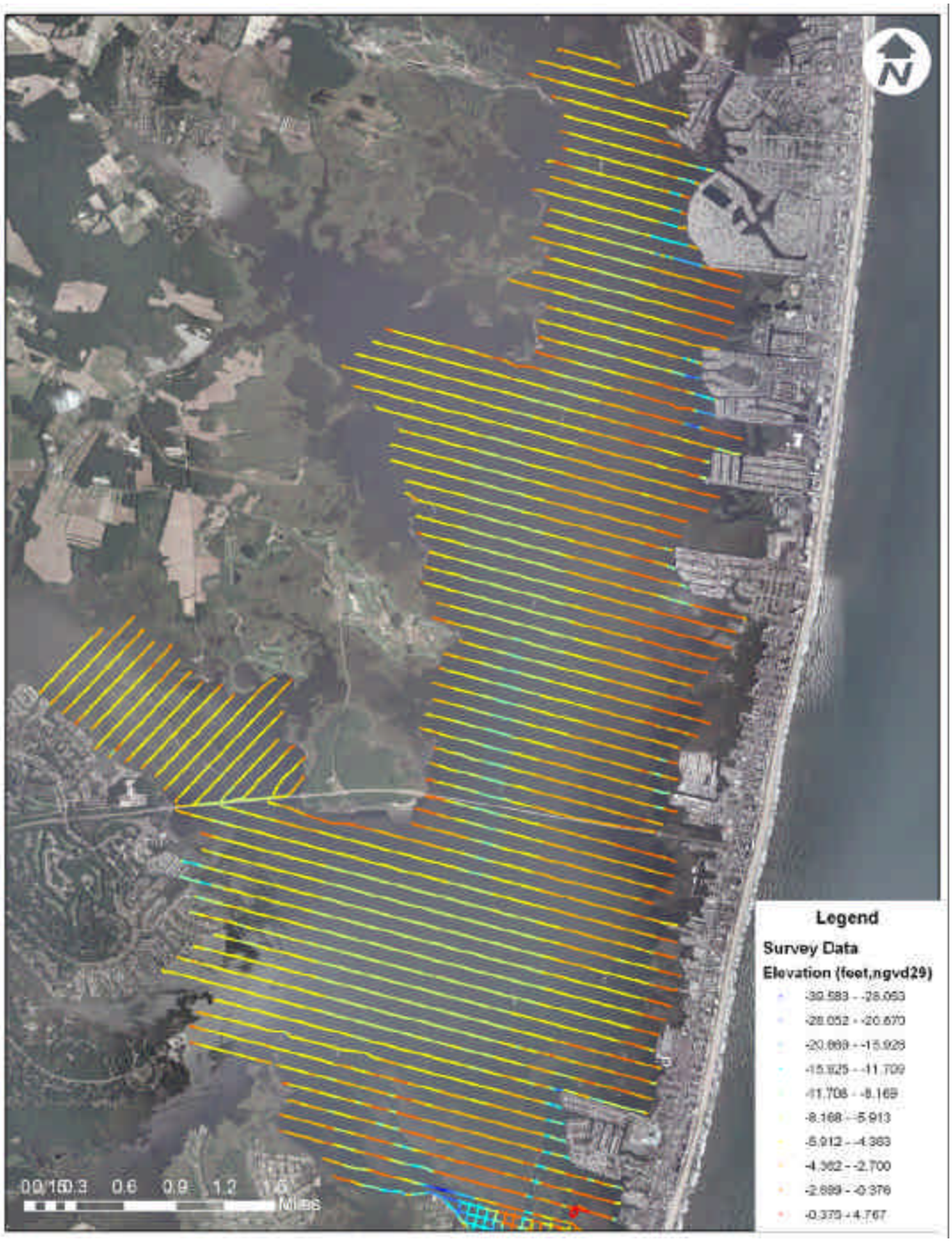

Figure 2-7. Map showing hydrographic and topographic data collected in the Assawoman Bay area.

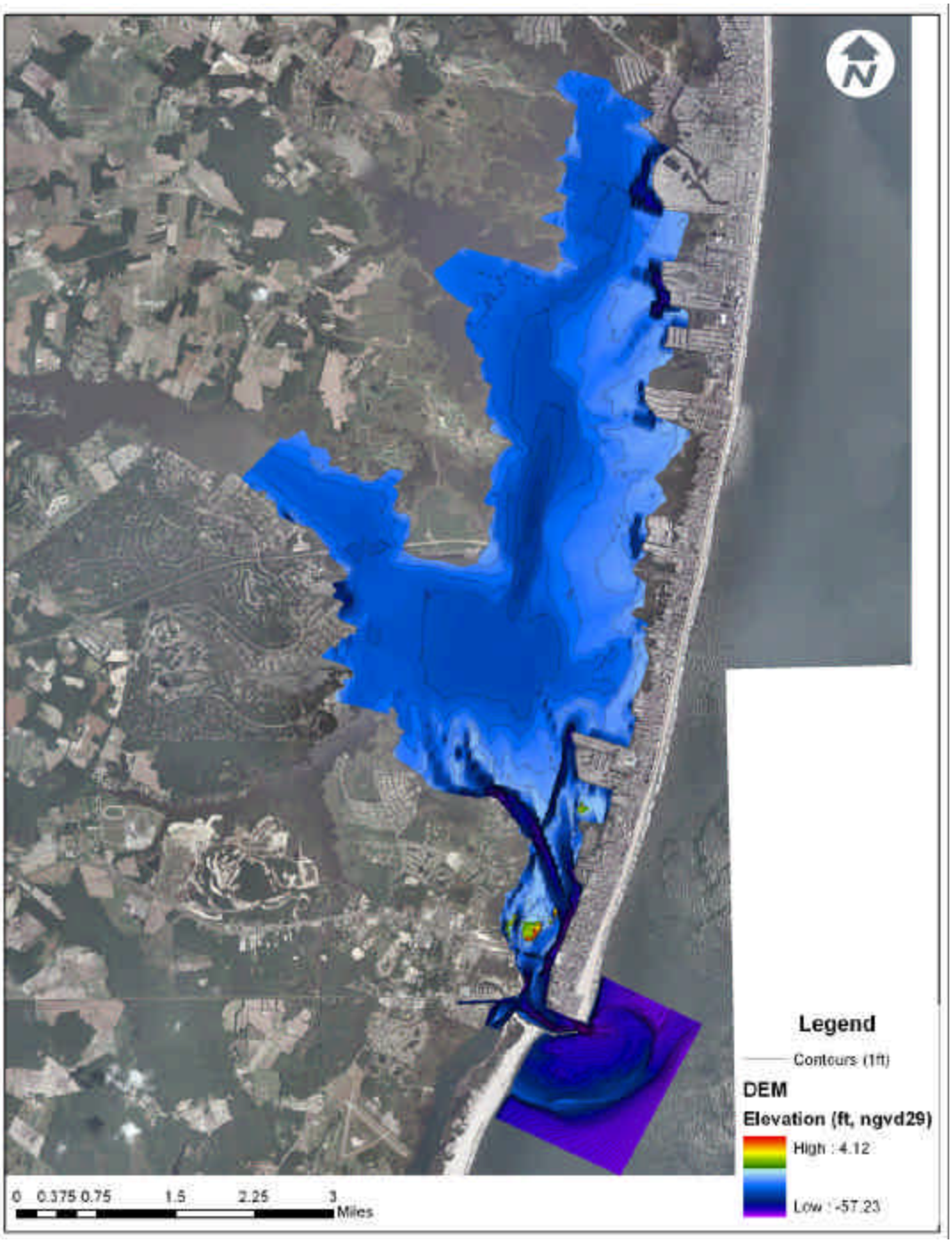

Figure 2-8. Map illustrating the final 30' DEM with contours.

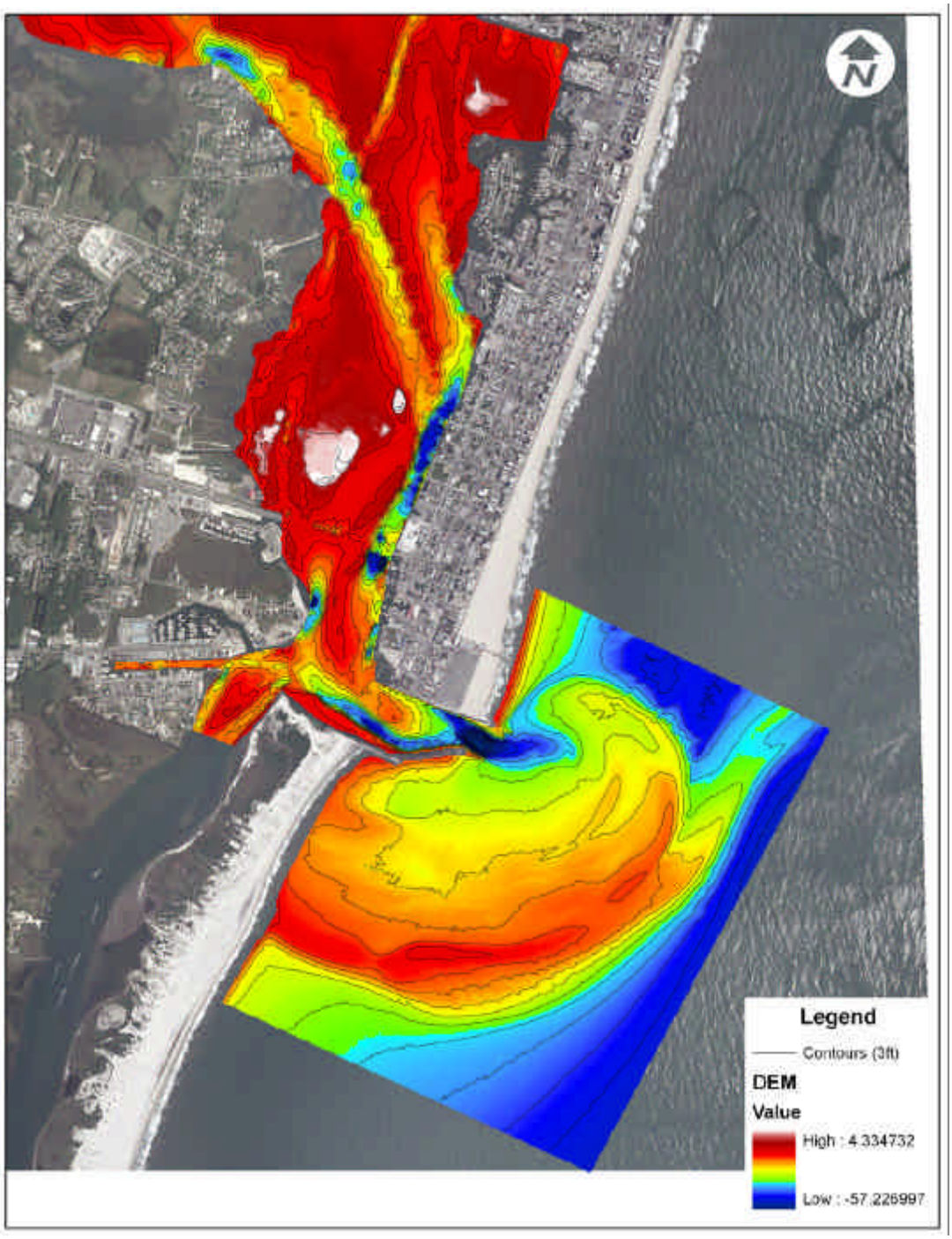

Figure 2-9. Map illustrating the final 30' DEM with contours for the area of interest (note different color scale).

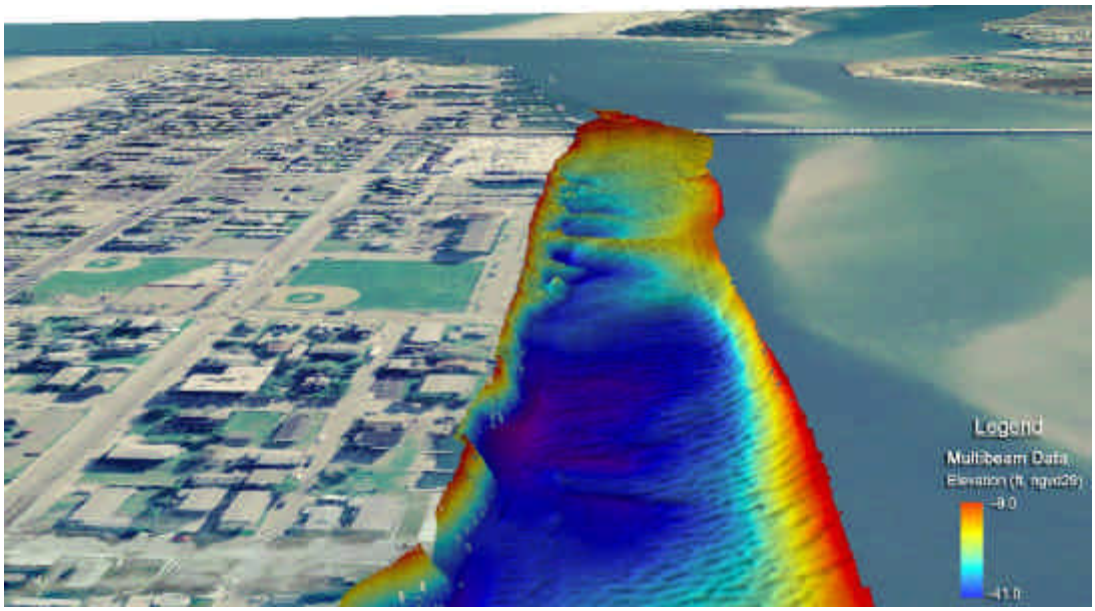

Figure 2-10. Map showing 3D illuminated and rendered multibeam data collected in the vicinity of the Rt.50 Bridge. View is looking to the south.

2.2 Hydrodynamic Measurements

Hydrodynamic measurements were made in Isle of Wight Bay during April and May, 2007. The measurements provided on-site observations of physical flow conditions in the vicinity of the existing bridge and a source of calibration and validation data for later numerical modeling.

Water level variations and flows were measured at locations north, south and along the existing U.S. 50 bridge (Figure 2-11). Subsurface water level gauges were deployed on existing pilings at White Marlin Marina, about one block south of the bridge, and at the end of 2nd Street, north of the bridge. These gauges collected water surface elevation data at a 6-minute interval for one month beginning on April 18, 2007.

Water level data were also collected during the same time period by a NOAA tide gauge located at the U.S. Coast Guard Station (USCG). A side-looking acoustic Doppler current profiler was co-located with the water level gauge at 2nd Street to measure currents 10 meters out in the navigation channel, about 1.5 meters below mean sea level. This current meter collected current speed data every 6 minutes for about 36 hours on April 18-20, 2007. Current flow data were also collected for a 13-hour tidal cycle on April 19, 2007 using a down-looking acoustic Doppler current profiler mounted on a boat. The boat visited six fixed locations along the north side of the bridge once per hour for the 13-hour period in order to characterize the flow distribution along the bridge.

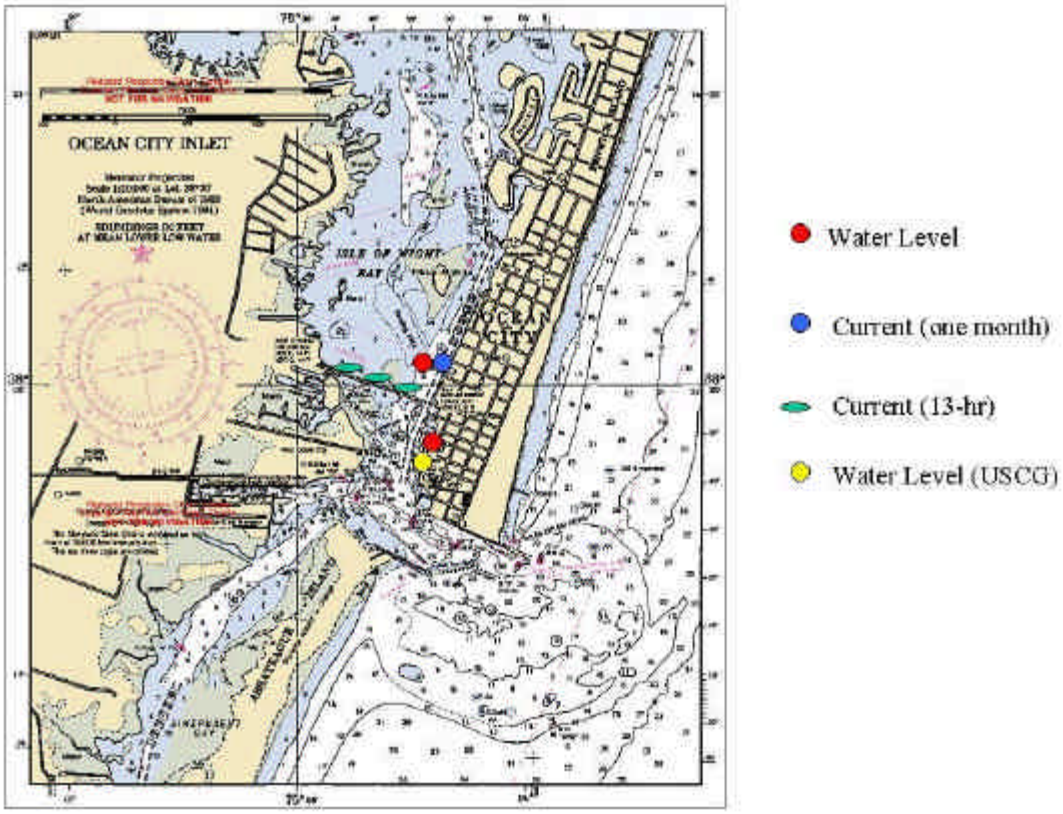

Figure 2-11. Field gauging locations, April and May, 2007

After retrieval of the gauges, data were processed to produce time histories of the water levels and current speeds over the measurement periods. Water level data were referenced to the mean tide level during the measurements and are shown in Figures 2-12 and 2-13. Figure 2-12 illustrates the water levels entire length of the deployment period. Figure 2-13 shows the same data for a 10-day portion during which weather conditions were calm and the water level variation was primarily astronomical tide. The reduction in tide amplitude from the southern gauge to the northern gauge is evident as the tide travels through the flood shoal and bridge area.

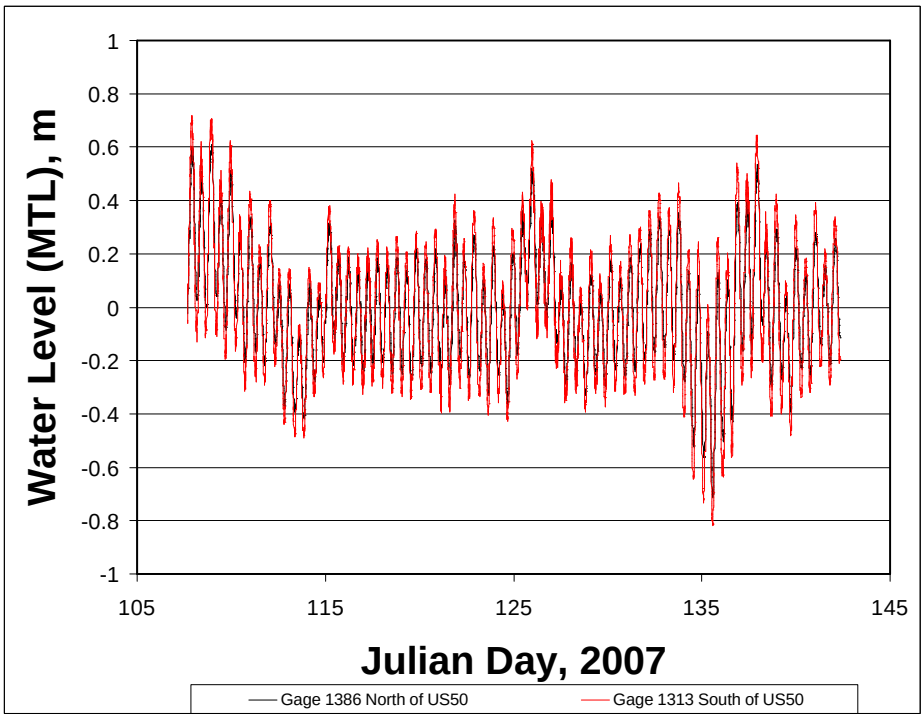

Figure 2-12. Time history of water levels north and south of U.S. 50 bridge, April and May, 2007

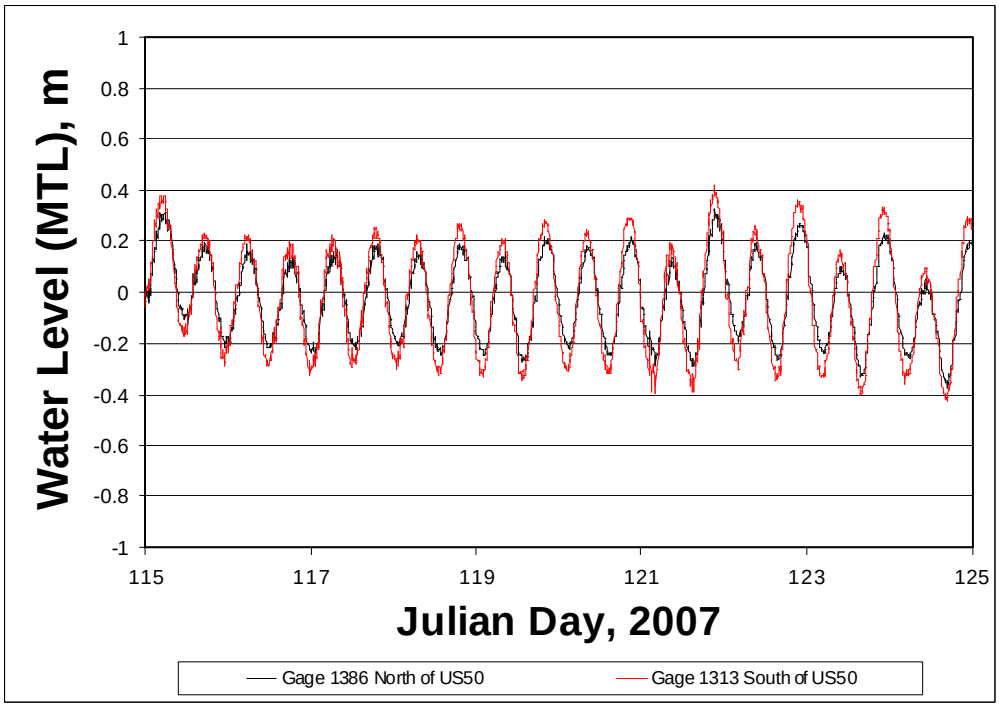

Figure 2-13. Time history of water levels north and south of U.S. 50 bridge, April 25-May 5, 2007

Current data collected by the fixed gauge north of the bridge (main channel at 2nd Street) is presented in Figure 2-14, along with the water level data north and south of the bridge. The currents about 10 meters out in the navigation channel peaked at nearly 100 cm/s during the ebb (falling) tide and over 70 cm/s during the flood (rising) tide. The locations of currents measured hourly for 13 hours during a single tidal cycle on April 19, 2007, are shown in Figure 2-15. The locations were selected to provide the numerical model with the distribution of flow beneath the bridge. Figure 2-16 shows the data at each of the six locations (numbered from east to west) as a function of time during the measurement day. The strongest flows, as expected, were in the east channel stayed relatively high toward the west until the flood shoal and scour protection blocked flow in the central portion of the bridge (stations 4 and 5). The westernmost measurement station (station 6) showed more flow speed because a flow/navigation channel is located at the west end of the bridge. At these locations, nearly under the bridge, flow speeds reached 150 cm/s in the main channel during ebb tide and 100 cm/s during flood tide.

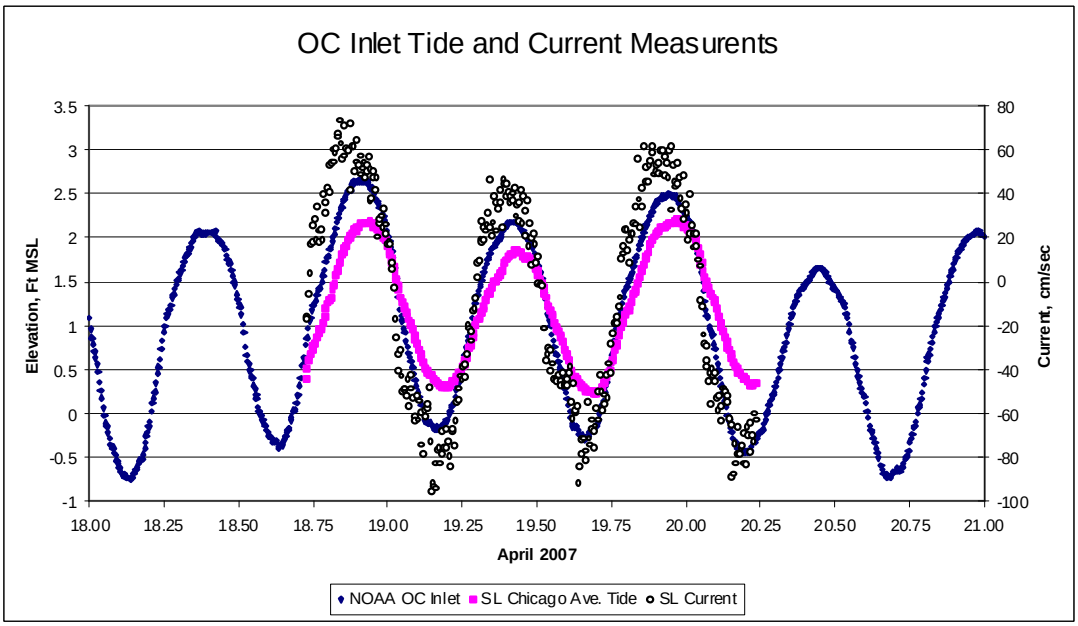

Figure 2-14. Water level at the NOAA (USCG Inlet) gauge, water level at Chicago Avenue, and current speed in the east channel at 2nd Street (dots), April 18-20, 2007.

Figure 2-15. Locations of current measurements and example flow vectors, April 19, 2007

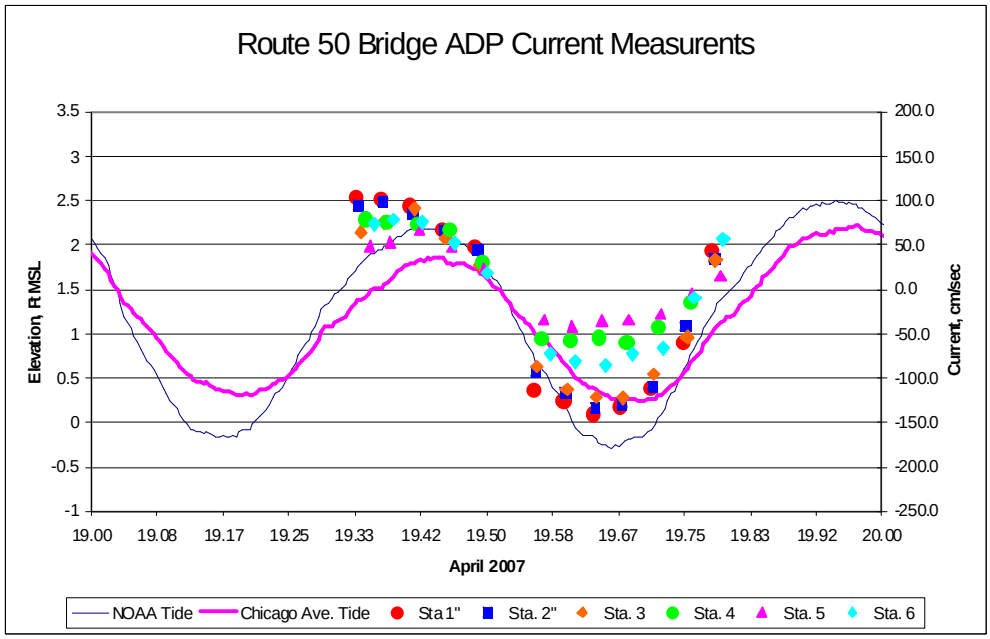

Figure 2-16. Current speeds (symbols) along the bridge during a tidal cycle on April 19, 2007. Concurrent water levels north and south of the bridge are shown as curves

3 Flood Shoal Processes

The historic evolution of the flood shoals inside Ocean City Inlet provides insight into the correlation between engineered projects and sediment deposition patterns. The evolution is evident in a series of aerial photographs taken over about a 70-year period since 1935. Ocean City Inlet was created by a hurricane in 1933 and, in the year that followed, the inlet was stabilized by jetties. As a result, the main flood shoal formed inside and south of the inlet and a smaller one formed to the north of the inlet. By 1938 (Figure 3-1), a newly-dredged navigation channel had been created along the eastern shore of Isle of Wight Bay and the primary natural channel was along the west side of the bay. A bridge crossed the bay just north of Ocean City Inlet and the present U.S. 50 Bridge had not yet been constructed. The flood shoal in Isle of Wight Bay was broad, extending from the 1938 bridge north to where the U.S. 50 Bridge would be located.

Figure 3-1. Aerial photograph of Ocean City Inlet and Isle of Wight Bay dated May 7, 1938

In 1944 (Figure 3-2), the U.S. 50 Bridge had been constructed and co-existed with the old bridge. The main flood shoal south of Ocean City Inlet continued to grow, while the flood shoal in Isle of Wight Bay had consolidated in size beneath the new bridge. The channel along eastern Isle of Wight Bay had widened and a new channel had formed to the northeast of the consolidating flood shoal. The natural channel along the western shore also continued to establish itself. By 1948, the old bridge had been removed with the exception of about 50 feet extending from the western shoreline. New shoals formed several blocks north of the U.S. 50 Bridge.

Figure 3-2. Aerial photograph of Ocean City Inlet and Isle of Wight Bay dated October 31, 1944.

By 1952, the main flood shoal south of Ocean City Inlet had merged with northern Assateague Island in the form of a spit, reducing the width of northern Sinepuxent Bay. The result was that more of the flow through the inlet was diverted toward the north into Isle of Wight Bay. In turn, by 1955 (Figure 3-3), the new shoals in Isle of Wight Bay north of the U.S. 50 Bridge grew considerably into what would be the beginnings of Skimmer Island. The shoal beneath the bridge was shrinking and being forced to the north. The three primary flow channels, the east channel, the branch cutting to the northwest from the east channel, and the channel along the western shore, were becoming wider. A 1961 photograph shows this process continuing with the northern reaches of Skimmer Island and an island along the western shoreline becoming subaerial.

Figure 3-3. Aerial photograph of Ocean City Inlet and Isle of Wight Bay dated March 14, 1955.

Through the ensuing 15 years, the shoal that would become Skimmer Island continued to migrate to the south and west as tidal flows pushed sediment north from beneath the U.S. 50 Bridge. A 1976 photograph (Figure 3-4) shows that the northern end of Assateague Island and the entrance to Sinepuxent Bay became more stable, creating more consistent tidal conditions in Isle of Wight Bay. The channel to the east and north of Skimmer Island continued to widen, as did the channel along its southwestern side. A small channel along the western shoreline persisted as well. A numerical model of flood tide flows around this time estimated that approximately 85% of the flow entering the inlet was flowing into Isle of Wight Bay and 15% was to Sinepuxent Bay (Dean et al, 1978).

Figure 3-4. Aerial photograph of Ocean City Inlet and Isle of Wight Bay dated March 24, 1976.

In 1987, a major scour protection system was constructed by the Maryland SHA beneath the U.S. 50 Bridge. The system was constructed of stone riprap along the entire length of the bridge because pile tips were becoming exposed as the sediment was pushed north into the Skimmer Island shoal. This rock essentially formed a very shallow weir (4-5 feet deep) across the bay, forcing most of the tidal flows into the east channel where the bottom was armored at a depth of approximately 25 feet (Offshore & Coastal Technologies, Inc., 1987). Figure 3-5 presents an aerial photograph taken in 1989, showing that the scour protection rapidly accelerated the southwesterly growth of the Skimmer Island flood shoal, the deepening of the east channel and the widening of the channel north of that shoal.

Figure 3-5. Aerial photograph of Ocean City Inlet and Isle of Wight Bay dated 1989.

The flow channel along the southwestern boundary of the Skimmer Island flood shoal became more constricted and the channel along the western shoreline became very narrow. This process continued and Skimmer Island eventually became subaerial by the mid-1990's (Figure 3-6) with well-established vegetation and bird populations. A U.S. Army Corps of Engineers study of the flood shoals at Ocean City Inlet measured polygons around shoal areas in historical aerial photographs and showed that the flood shoal volumes were still growing at a slow but constant rate until 1995, likely due to the consistent source of sand form the Ocean City beach nourishment project along the ocean.

Figure 3-6. Aerial photograph of Ocean City Inlet and Isle of Wight Bay dated 1998.

In 2002, the outer leg of the south jetty at Ocean City Inlet was sand tightened and raised in elevation. This rehabilitation project reduced the width of the inlet and affected the flow patterns. In turn, the ebb shoal and flood shoal experienced hydrodynamic forcing that pushed the ebb shoal farther oceanward and reduced the rate of southerly migration of Skimmer Island. The change in current patterns in 1985 and 2007 was calculated using a numerical model and is shown in Figure 3-7.

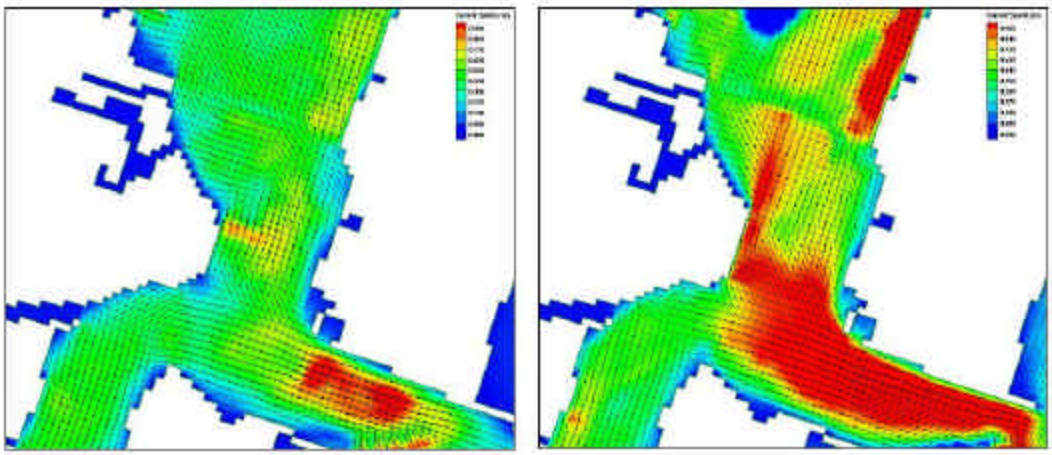

Figure 3-7. Comparison of flood tide currents in 1987 (left) and 2007 (right), with yellow and red colors indicating strong currents and blues indicating weak currents.

The resulting reduction in southerly migration of Skimmer Island is illustrated visually in Figure 3-8, where the high water line on Skimmer Island was surveyed during successive years using a hand-held GPS unit (Maryland Department of Natural Resources, 2007). The method of measurement was consistent for each survey and is a good indicator of the changes in the position of the island.

By 2005, Skimmer Island was well-established and vegetated, as shown in Figure 3-9. A polygon analysis of the area of Skimmer Island for this study indicates that the size of the island became more compact by 20% since 1998. The east channel continued to the primary flow conduit to and from a wide channel along the northern side of Skimmer Island. During flood tide, flows enter the inlet and up the western side of the bay until they encounter the U.S. 50 Bridge scour protection system. There, the flow splits into the western channel (along the western shoreline), the channel south of Skimmer Island, and the east channel. During ebb tide, most of the bay empties through the east channel and down to the inlet.

In summary, the hydrodynamic and sedimentation processes in the flood shoals at Ocean City have been largely a function of engineering projects, after the Inlet's original natural establishment by the Hurricane of 1933. Changes to the area that led to the formation and migration of Skimmer Island have included the early dredging of navigation channels, the construction of the U.S. 50 Bridge, the

stabilization of the north end of Assateague Island, the installation of the U.S. 50 Bridge scour protection, and the rehabilitation of the south jetty at Ocean City Inlet.

Figure 3-8. Shoreline surveys 2004-2007 on a 2004 photograph (MD DNR, 2007).

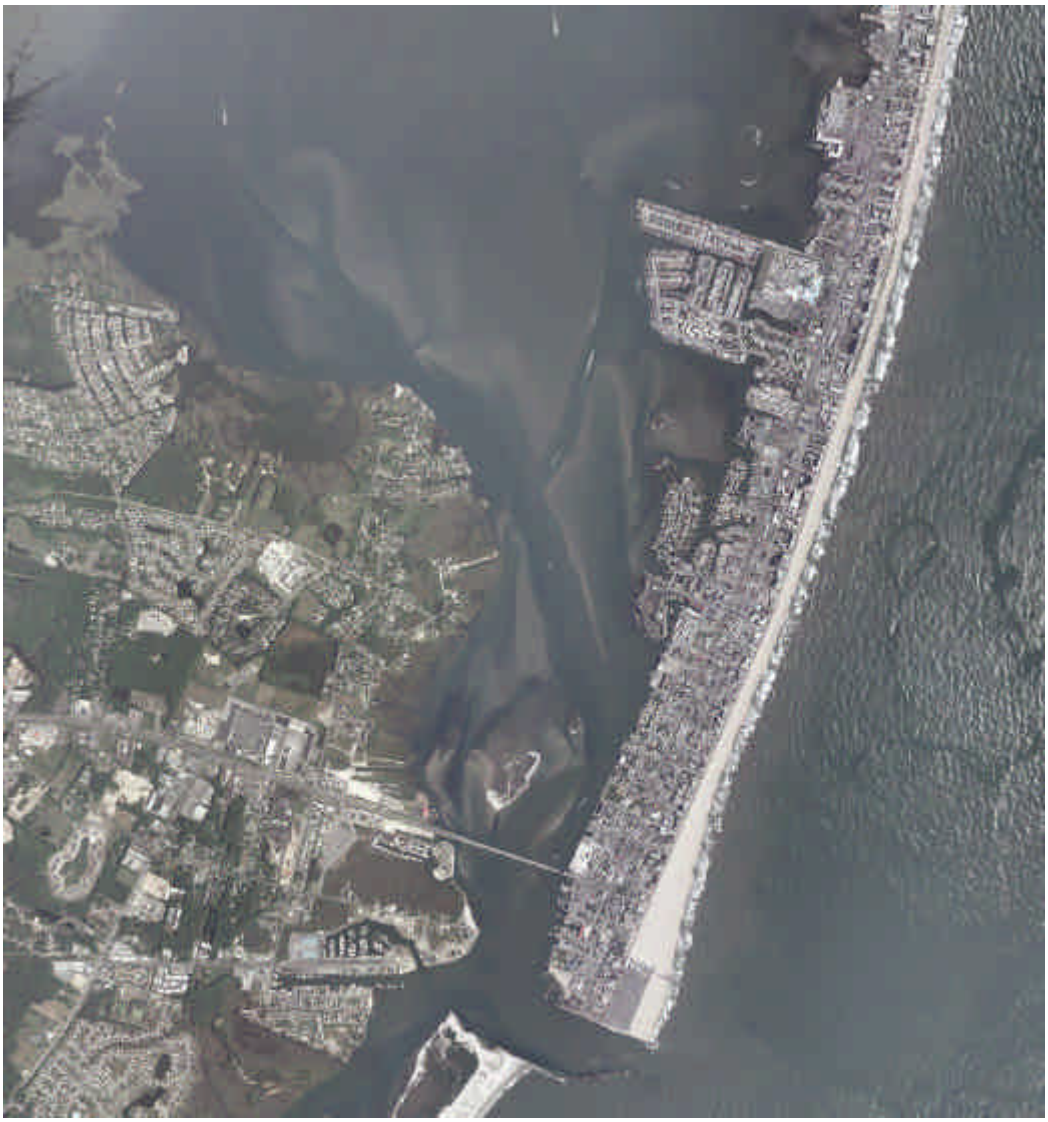

Figure 3-9. Aerial photograph of Ocean City Inlet and Isle of Wight Bay dated 2005.

4 Numerical Modeling

4.1 Introduction

Numerical modeling of hydrodynamics, sediment transport, and morphology change was conducted to evaluate the response of the currents and sediment movement in the vicinity of the present U.S. 50 Bridge, locations of proposed bridge alternatives, and Skimmer Island. The modeling approach was designed to calculate tidally-driven processes that control the currents and sediment movement in the study area. Descriptions of the models, modeling approach, verification, and results for alternatives are provided.

4.2 Model Description

The model selected to conduct the hydrodynamic and sediment transport analysis for the U.S. 50 Bridge alternatives is CMS-FLOW (formerly CMS-M2D), Version 3.2 (Buttolph et al. 2006). This model is a finite-volume numerical representation of the two-dimensional depth-integrated continuity and momentum equations of water motion and also contains integrated representation of sediment transport and morphology change. Sediment transport is represented by two total load transport rate formulations, the advection-diffusion equation, and the sediment continuity equation for updating change in water depth. Wave forcing can be included in CMS-FLOW through coupling with a wave model (waves were not included in the analysis for the U.S. 50 Bridge). CMS-FLOW has been successfully applied in numerous applications involving structural alternatives and evaluation of sand movement.

CMS-FLOW operates on a staggered, rectilinear grid that can have constant or variable cell sizes. Momentum equations are solved in a time-stepping manner first, followed by solution of the continuity equation, in which the updated velocities calculated by the momentum equations are applied. Optional sediment transport calculations are conducted on updated velocity and water-surface elevation values, together with wave properties if they are included in a specific simulation. Calculated changes in water depth by sediment movement are provided to the hydrodynamic calculations so that full feedback between the hydrodynamics and sediment transport is achieved.

For support of engineering applications, features of CMS-FLOW include robust flooding and drying, wind-speed dependent (time-varying) wind-drag coefficient, variably spaced bottom-friction coefficient, wave-stress forcing that can vary in space and time, efficient grid storage in memory, hot-start options, and sediment transport and morphology change calculations. Features of the sediment transport component include three transport formulation options, specification of sediment and water properties, control over timing of transport calculations and morphology change calculations, representation of hard or non-erodible bottom, and

representation of avalanching of steep bottom slopes. CMS-FLOW operates exclusively in SI units and requires that input be provided in metric units.

CMS-FLOW has been designed as a project-scale model that can be readily applied to examine engineering issues in embayments, coastal inlets, and the nearshore zone. The model has been developed to maximize flexibility in grid specifications and forcing, and includes the capability to obtain boundary conditions from a larger-scale regional model and apply them to a finer-scale local grid.

A graphical interface for CMS-FLOW is implemented within the Surfacewater Modeling System (SMS), Versions 8.1 and higher (Zundel 2000). SMS Version 9.2 was used for the U.S. 50 Bridge Study. Features of the CMS-FLOW interface cover grid development, control file specification, boundary condition and wind specification, coupling with regional and wave models, model runs, post-processing of results, and input and output visualization. The SMS provides tools for grid generation and modification such as assigning bathymetric data sets for interpolating to the CMS-FLOW grid, manual modification of depths and friction coefficients, cell size adjustment, and insertion or deletion of calculation cells. A model control dialog provides the user with a convenient interface for specifying timing control, model options, wind and wave forcing, sediment transport and morphology change options, and output options. The SMS provides coordinate system and unit conversion utilities so that spatial information can be converted to different coordinate systems and to different units.

CMS-FLOW can be driven by larger-domain circulation models through boundary specification capabilities contained within the SMS. The boundary conditions dialog allows access to solutions from larger-domain models that can be extracted and mapped to CMS-FLOW boundaries. The user can choose to specify water-surface elevation or a combination of water-surface elevation and velocity as boundary input for CMS-FLOW. This capability provides CMS-FLOW with boundary conditions that preserve tidal phase and other spatial and temporal variations calculated by a larger or regional scale model.

Because CMS-FLOW is a robust hydrodynamic model, it has limited adjustments available to the user to achieve an accurate result. Input bathymetry and physical forcing, together with good grid design are the most critical elements in achieving a quality outcome from CMS-FLOW. Thus, there is no user-defined eddy viscosity, which is often increased beyond its natural value to introduce artificial damping of models to keep them stable. CMS-FLOW calculates the eddy viscosity based on the physical properties of the water. The only adjustment parameter that the user has in CMS-FLOW that exerts control over the hydrodynamics is the bottom friction coefficient, which is in the form of Manning's n. This parameter should be set to a representative value based on the physical roughness of each cell.

CMS-FLOW has three formulations for calculation of sediment transport: Watanabe formulation (Watanabe 1987), the Lund-CIRP formulation (Camenen and Larson 2005, 2006), and the advection-diffusion equation. The Lund-CIRP formulation was selected for the U.S. 50 Bridge study. The Lund-CIRP formulation computes bed load and suspended load independently, and combines them to obtain the total load. The total load is then applied in the sediment continuity equation to compute the change in depth. Application of the Lund-CIRP formulation requires that the user supply the following sediment and water properties: d50 (mm), sediment density (kg/m3), water density (kg/m3), water temperature (deg C), a transport slope coefficient, sediment porosity, the option of whether or not to include the effect of ripples in the calculations, and separate scaling coefficients for the suspended load and bed load. The transport slope coefficient is a parameter that enhances the degree of downhill transport and inhibits uphill transport. For the present study, the transport slope coefficient was set to 3.0.

The transport scaling coefficients for bed load and suspended load can be applied to independently adjust the transport rates. These coefficients are effectively multipliers for the transport rates and can be applied as calibration coefficients for sediment transport. The default value for the transport scaling coefficients is 1.0, which does no adjustment to the transport rates. Because this study required long-term (multiple-year) simulations of sediment transport and morphology change, the transport scaling coefficients were applied as tools to boost the transport rates to represent longer periods of time than the actual simulation. By this method, a simulation in which a few months of hydrodynamics are calculated can represent a few years of morphology change.

Representation of sediment transport in CMS-FLOW includes representation of non-erodable (hard) bottom (Hanson and Militello 2005, Buttolph et al. 2006). This capability allows the user to specify cells that cannot erode below a cell-specific depth. Material can accrete on top of the hard bottom and material overlying the hard-bottom can also be eroded away. However, once the level of the hard material is reached, it cannot be eroded. The algorithm that treats the hard-bottom constraint conserves sediment. This algorithm can be applied to areas of rock bottom or hard pan, as well as structures such as jetties, and scour protection.

4.3 Overview of Modeling for U.S. 50 Bridge

Numerical modeling for the U.S. 50 Bridge Study consists of two primary elements. The first element is the calculation historical morphology change north of the existing U.S. 50 Bridge with the aim of demonstrating that the model reproduces the trends in shoal development and migration that have occurred since about 1985. This element provides confidence that the model is capable of predicting the future response of the Skimmer Island shoal to the present bridge (existing condition) and structural alternatives (new bridge design and placement).

The second element is calculation of hydrodynamics and sediment transport for present conditions (2007 bathymetry) for the existing condition and action alternatives. This element includes: verification of hydrodynamics by comparison of calculated currents and water levels to measurements and predicted tide, detailed (super-fine resolution) calculation of hydrodynamics of the existing condition and action alternatives to discern fine details of flow patterns, and calculation of sediment transport and morphology change over a 7.5-year time interval to predict the morphologic response of Skimmer Island to each bridge configuration. Table 4-1 summarizes the modeling elements and purpose of each modeling scale. Results from these model runs are compared and evaluated to provide information that will be applied in the decision-making process of alternative selection.

Table 4-1. Modeling Elements and Purpose

Element	Scale	Purpose
Historical	Regional	Provide boundary conditions for local model.
Historical	Local	Calculate hydrodynamics and sediment transport over 21-year time interval to verify functioning of morphology change model.
2007	Regional	Provide boundary conditions for local and super-fine models.
2007	Local	Calculate hydrodynamics and projected morphology change for existing U.S. 50 Bridge and alternatives over a 7.5-year interval.
2007	Super-fine	Calculate detailed hydrodynamics of existing U.S. 50 Bridge and alternatives.

Both modeling elements (historical bathymetry and 2007 bathymetry) were conducted by development of a regional model which was run to provide boundary conditions for more detailed local models. The regional models included Ocean City and Chincoteague Inlets, as well as the entire back bay system that is influenced by these two inlets. By coupling the local models to the regional model solution, the spatial and temporal variations in water movement at the local model boundaries are preserved. This method provides flexibility in design of the local model grid, allowing for boundary placement to be specified at appropriate locations.

All modeling for the U.S. 50 Bridge analysis was conducted with tidal forcing. Storm-induced water levels and currents were not included in the calculations, nor were the effects of waves and wind.

4.4 Historical Model

Calculation of past shoal behavior was conducted by developing a regional grid over which hydrodynamic calculations were conducted, and extracting water-surface elevation and velocity values from this regional model and applying them to the boundaries of a local model. The local model was then applied to compute hydrodynamics and sediment transport at the study area.

Bathymetric information for the regional and local models was obtained from navigation charts. This bathymetry is estimated to represent the time period of the mid 1980's. Figure 4-1 shows the regional model with the grid shown on the left and bathymetry shown on the right. The regional model contains 65,341 computational cells with minimum cell dimension of 37.8 m and maximum cell dimension of 182.5 m.

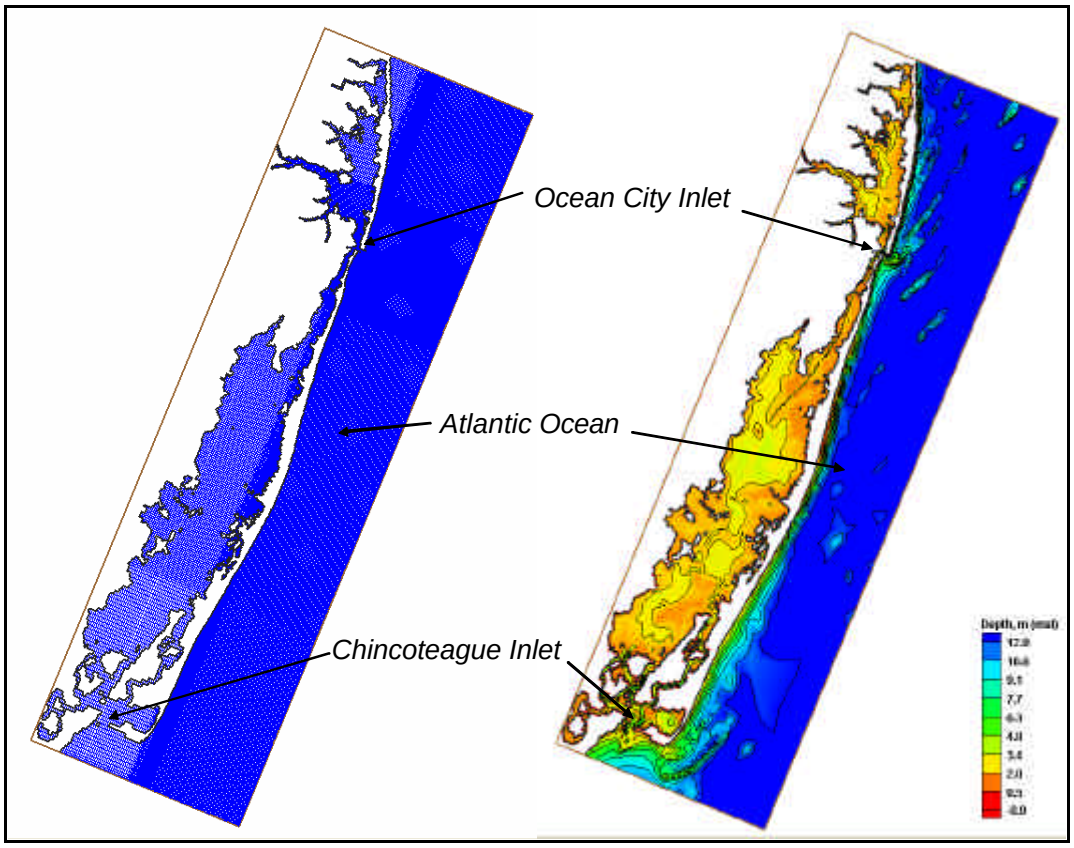

Figure 4-1. Regional model for historical simulation, computational grid (left) and bathymetry (right)

The local model is shown in Figure 4-2 with the grid shown on the left and the bathymetry shown on right. The local model contains 11,418 computational cells. Local model cells have uniform dimension of 25 m on each side. The bridge, scour protection, and south jetty were all specified as hard bottom with the ambient cell depth set as the depth of non-erodable substrate. Because 25-m resolution is not

sufficient to represent each piling of the existing bridge, the effects of the bridge on the hydrodynamics were represented through an increase in the Manning coefficient at the bridge. Cells spanning the bay at the bridge location were assigned a Manning's n value of 0.2, and the scour protection under the bridge was assigned a Manning's n of 0.09. Cells located in the ocean and most of the bay were specified to have Manning's n values of 0.029. Within the inlet, the Manning's n values were increased to represent rough surfaces (jetty stone) and turbulent losses through the inlet. Values of Manning's n through the inlet ranged from 0.031 to 0.2, with the largest values representing jetty stone.

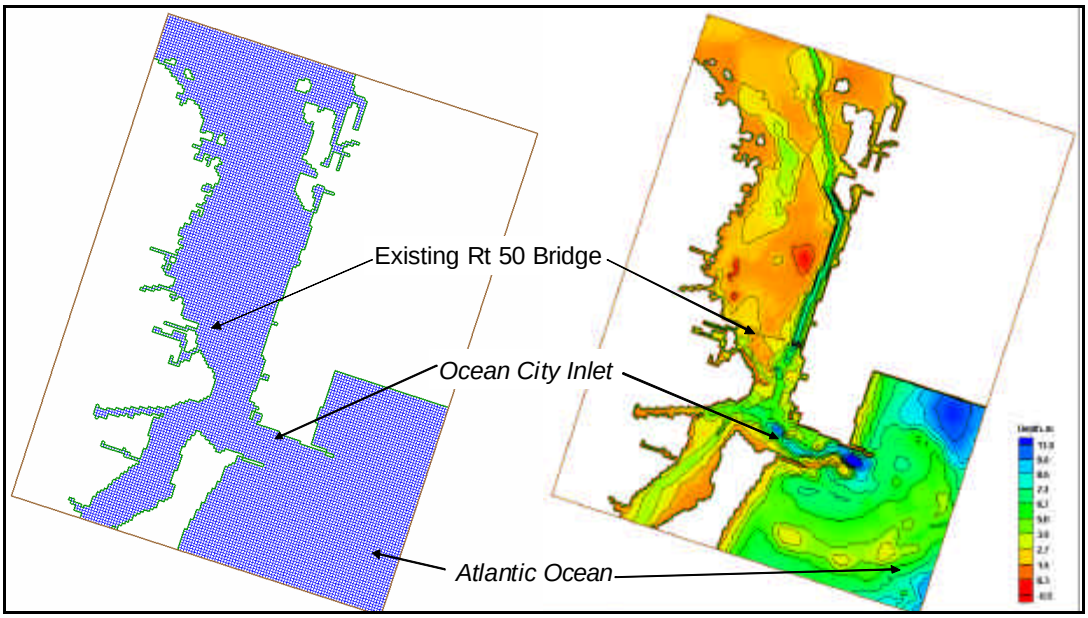

Figure 4-2. Local model for historical simulation, computational grid (left) and bathymetry (right)

Forcing for the regional model was obtained from the NOAA Center for Operational Oceanographic Products and Services (CO-OPS) web site (http://www.co-ops.nos.noaa.gov/). Water-surface elevation from 1985 measured at the Ocean City Fishing Pier was obtained at 6-min intervals and referenced to Mean Sea Level (msl) at the Ocean City Fishing Pier for input into the model. Figure 4-3 plots the water-surface elevation from the Ocean City Fishing Pier for January through March 1985 which was applied as forcing for the regional model. Because the regional model was run for the purpose of providing hydrodynamic boundary conditions for the local model, sediment transport and morphology change were not calculated by the regional model.

Forcing for the local model was mapped from the hydrodynamic solution of the regional model. Figure 4-4 provides examples of the water level and current field calculated by the regional model for high and low tide levels. Water-surface elevation and current velocity calculated by the regional model were spatially-

interpolated from the regional model cells to the cells located on the local model water boundaries. This interpolation was conducted at 0.5-hr intervals, corresponding to the output time interval of the regional model solution.

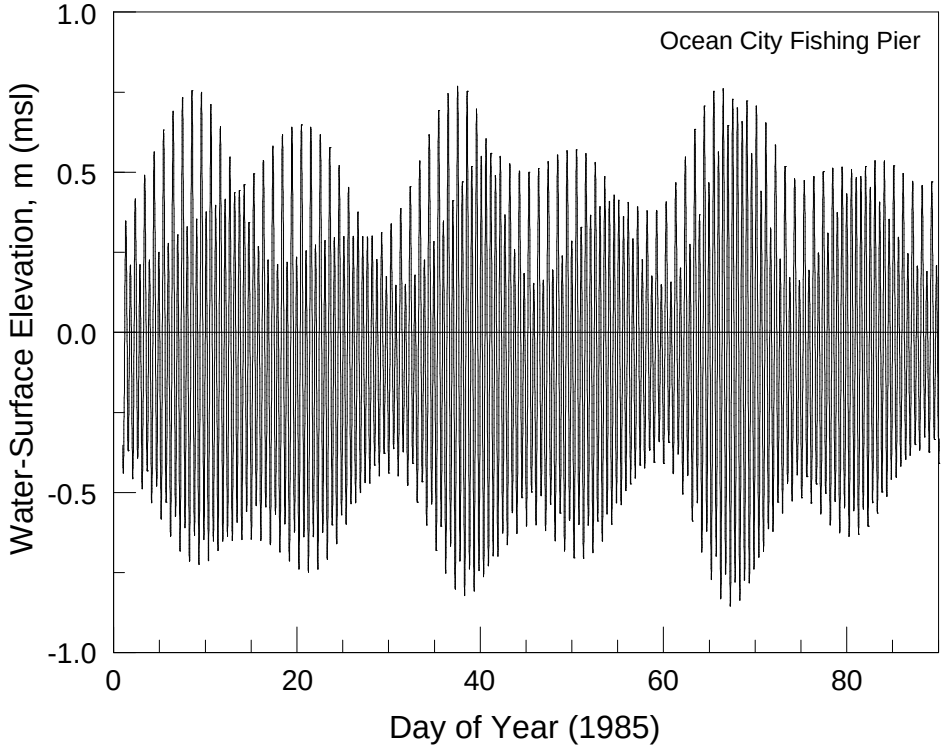

Figure 4-3. Water-surface elevation at Ocean City Fishing Pier, January through March 1985

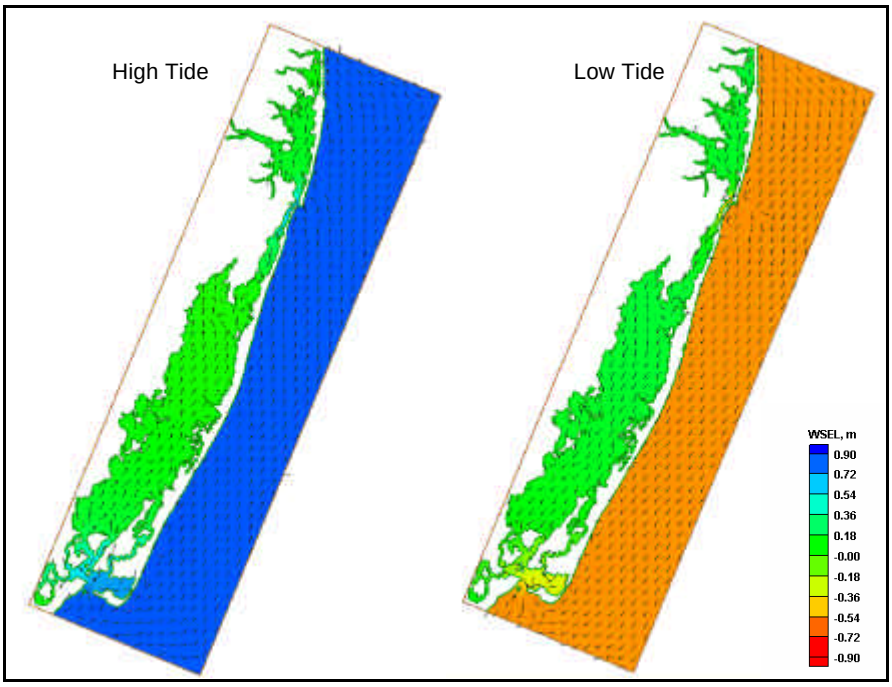

Figure 4-4. Water level and current vectors for the regional model at high and low tides

The local model was run for a 3-month time interval. Sediment transport scaling coefficients were set to values of 30 for both bed load and suspended load. This increase enabled the 3-month simulation to represent a time interval of approximately 7.5 years by inducing bathymetric change that is 30 times greater than calculating transport with a scaling coefficient of 1.0.

Examples of peak ebb and flood current for the historical local model are shown in Figure 4-5 and Figure 4-6, respectively. Triangles denote cells that have been specified as non-erodable for sediment transport computations. During both flood and ebb, the strongest current is located in the inlet and navigation channel east of Skimmer Island. During both tidal phases there is also deceleration in the area north of the U.S. 50 Bridge where shoaling has historically taken place. This reduction in current speed promotes accumulation of material and thus the migration of sand into this area.

Validation of the sediment transport and morphology change component of the modeling was conducted by simulation of shoal migration and change over a time period representing 21 years. Initial bathymetry was digitized from navigation charts and is representative of the mid-1980's. Thus, the modeling time period for the validation is from about 1985 to 2006.

For validation of the morphology change over the 21-year time interval, comparisons are made between the actual historical movement and shape of the shoal and the calculated morphology change. These comparisons are for overall

trends and properties, such as general shoal shape and migration direction, as well as other changes that have occurred in the study area, such as widening of the east navigation channel.

Figure 4-7 shows historical shorelines superimposed over an aerial photograph of Skimmer Island. The 1985 shoreline extends from the northeast island in a linear trend southwestward toward the U.S. 50 Bridge. By 1998, the northeast island had reduced in size and the shoreline of Skimmer Island had migrated westward and changed form, becoming wider and horseshoe-shaped. The shoals continued to change and by 2004 the northeast island had reduced in size a little more, and Skimmer Island migrated toward the southwest, the shape becoming triangular in the center with spits extending to the northeast and southwest.

Calculated morphology is shown in Figure 4-8 at 7-year intervals. Contours have been colored to be similar to the aerial photograph shown in Figure 4-7 to aide in the visual comparison. The initial condition is approximately 1985, 7 years is 1992, 14 years is 1999, and 21 years is 2006. During the first 7-year interval, the east channel has widened substantially and the northeast island reduced in area. Deposition has taken place directly north of the central part of the bridge and a horse-shoe shaped shallowing has occurred in the central shoal area.

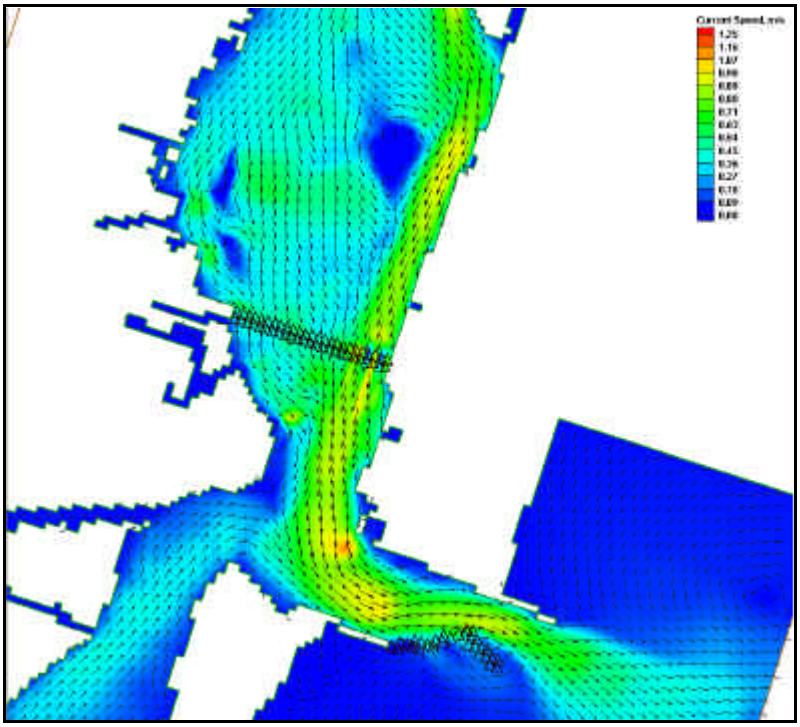

Figure 4-5. Peak ebb current for navigation chart bathymetry

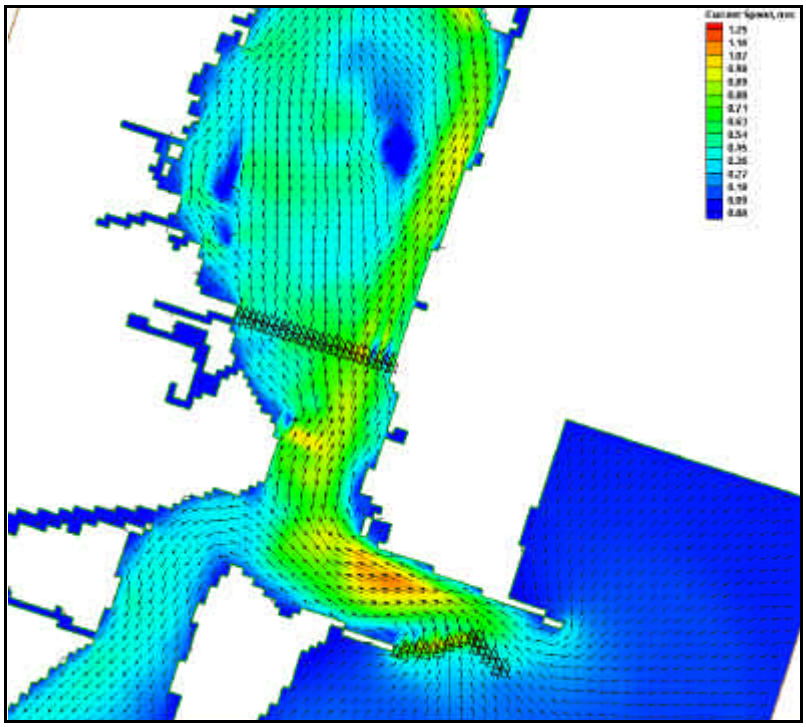

Figure 4-6. Peak flood current for navigation chart bathymetry

Figure 4-7. Skimmer Island historical shorelines and recent aerial photograph showing shoal extent

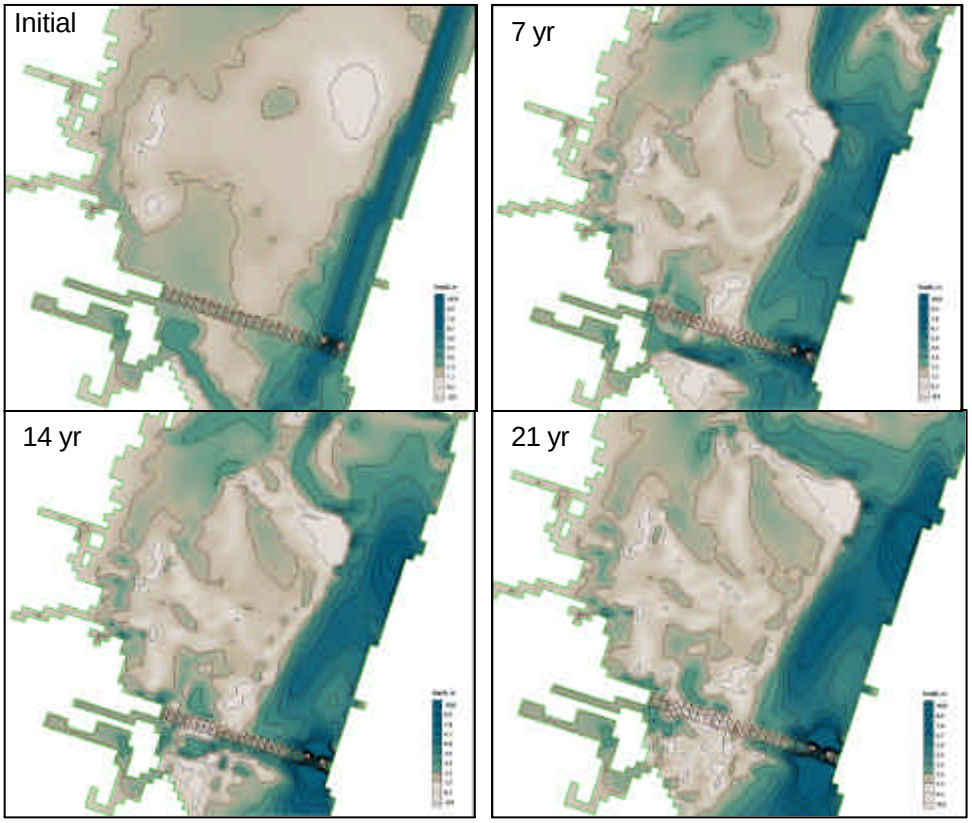

Figure 4-8. Calculated morphologic evolution at 7-year intervals.

By the 14-year (1999) time period, the channel north of the northeast island has migrated sharply to the west, which has induced part of the northwest island to grow a westward spit. This calculated sharp westward migration is too strong as the actual channel migrated more modestly toward the northwest. The central shoal area, however, shows trends similar to changes that have occurred historically. Shoaling has continued to occur, causing shallow areas to gain elevation and the horseshoe shape is beginning to narrow.

At 21 years (2006), the patterns that have occurred in the 1999 image are still present, but have evolved such that the shoal is building elevation and its various branches become more linear rather than wide and horseshoe-shaped. The deposition area just north of the central part of the U.S. 50 Bridge has continued to gain area and elevation. The east navigation channel has slowed significantly in its migration, although it has migrated further westward than what occurred historically.

The validation simulation for the Skimmer Island area has reproduced the overall trends in shoal migration and change of form. Changes calculated through time are consistent with those observed at the site. Historical migration of the navigation channel was also calculated, although this process was overpredicted.

4.5 2007 Model of Existing Condition and Alternatives

For simulation of present conditions and prediction of future changes, the regional and local models were updated with the 2007 bathymetric survey data. Scour protection under the existing U.S. 50 Bridge was assigned as non-erodable material having a Manning's n value of 0.09. In addition, changes to the south inlet jetty from the rehabilitation project as well as the scour protection constructed at the toe of the jetty were implemented. The local model with updated bathymetry is shown in Figure 4-9 (the updated regional model contains the same bathymetry as the local model so is not shown). The 25-m resolution of the local model is too coarse to represent individual bridge piers in the alternatives. Thus, the bridge piers for the alternatives were represented through assignment of the Manning friction coefficient to 0.15 along the span of each alternative. This friction coefficient is lower than that assigned to the existing U.S. 50 Bridge because the piers are farther apart and there are fewer of them. The local models developed for the alternatives are identical to that for the existing condition except for the modification of the friction coefficient along the proposed bridge spans.

In addition to the regional and local models, a super-fine resolution (SFR) model was developed to calculate details of the hydrodynamics in the vicinity of the present U.S 50 Bridge and the proposed alternatives. The SFR model covers the same computational area as the 2007 local model and uses the same bathymetry, but is more highly-resolved. Figure 4-10 shows the computational grid for the SFR model for the existing condition. Cell dimensions for the SFR model range from a minimum of 4.7 m to a maximum of 19.9 m. Maximum resolution is located in the area of the existing U.S. 50 Bridge and alternative locations. The existing condition SFR model contains 45,231 cells. Manning coefficients were specified to correspond with the local model friction coefficients.

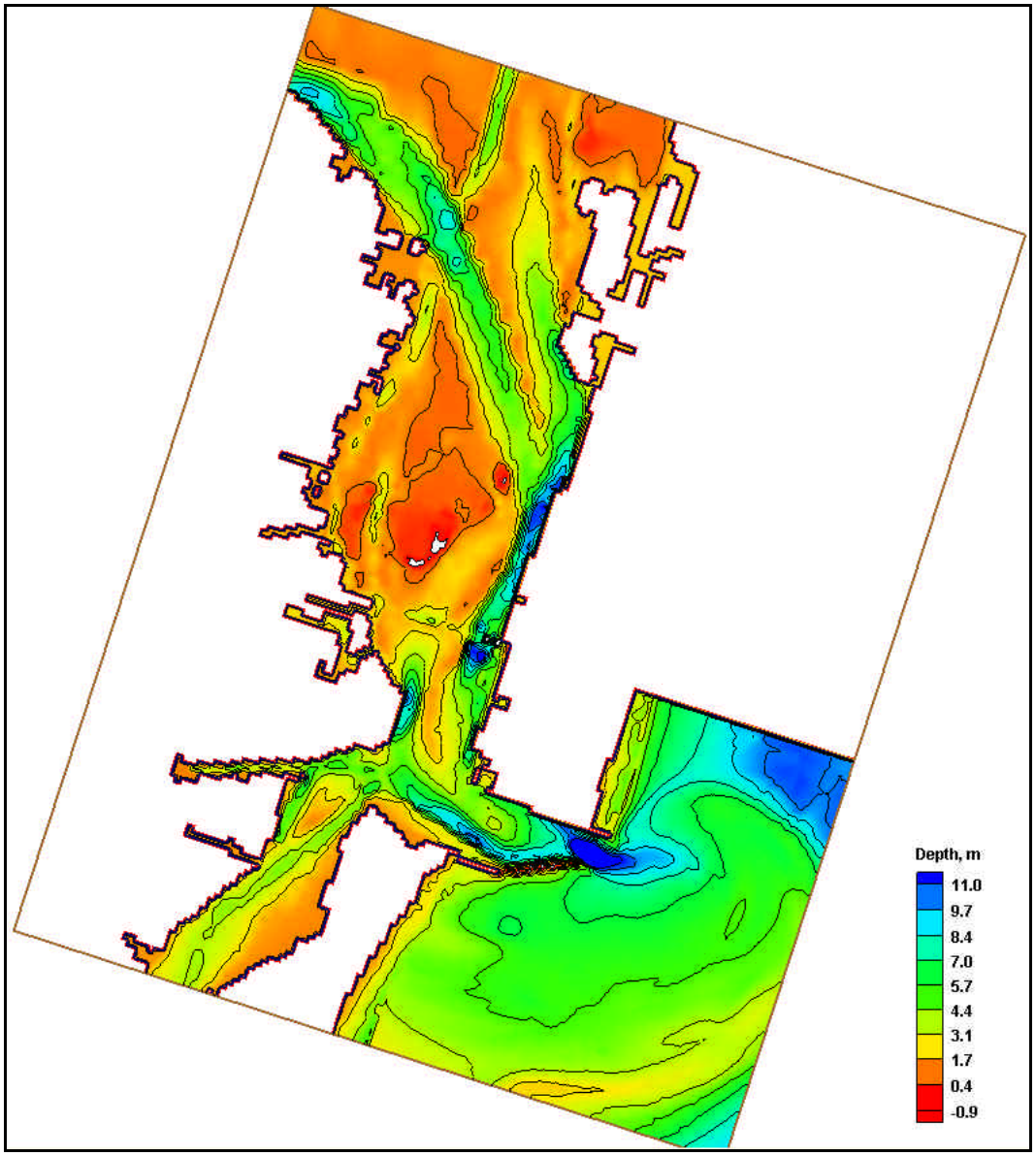

Figure 4-9. Local model with 2007 bathymetry

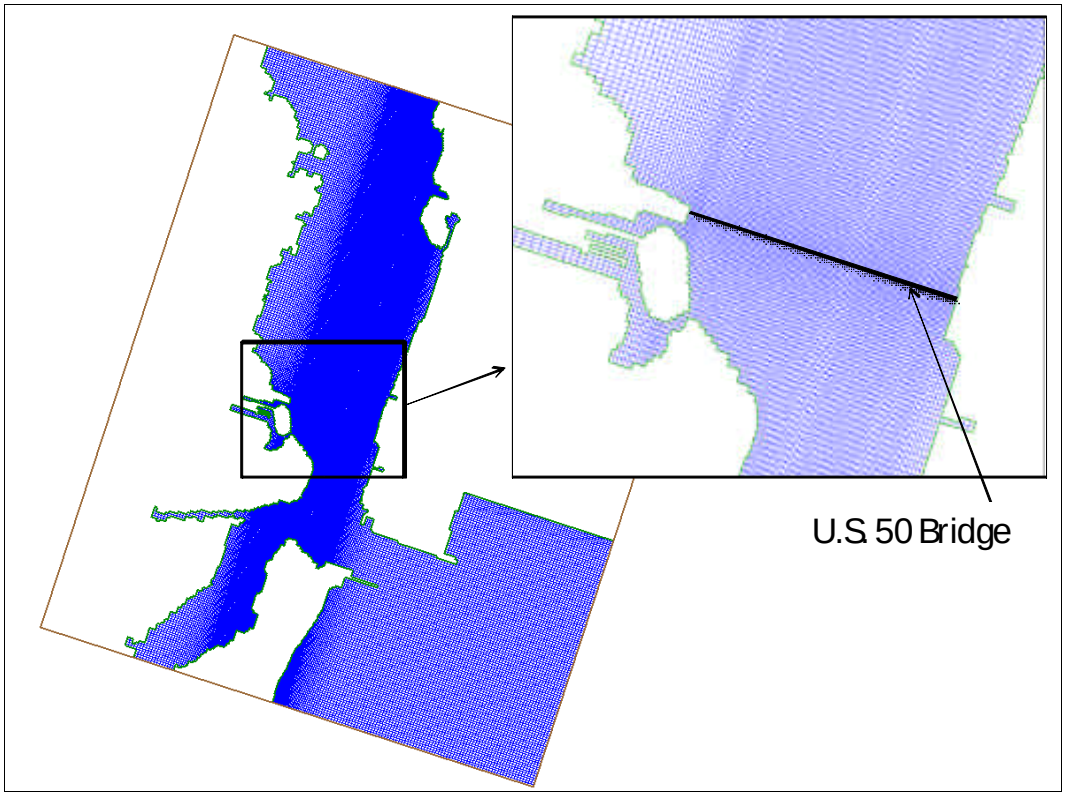

Figure 4-10. Computational grid for super-fine resolution model

Details of the SFR models for the existing condition and alternatives are shown in Figure 4-11. The existing U.S. 50 Bridge was represented through an increase in the friction coefficient along the span of the bridge to a value of 0.2. Sizes of the existing pilings were not close enough to the grid cell sizes to represent them individually. Because of the dimensions and spacing of the proposed bridge piers for the alternatives are closer to the cell sizes of the SFR grids, they were individually included in the model as land cells. This treatment of the bridge piers enabled the model to calculate the diversion of flow around each pier and represent the acceleration of flow induced by the presence of the piers. Inclusion of wall friction coupled with a Manning coefficient of 0.031 between piers represented the turbulent losses at the proposed alternatives. For Alternative 5B, the existing U.S. 50 Bridge was removed by reduction of the Manning coefficient from 0.2 (bridge in place) to 0.031 (bridge removed).

Specification of boundary conditions was conducted with the same method as applied for the historical model. A simulation with the regional model was conducted and the hydrodynamic solution from the regional model was mapped to the boundaries of the local and SFR models to be applied as forcing. Thus, both the local and the SFR models are forcing with mapped information from the regional model

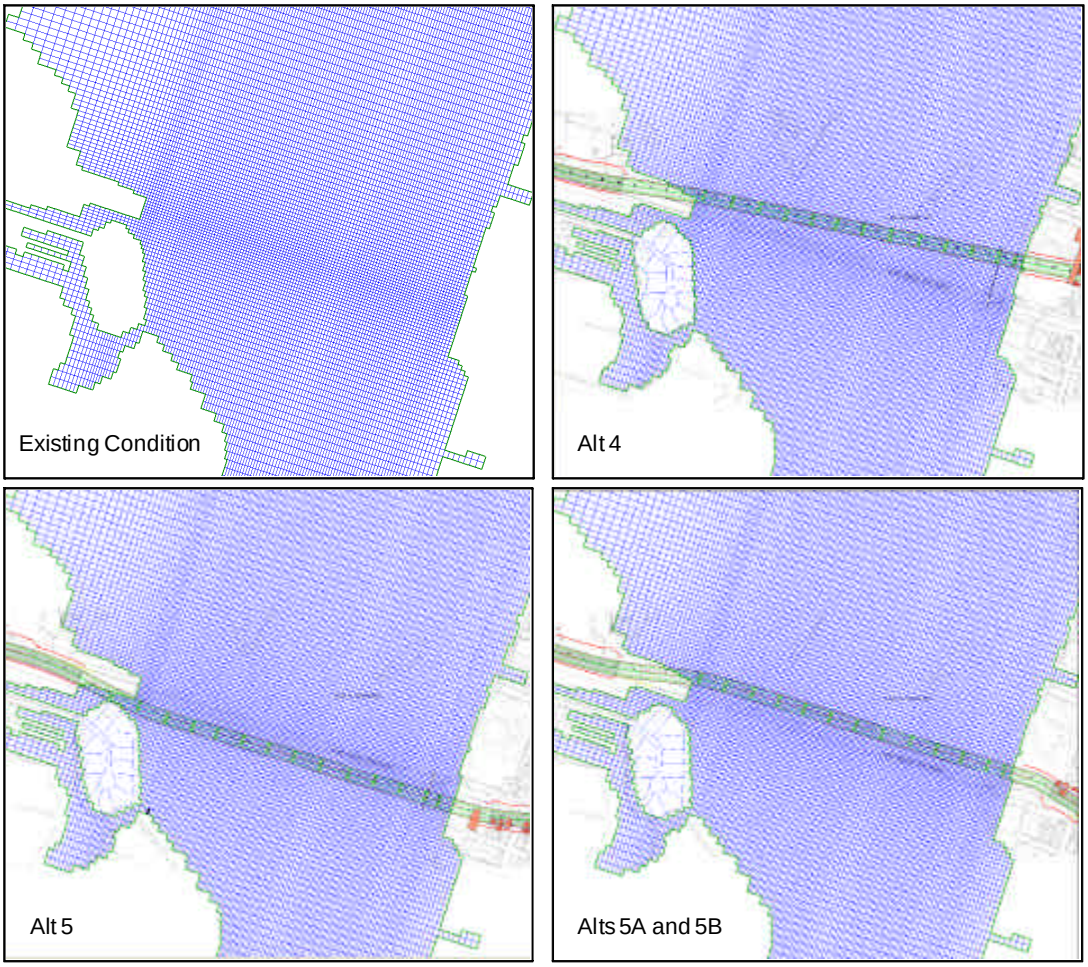

Figure 4-11. Grids for SFR models of existing condition and alternatives

Model validation was conducted for the April-May 2007 measurement interval. For the model validation, the regional model was forced with predicted tidal elevations for the Ocean City Fishing Pier obtained from the NOAA CO-OPS web site for the time interval of April 15 to May 22, 2007 (Figure 4-12). The predicted tide was selected as forcing for the calibration interval because gauge data in the Atlantic Ocean near Ocean City were not available for the measurement interval. Predicted tides are constructed from tidal constituents and therefore do not include modifications to the water-surface elevation owing to storms, wind, or other non-tidal influences.

Water levels were compared at three locations: the measurement site located approximate 600 ft south of the bridge, the site located approximately 600 ft north of the bridge, and predicted tide for the NOAA Inlet Gauge. For comparison to calculations, the measurements were high-pass filtered to remove much of the influence of an offshore storm event and other non-tidal processes on the water-surface elevation.

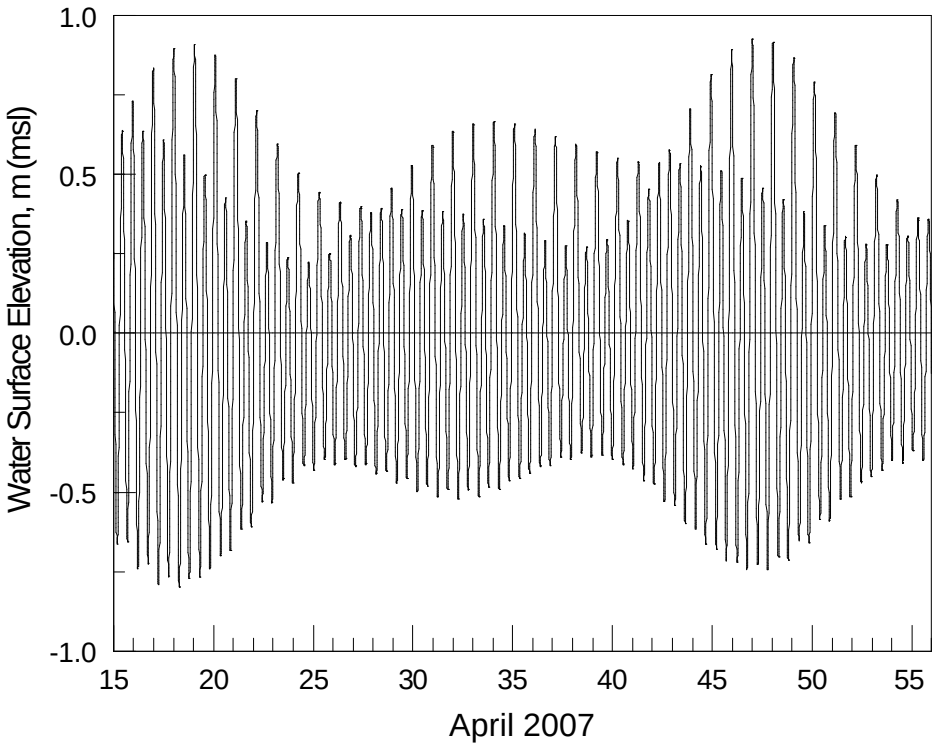

Figure 4-12. Predicted tide at Ocean City Fishing Pier for the April-May 2007 calibration period

Comparison of measured and calculated water levels for the gauge located 600 ft south of the U.S. 50 Bridge is shown in Figure 4-13. Calculations compare well to measurements, following the spring-neap cycle. During peak spring tide, the model appears to over-predict the peak high tides by 8 to 10 cm, however, this discrepancy may owe to the high-pass filter not removing the entire non-tidal component of the water-surface elevation signal from the measurements. Outside of these intervals of discrepancy, the model calculates high and low tide values within about 0 to 3 cm of measurements.

Comparison of measured and calculated water levels for the gauge located 600 ft north of the U.S. 50 Bridge is shown in Figure 4-14. Water levels are over-predicted by up to 10 cm during peak spring tide, and differences during the remainder of the spring-neap cycle range from 0 to 3 cm.

Figure 4-15 compares the predicted and calculated water levels at the NOAA Inlet Gauge, located near the Coast Guard Station. This comparison shows good agreement between the model and the predicted tide. During the first half of the comparison, the discrepancy between calculations and prediction is less than 2 cm. During the second half of the comparison from the latter neap to the first half of spring tide, a small shift of overall water level (downward in the predictions, upward

in the calculations) can be seen, but which realigns to better agreement by the last two days of the comparison.

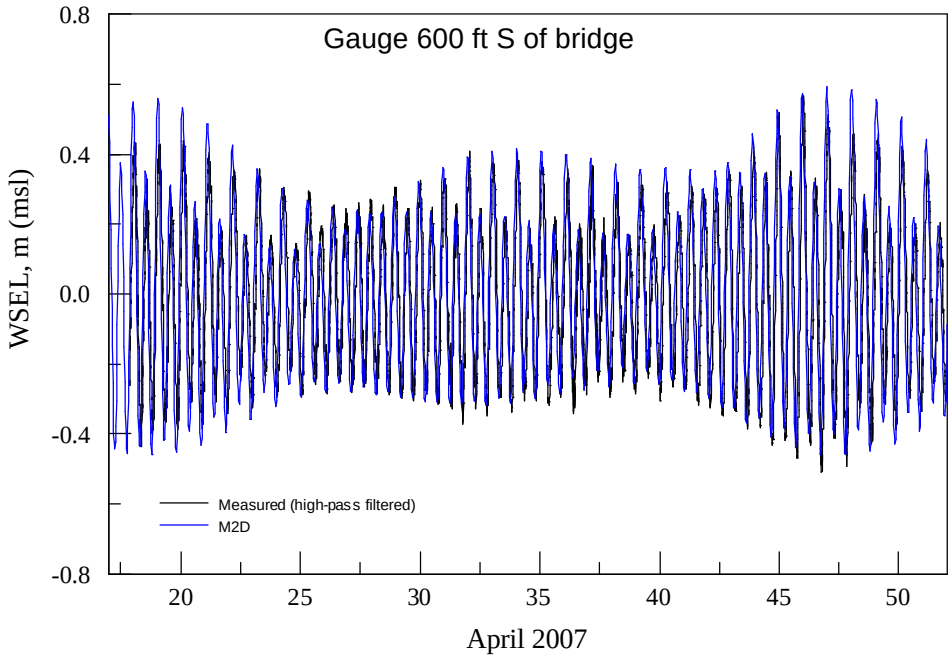

Figure 4-13. Comparison of measured and calculated water level at the gauge located 600 ft south of the U.S. 50 Bridge

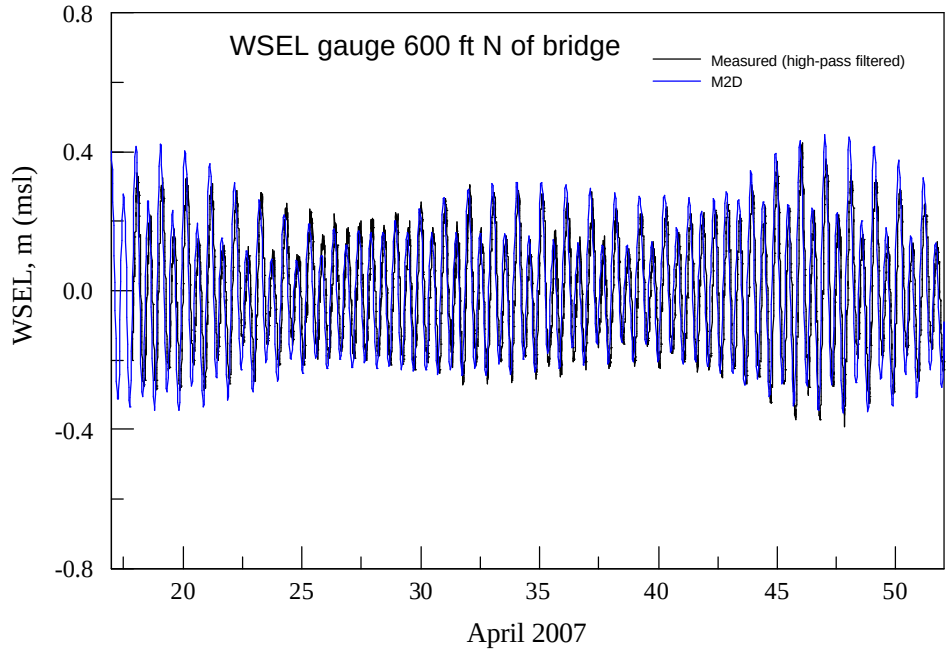

Figure 4-14. Comparison of measured and calculated water level at the gauge located 600 ft north of the U.S. 50 Bridge

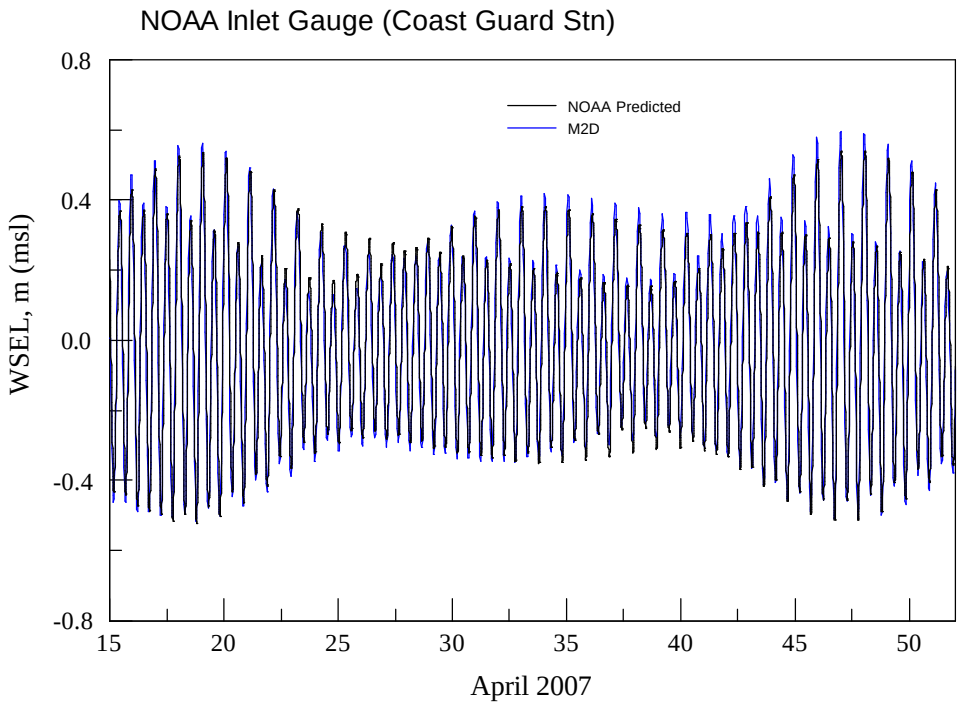

Figure 4-15. Comparison of predicted and calculated water level and the NOAA Inlet Gauge

Currents measured over three tidal cycles starting April 18 and ending April 20, 2007 were applied to verify the hydrodynamic calculations (Figure 4-16). During the measurement interval, an offshore storm modulated the water levels in the ocean and back bays, which suppressed the current speed during flood. Comparison of the calculated and measured current speed shows the model over-predicts the peak flood current by about 0.5 m/sec. This discrepancy in part owes to the non-tidal influence of the storm, which was not included in the model. During peak ebb current, the model over-predicts the current speed by 0.2 to 0.3 m/sec, giving an error in peak speed of about 25%. This range of error is typical for currents.

Production simulations for the SFR and local models were conducted through implementation of boundary conditions obtained from the regional model. The regional model was run for the time interval of January 1 to March 30, 2007 with predicted tides from the NOAA CO-OPS web site for the Ocean City Fishing Pier (Figure 4-17). The SFR model was run for the first 15 days of this time period and the local model was run for the entire 3-month time interval.

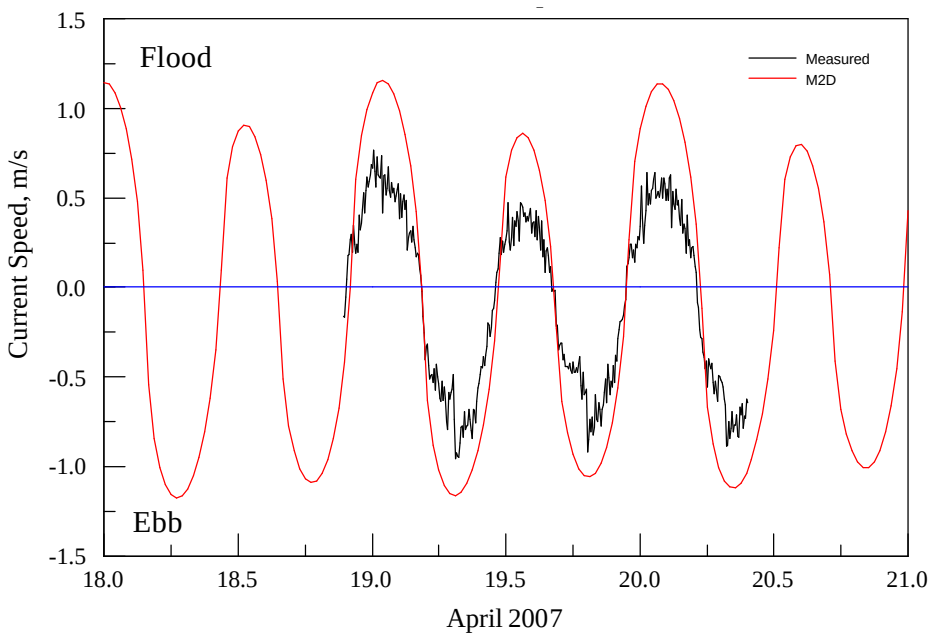

Figure 4-16. Comparison of measured and calculated current speed

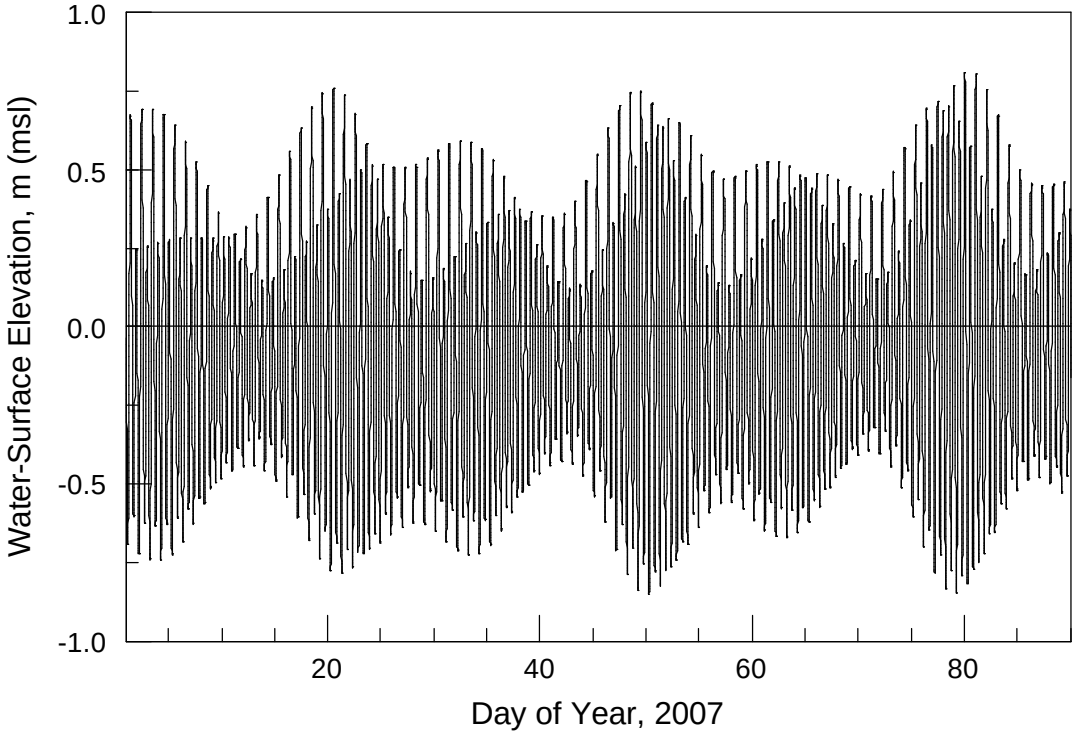

Figure 4-17. Predicted tide at Ocean City Fishing Pier, January through March 2007

Results of the SFR model provide details of flow fields in the vicinity of the bridge, as well as their influence to the south of the existing U.S. 50 Bridge and in the Skimmer Island area. Contour plots of representative peak ebb and peak flood velocity fields provide spatial information on the distribution and details of the currents. Peak flood current for the existing condition and Alternatives 4, 5, 5A, and 5B are shown in Figures 4-18 through 4-22, respectively. In all of the flood current figures, the primary flow from the inlet enters on the west side south of the existing U.S. 50 Bridge. The current spreads and decelerates in the vicinity of the bridge. North of the bridge, the primary current shifts to the navigation channel on the east. All of the proposed alternatives show narrow patterns of strong and weak velocity near the bridge piers, which indicate acceleration between the piers and sheltering behind them.

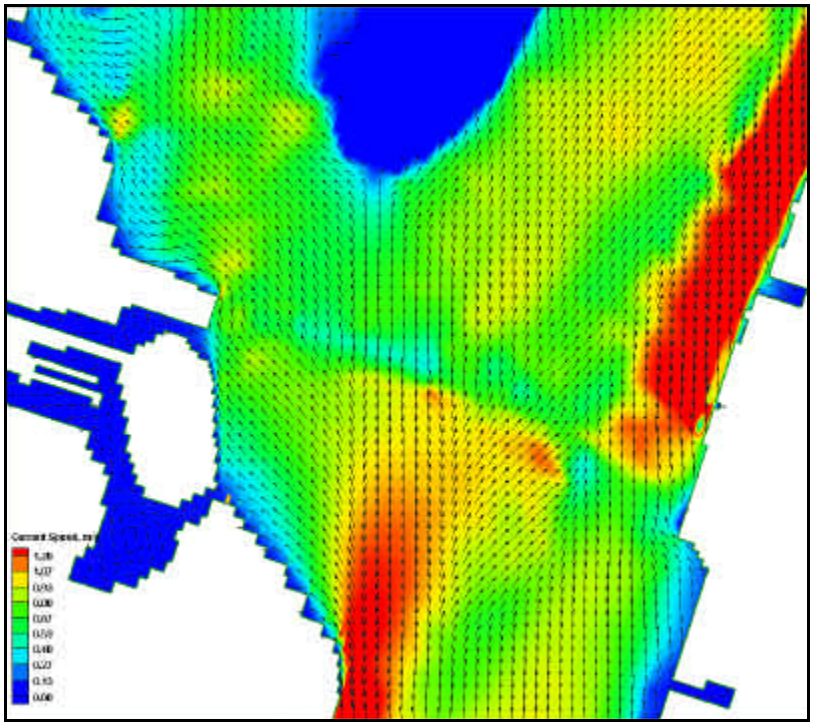

Figure 4-18. Peak flood current for existing condition calculated by SFR model

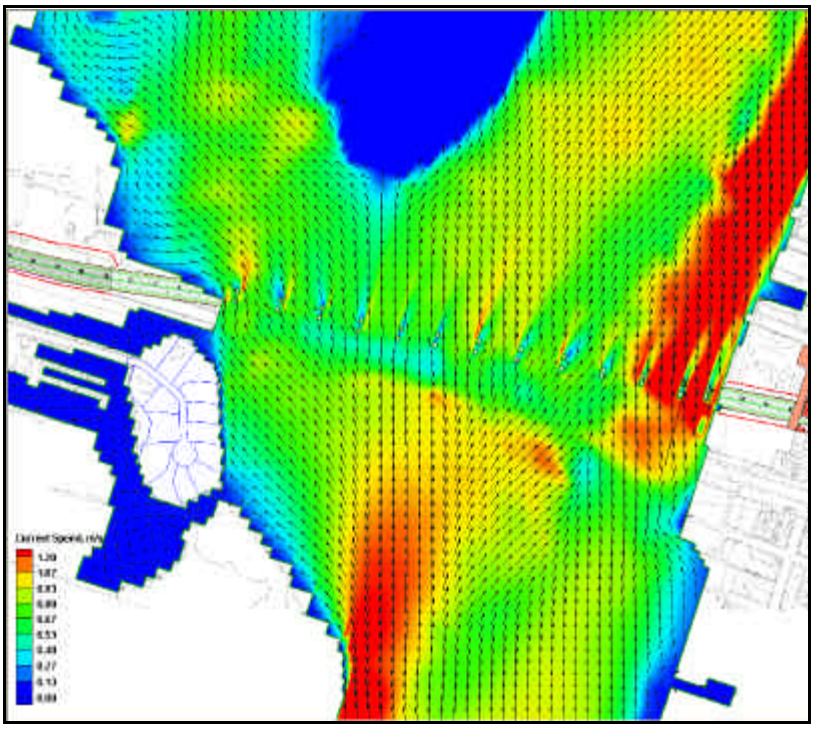

Figure 4-19. Peak flood current for Alt 4 calculated by SFR model

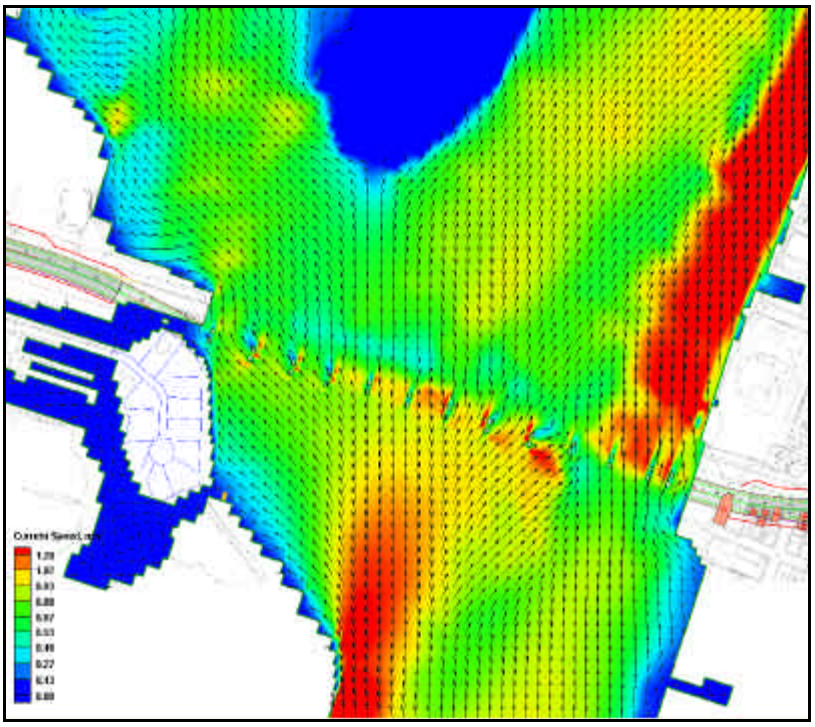

Figure 4-20. Peak flood current for Alt 5 calculated by SFR model

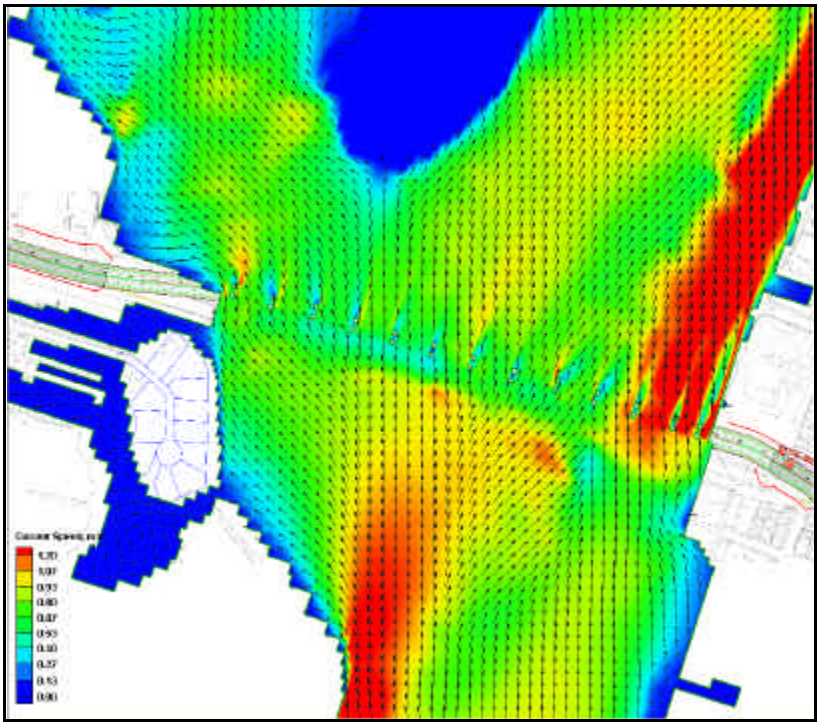

Figure 4-21. Peak flood current for Alt 5A calculated by SFR model

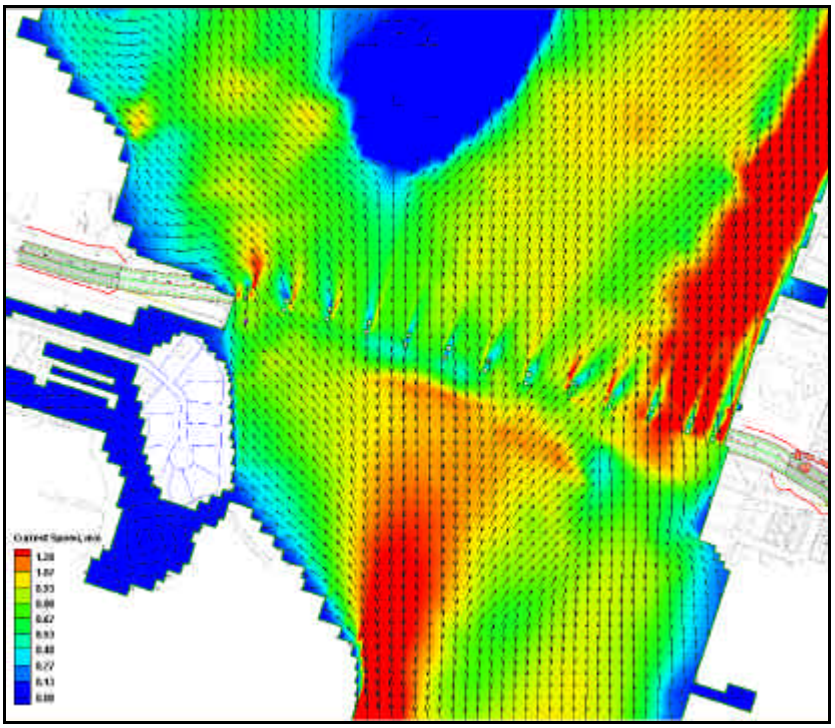

Figure 4-22. Peak flood current for Alt 5B calculated by SFR model

Peak ebb current for the existing condition and Alternatives 4, 5, 5A, and 5B are shown in Figures 4-23 through 4-27, respectively. General patterns of ebb flow are consistent among the existing condition and alternative simulations with the strongest ebb current flow being in the east navigation channel, both north and south of the location of the existing U.S. 50 Bridge. The proposed alternatives show some variation in the flow field owing to the presence and location of the bridge piers. Alternatives 4, 5A, and 5B show reductions in current speed in their central areas on the south side of the piers. Alternative 5 shows greater current speed between piers.

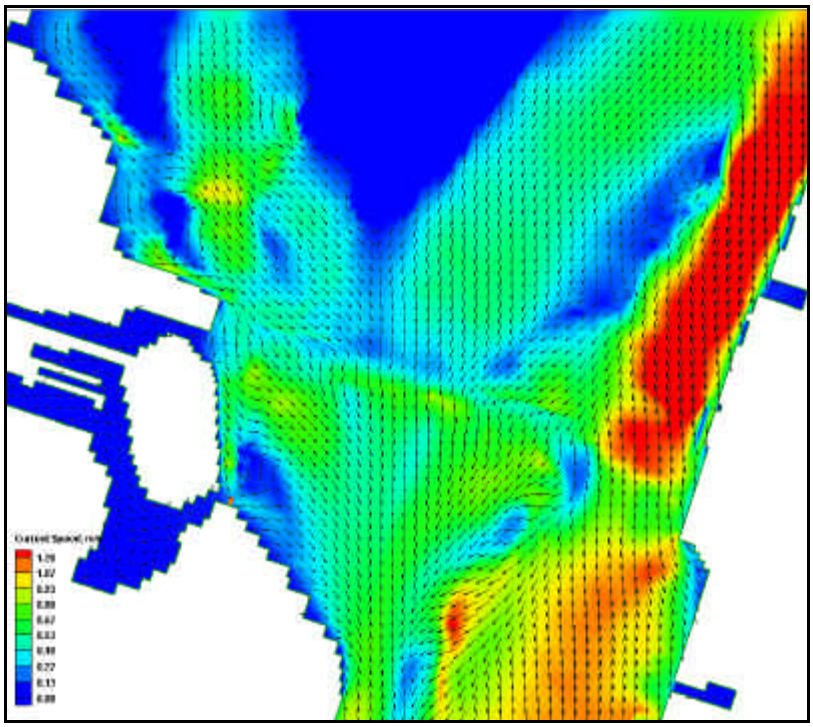

Figure 4-23. Peak ebb current for the existing condition calculated by SFR model

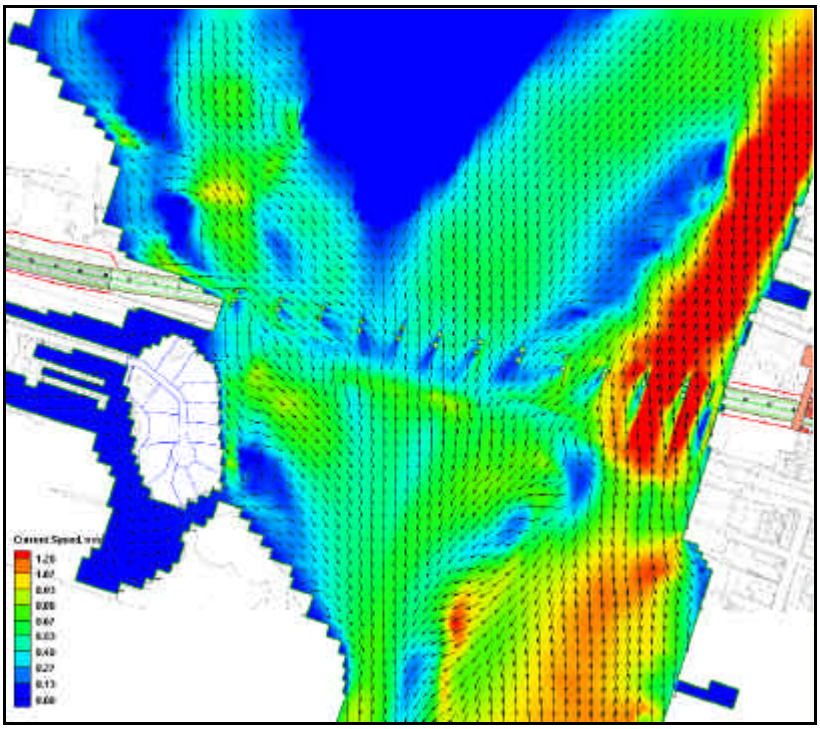

Figure 4-24. Peak ebb current for Alt 4 calculated by SFR model

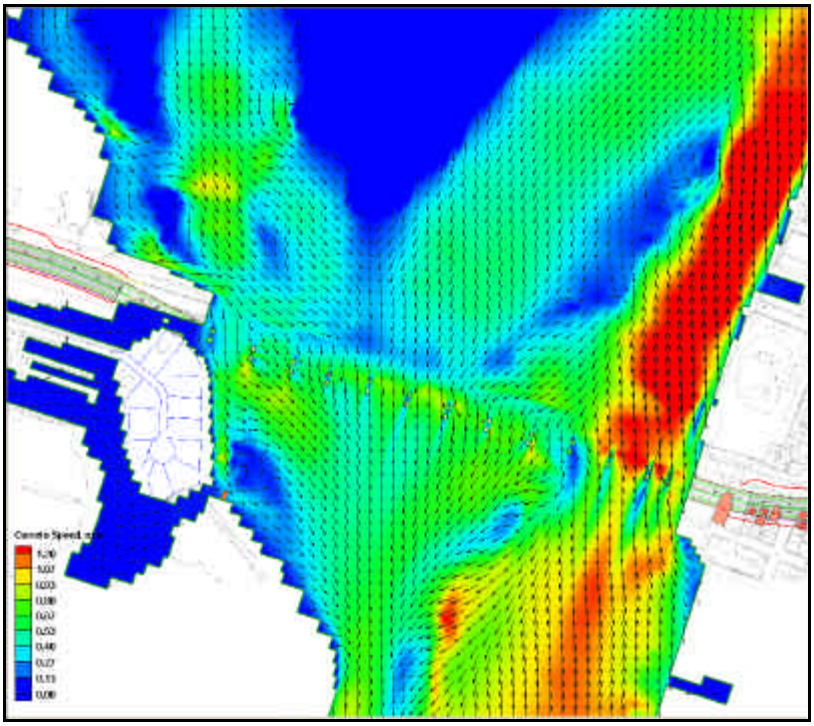

Figure 4-25. Peak ebb current for Alt 5 calculated by SFR model

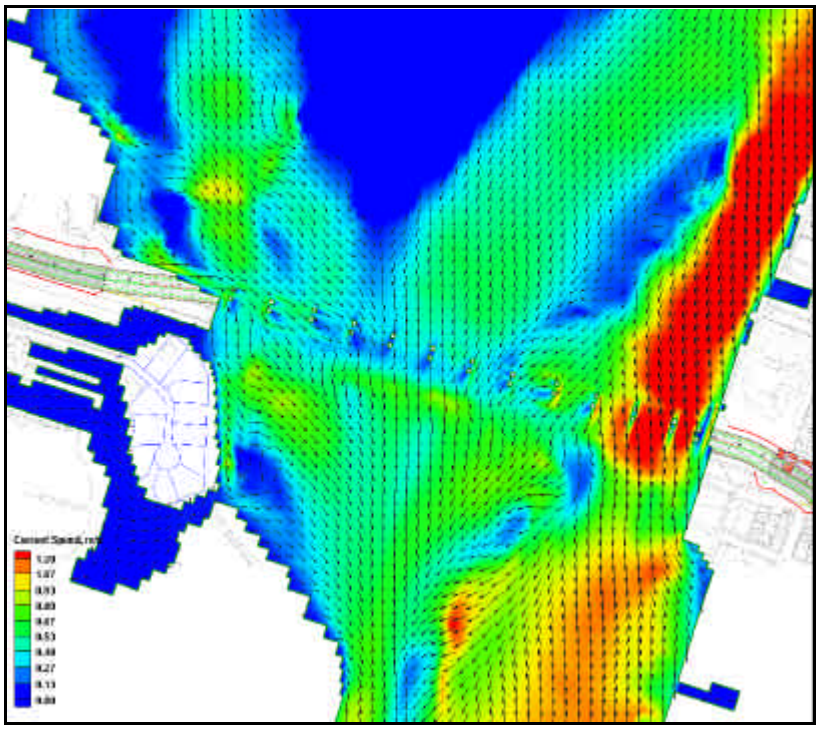

Figure 4-26. Peak ebb current for Alt 5A calculated by SFR model

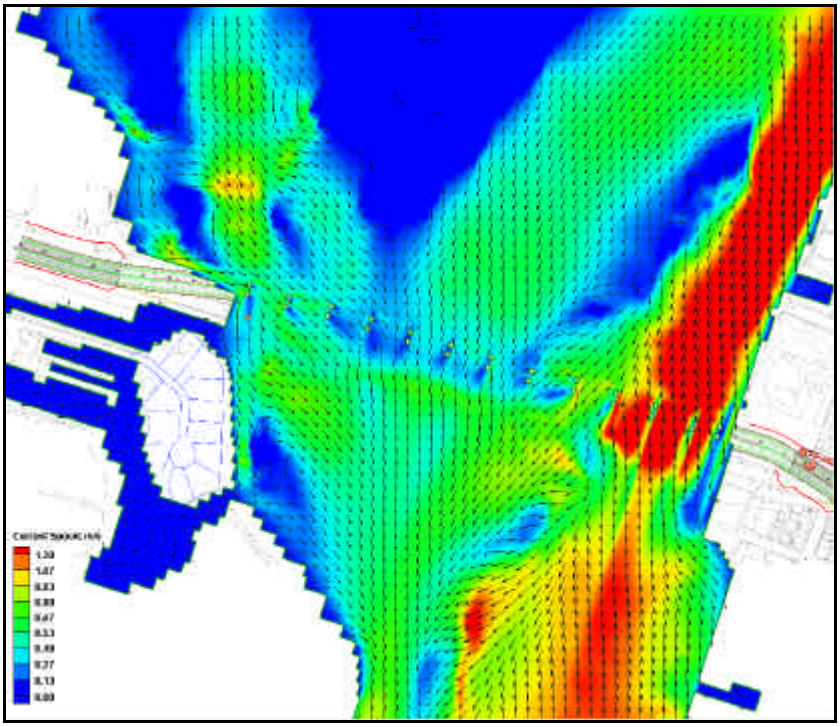

Figure 4-27. Peak ebb current for Alt 5B calculated by SFR model

To more easily discern changes in current speed owing to construction of the proposed alternatives, plots of current speed difference between the existing U.S. 50 Bridge and the proposed alternatives are provided. Differences were calculated by subtracting the current speed of the existing condition from the current speed of each proposed alternative at peak flood and at peak ebb. Plots of speed differences are contoured such that blue denotes that the proposed alternative has a weaker current speed than the existing condition, and yellow/red denotes that the proposed alternative has a stronger current speed than the existing condition.

Figures 4-28 through 4-31 display contour plots of the speed differences for Alts 4, 5, 5A, and 5B, respectively, at peak flood current. Alternatives 4, 5A, and 5B show a slight increase in current speed, under 5 cm/sec, in the central area north of the bridge, whereas Alt 5 shows a general slight decrease in the same area. The navigation channel on the east shows a decreased current speed in the range of 5 to 10 cm/sec over its length for Alts 4, 5, and 5A, whereas Alt 5B shows an increased current speed of about 8 cm/sec over most of the navigation channel. Outside of the Skimmer Island area and proposed bridge location, Alts 4, 5, and 5A generally have a slightly reduced current speed, 1 to 3 cm/sec, over the domain. Alternative 5B shows stronger currents, typically between 3 and 8 cm/sec, over most of the domain.

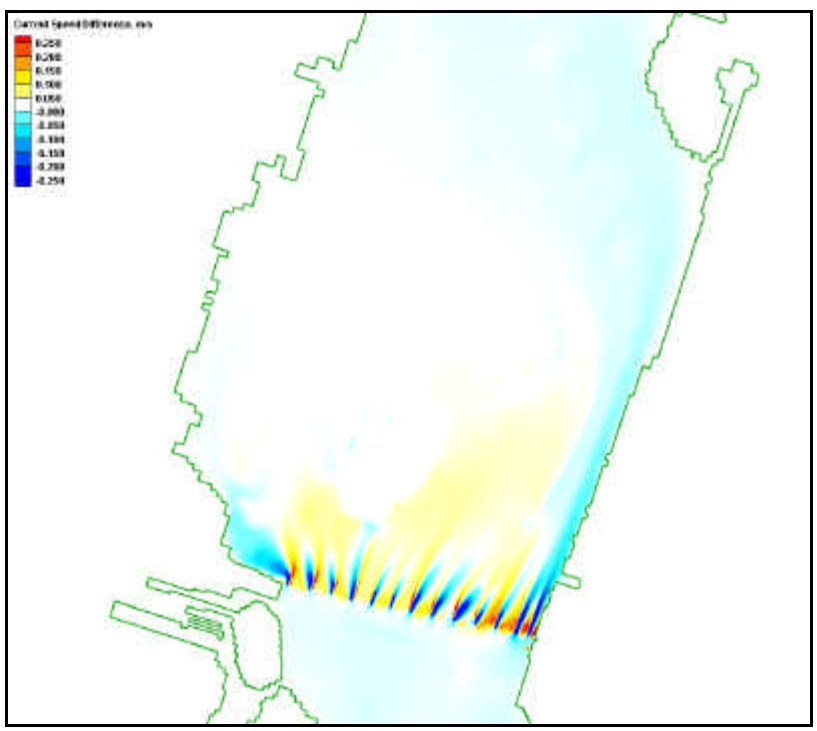

Figure 4-28. Difference in current speed between Alt 4 and the existing U.S. 50 Bridge at peak flood

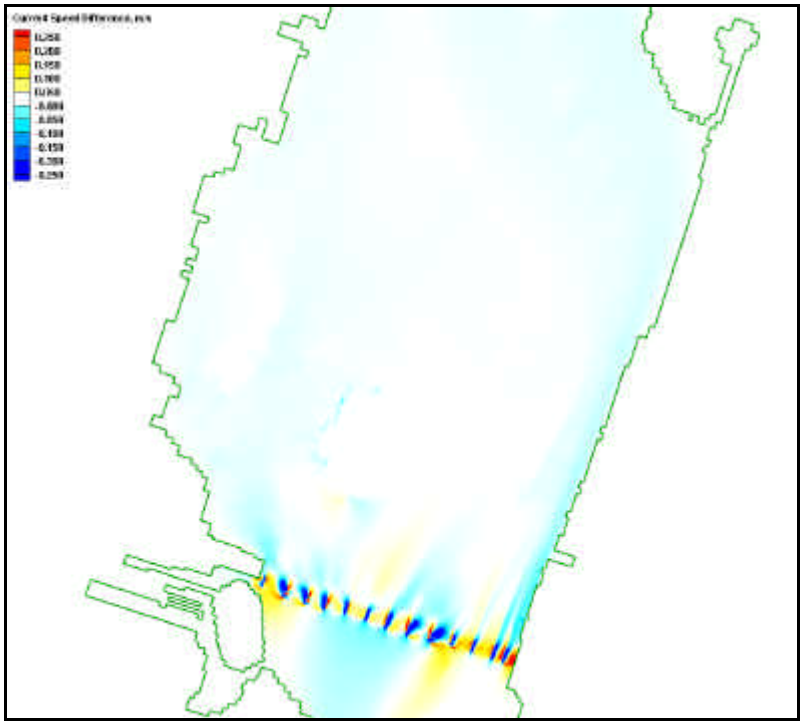

Figure 4-29. Difference in current speed between Alt 5 and the existing U.S. 50 Bridge at peak flood

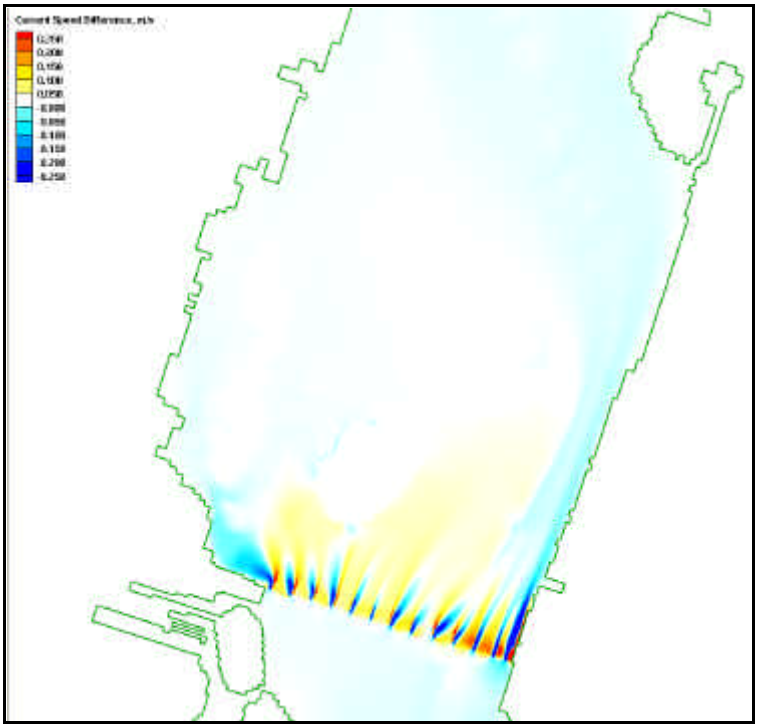

Figure 4-30. Difference in current speed between Alt 5A and the existing U.S. 50 Bridge at peak flood

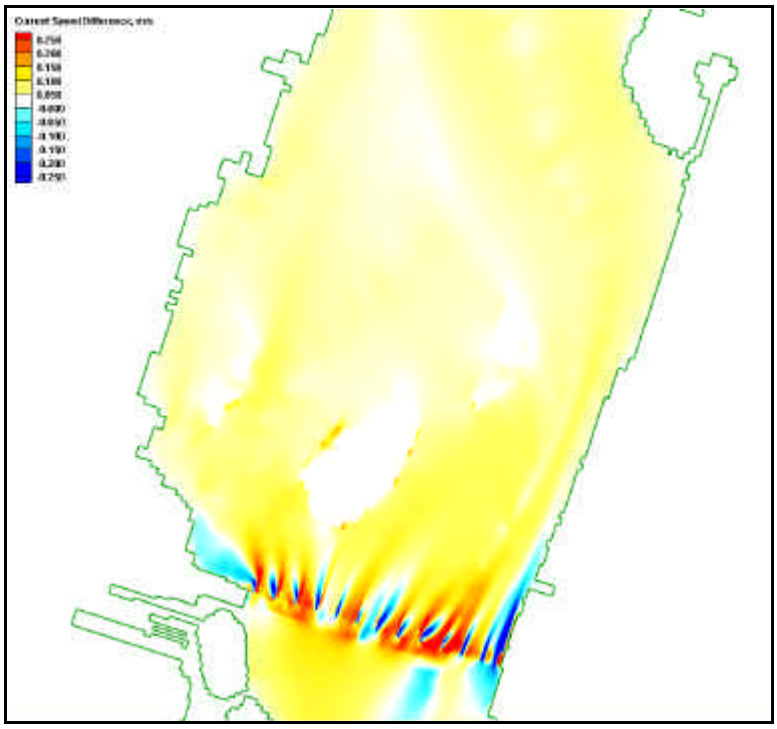

Figure 4-31. Difference in current speed between Alt 5B and the existing U.S. 50 Bridge at peak flood

Figures 4-32 through 4-35 display contour plots of the speed differences for Alts 4, 5, 5A, and 5B, respectively, at peak ebb current. Alternatives 4, 5A, and 5B show a slight increase in current speed, in the range of 1 to 3 cm/sec, in the eastern central area north of the bridge, whereas Alt 5 shows a very slight decrease, about 1 cm/sec, in the same area. The navigation channel on the east shows a decreased current speed of about 5 cm/sec over its length for Alts 4, 5, and 5A, whereas Alt 5B shows an increased current speed in the range of 5 to 9 cm/sec over most of the navigation channel. Outside of the Skimmer Island area and proposed bridge location, Alts 4, 5, and 5A generally have a slightly reduced current speed, 1 to 3 cm/sec, over the domain. Alternative 5B shows stronger currents, typically between 3 and 5 cm/sec, over most of the domain.

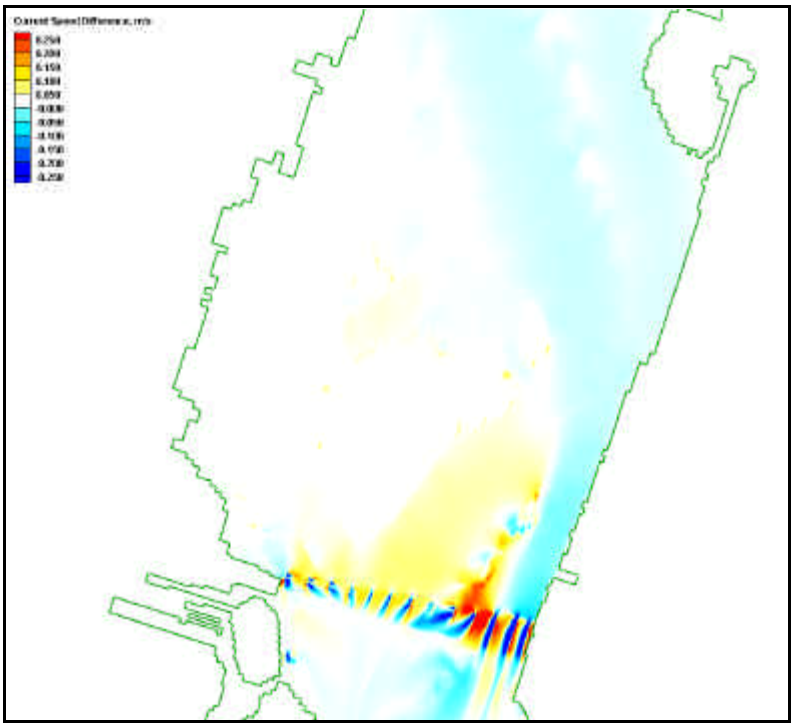

Figure 4-32. Difference in current speed between Alt 4 and the existing Rotue 50 bridge at peak ebb

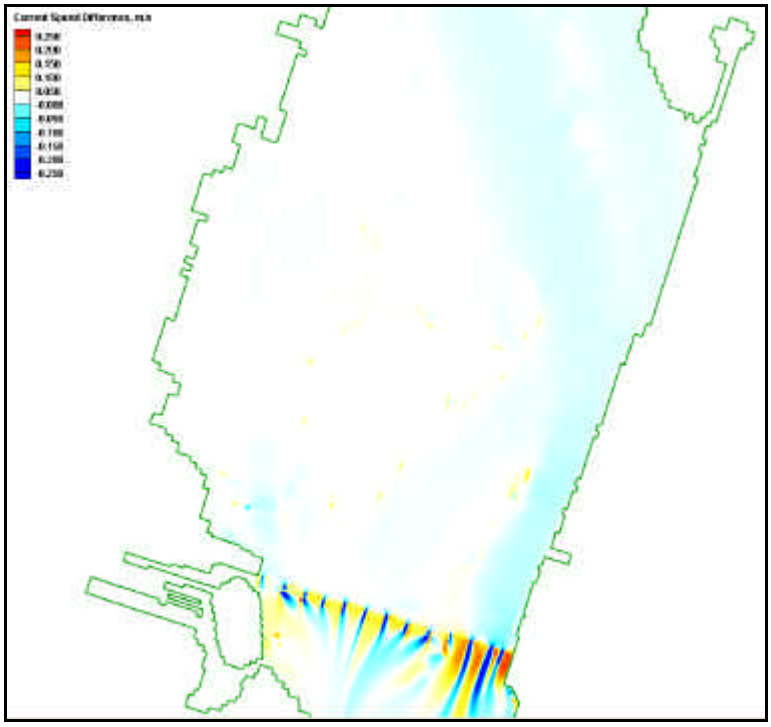

Figure 4-33. Difference in current speed between Alt 5 and the existing U.S. 50 Bridge at peak ebb

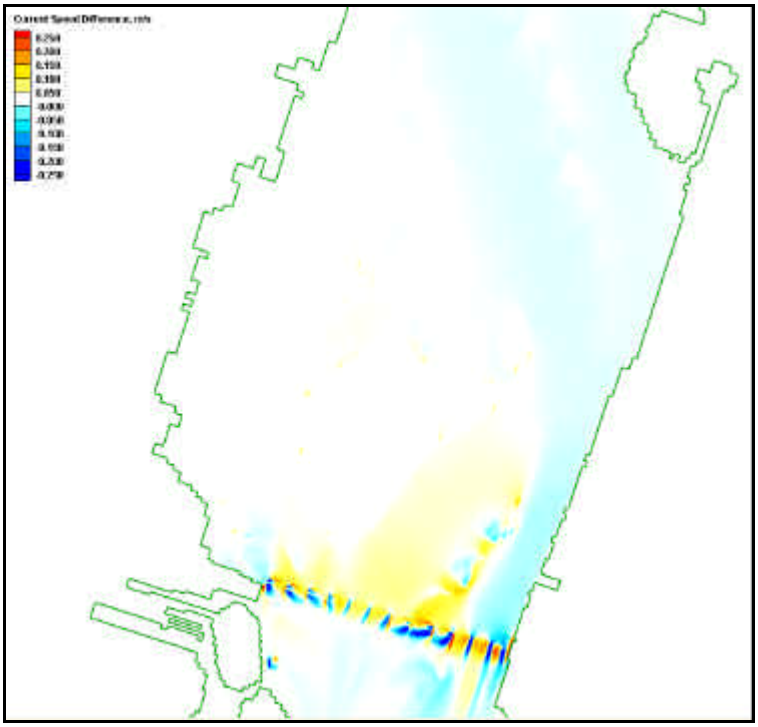

Figure 4-34. Difference in current speed between Alt 5A and the existing U.S. 50 Bridge at peak ebb

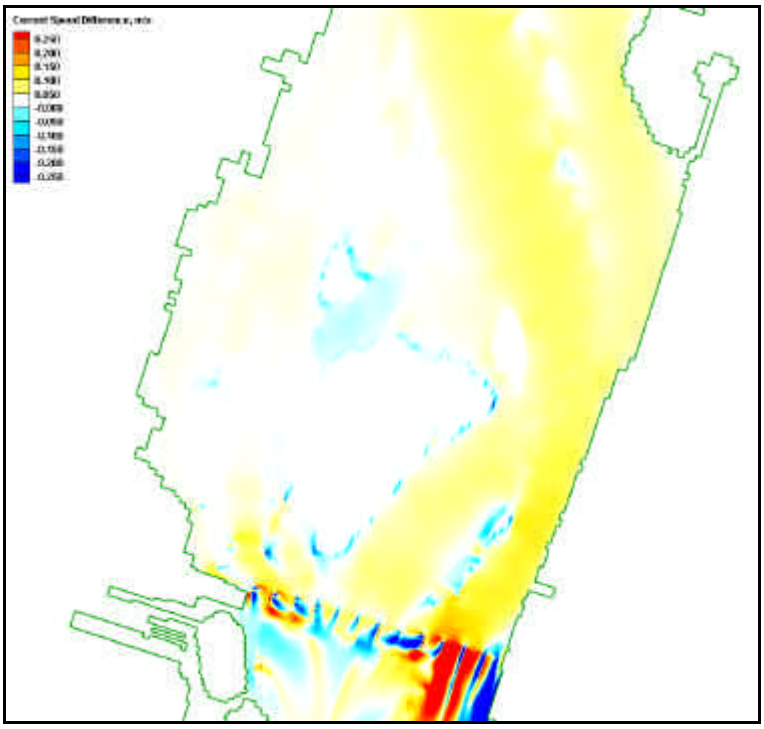

Figure 4-35. Difference in current speed between Alt 5B and the existing U.S. 50 Bridge at peak ebb

The local model was run for a time interval that represented five years of morphology change. This simulation was conducted by running a 90-day hydrodynamic simulation together with bed load and suspended load transport coefficients set to 30. Forcing for the regional model was NOAA predicted tide for January through March 2007 and the solution from the regional model was applied as forcing for the local model. Because of the large transport rate coefficients and corresponding fast morphology change, the calculation of depth change was conducted at 0.1 hr (6-min) intervals.

Local model initial bathymetry in the study area is shown in Figure 4-36. Morphology at the end of the 5-yr simulation period for the existing condition and Alts 4, 5, 5A, and 5B is shown in Figures 4-37 through 4-41, respectively. Bathymetry after the 5-year interval indicates that the proposed alternatives will not significantly change the patterns of morphologic change significantly as compared to the existing condition.

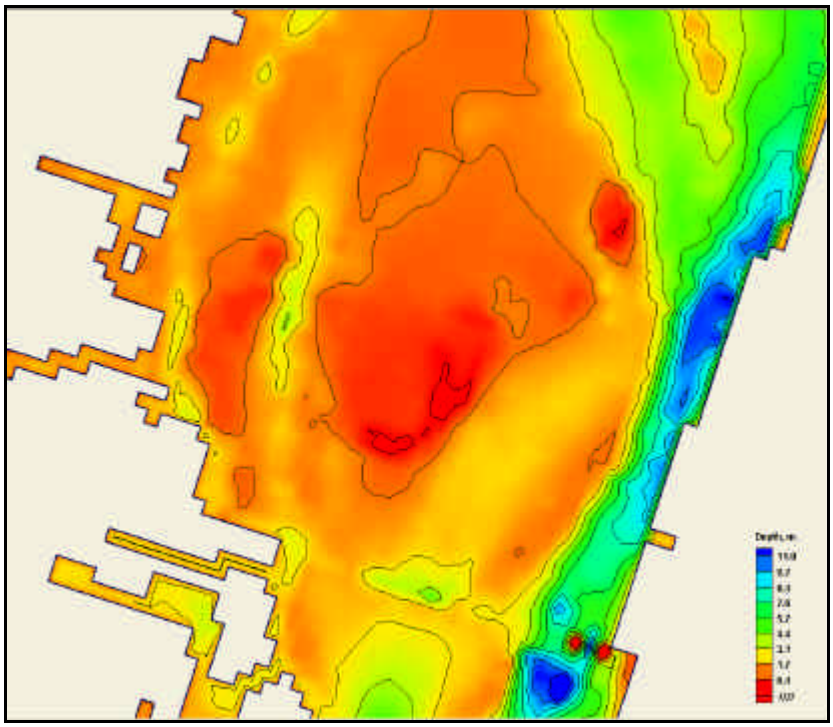

Figure 4-36. Initial (2007) bathymetry for evaluation of morphology change for alternatives

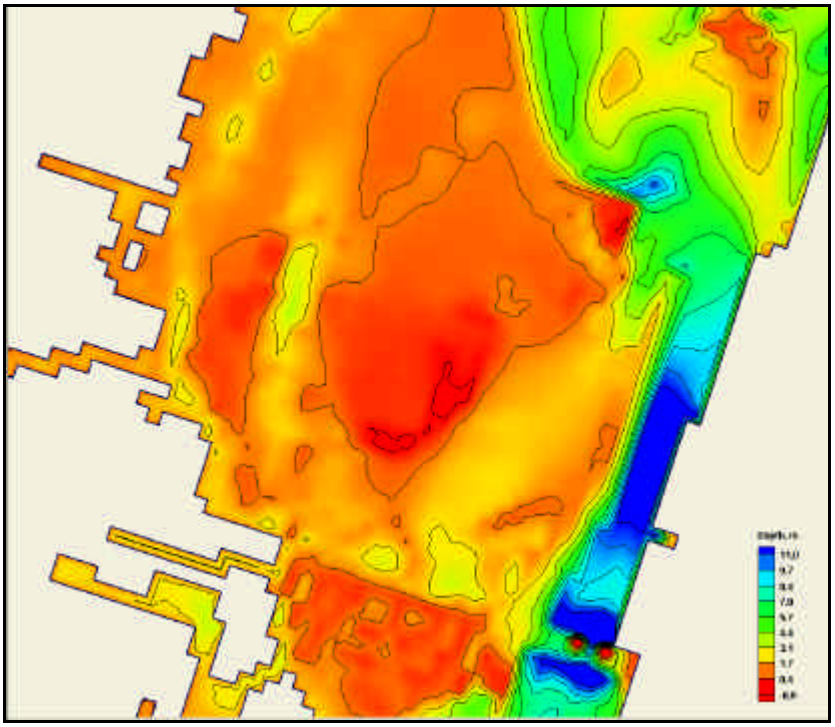

Figure 4-37. Calculated bathymetry after 5 yr, existing condition

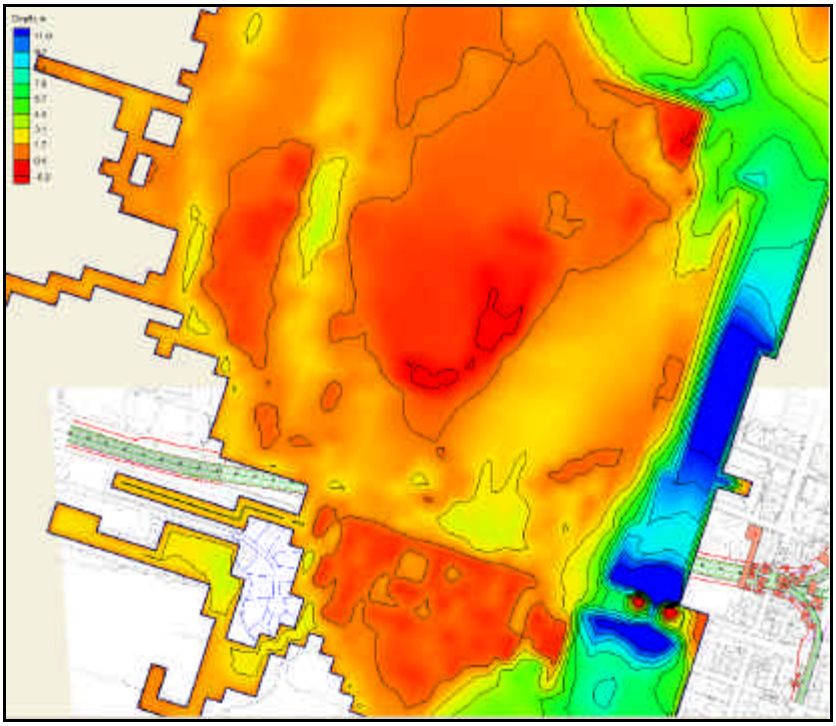

Figure 4-38. Calculated bathymetry after 5 yr, Alt 4

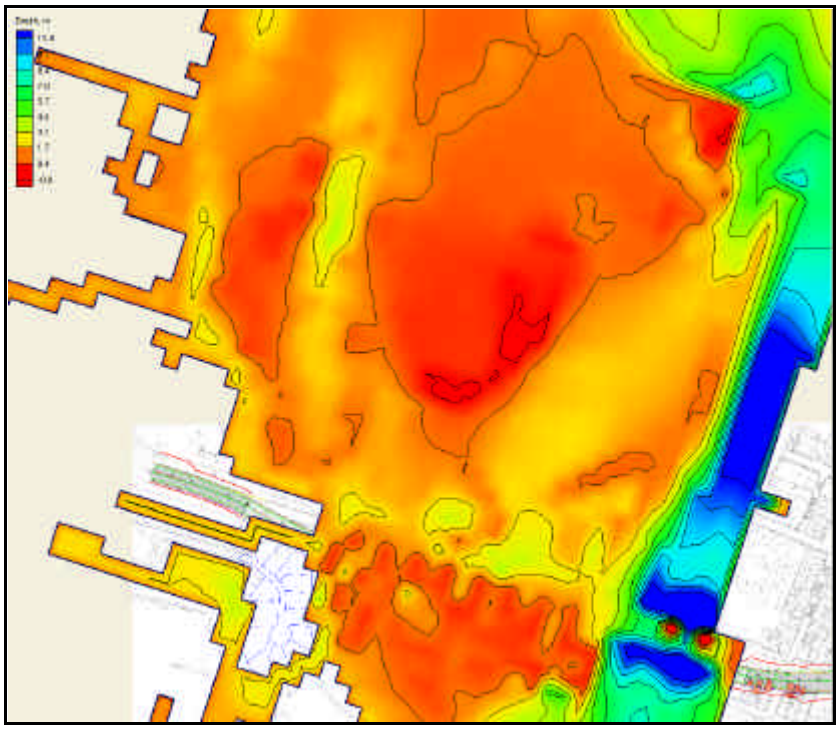

Figure 4-39. Calculated bathymetry after 5 yr, Alt 5

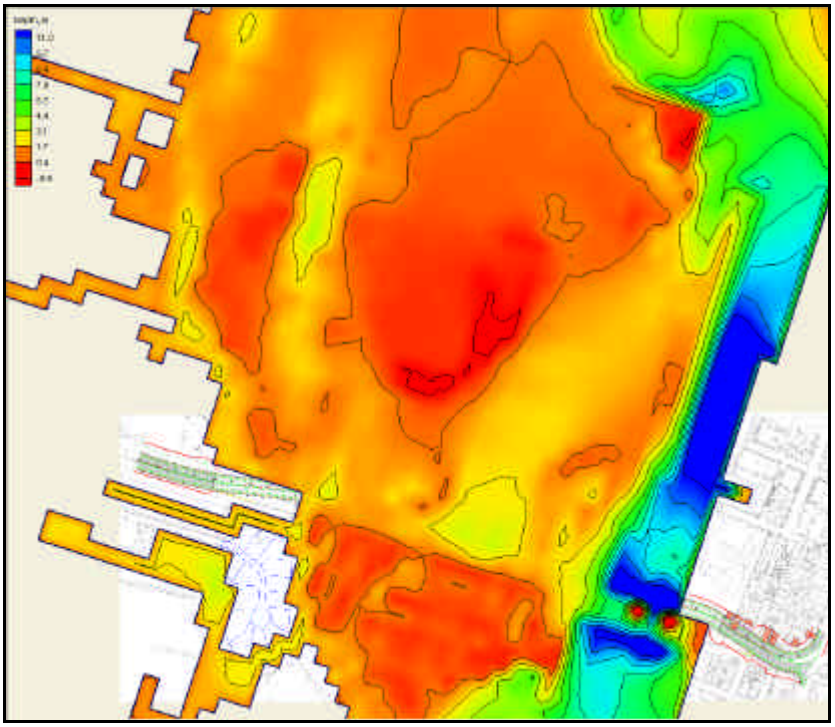

Figure 4-40. Calculated bathymetry after 5 yr, Alt 5A

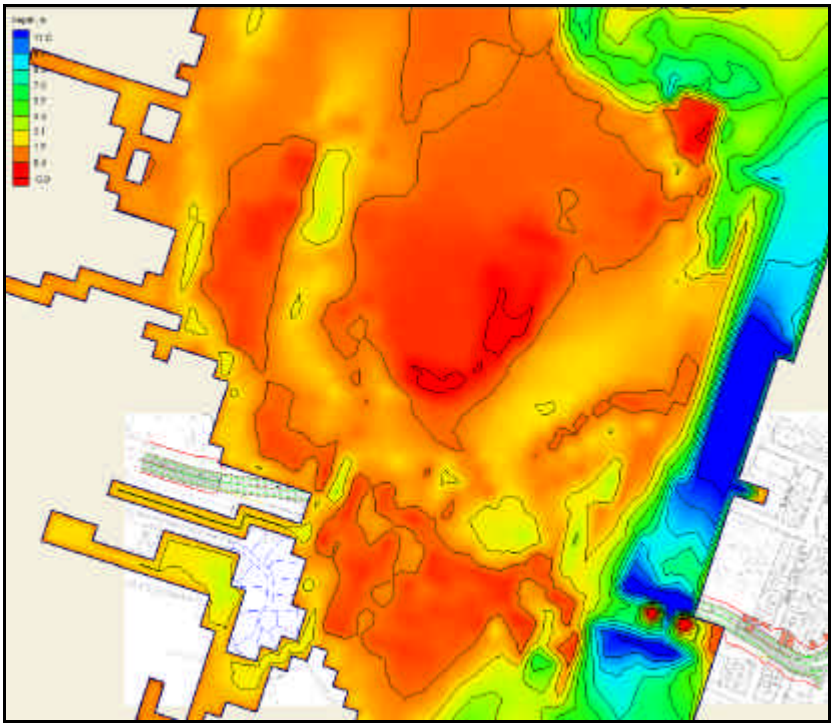

Figure 4-41. Calculated bathymetry after 5 yr, Alt 5B

Plots of calculated depth change over the 5-yr interval for the existing condition and Alts 4, 5, 5A, and 5B are shown in Figures 4-42 through 4-46, respectively. In these plots, blue denotes erosion and yellow/red denotes accretion. All of the simulations show similar patterns of morphologic change with differences being primarily in the amount and localized trends for erosion or deposition. In all cases, the navigation channel widens and deepens, indicating that it will remain self-sustaining for all proposed alternatives. Alternatives 4 and 5A have calculated depth change that is similar to the existing condition in magnitude and pattern. Alternative 5 was calculated to have areas of stronger erosion and of stronger deposition north of the present U.S. 50 Bridge as compared to the existing condition and Alts 4 and 5A. That is, the areas of accretion in Alt 5 are higher and areas of erosion are lower in elevation than those of the existing condition and Alts 4 and 5A, which will promote faster development of channels and shoals in Alt 5. Alternative 5B was calculated to have the greatest amount of shoaling north of the bridge, particularly in the western area of the bay just north of the proposed Alt 5B bridge location. Removal of the existing bridge allows for stronger current at the present bridge site, which will transport more material northward during flood tide.

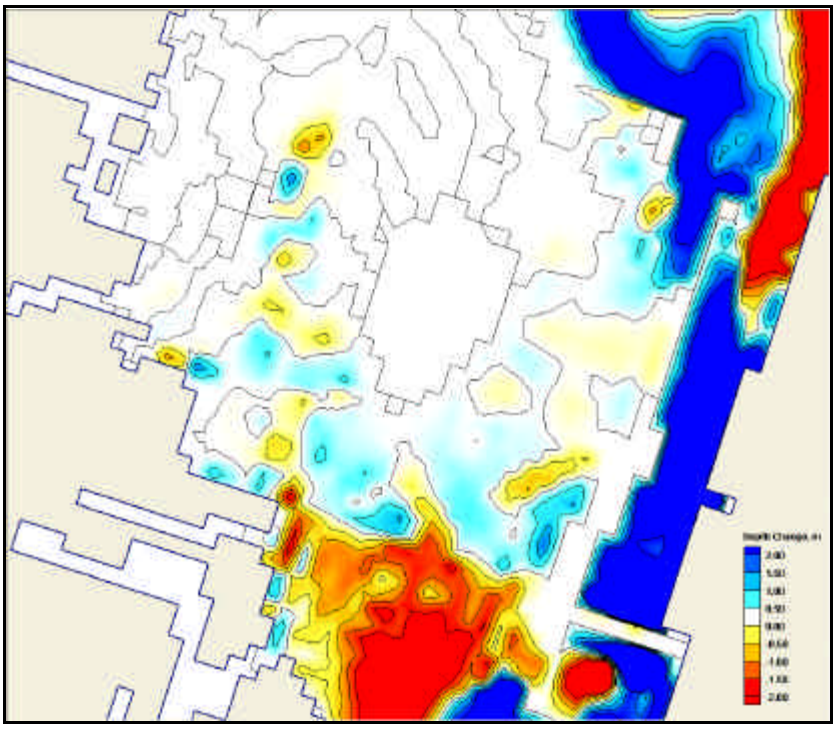

Figure 4-42. Calculated depth change over 5 years, existing condition

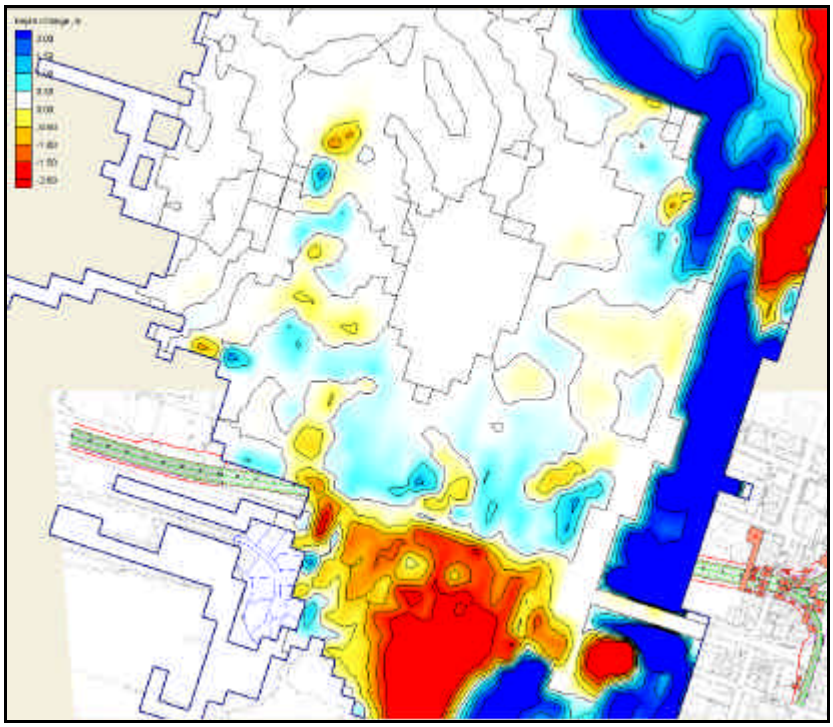

Figure 4-43. Calculated depth change over 5 years, Alt 4

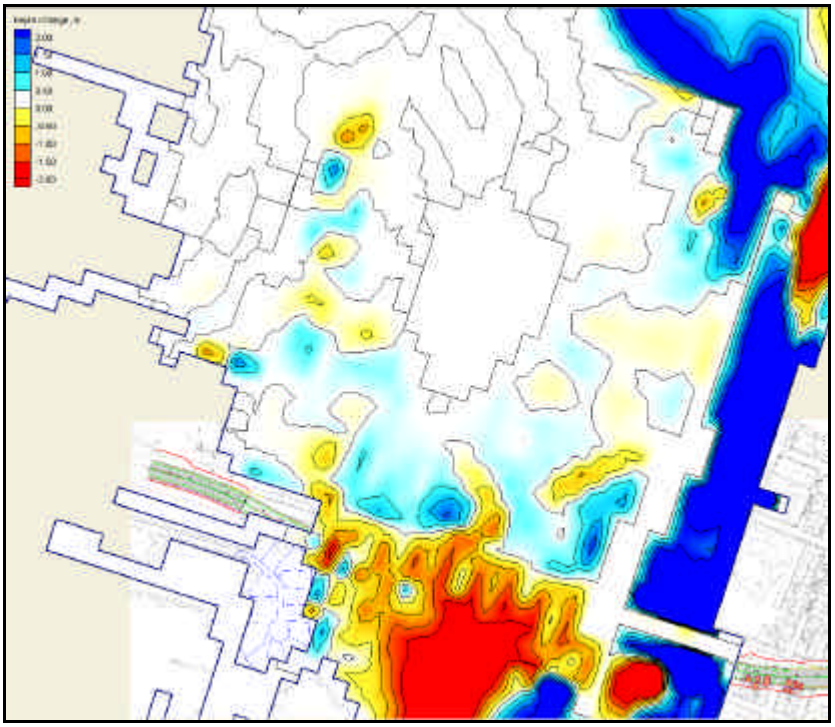

Figure 4-44. Calculated depth change over 5 years, Alt 5

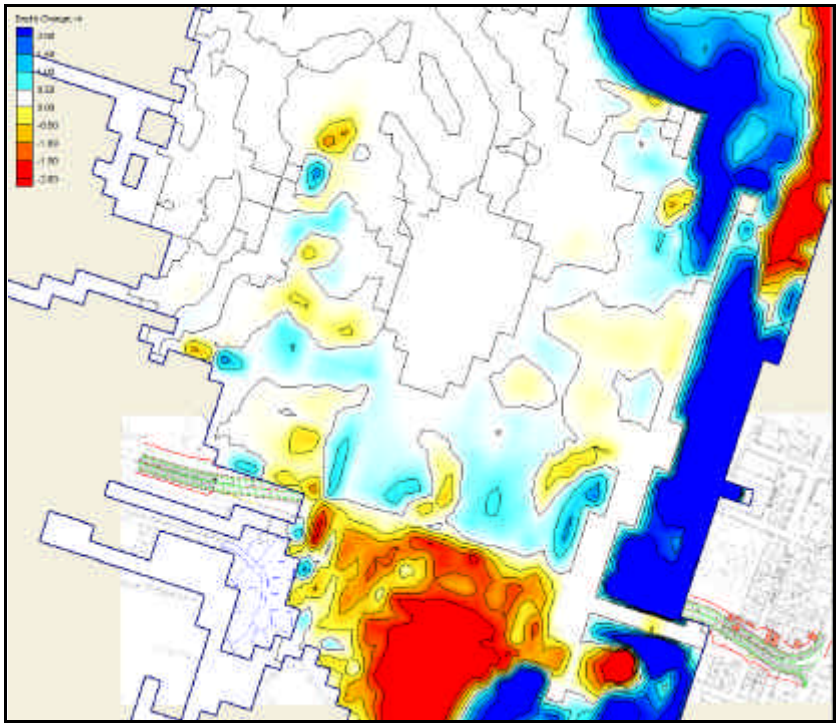

Figure 4-45. Calculated depth change over 5 years, Alt 5A

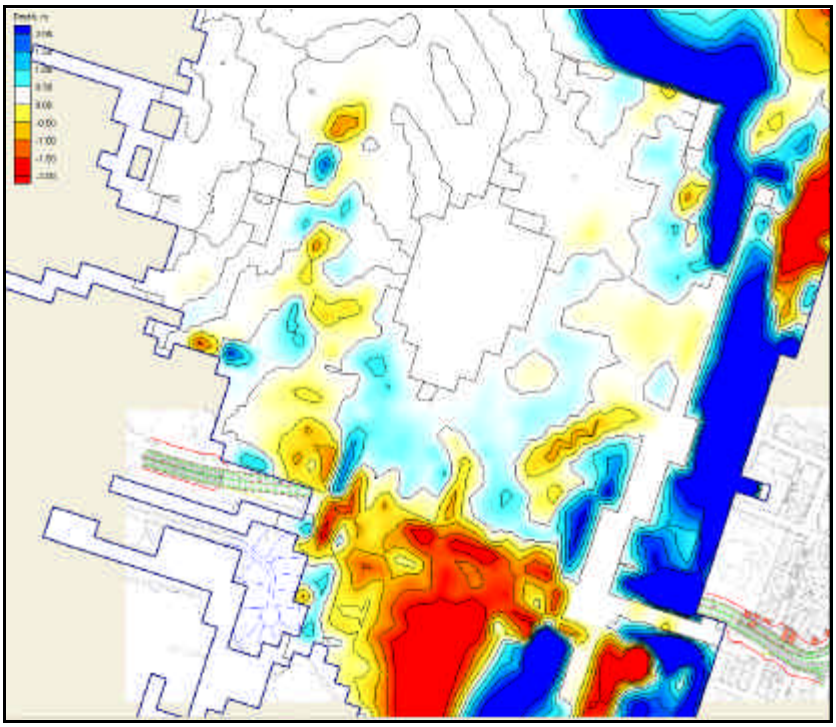

Figure 4-46. Calculated depth change over 5 years, Alt 5B

5 Summary and Conclusions

A detailed field measurement and numerical modeling study of Isle of Wight and Little Assawoman Bays was performed to evaluate the potential impacts of alternatives for a new U.S. U.S. 50 Bridge that will connect the mainland to Ocean City, Maryland. An analysis of historical processes and the numerical modeling indicate that the hydraulics and sedimentation processes are strongly controlled by the present bridge and stone scour protection. Numerical modeling of the alternatives presently under consideration indicates that impacts are expected to be confined to within about 1,500 feet of the new construction if the existing bridge and scour protection are left in place. The effects are estimated to be mainly very local changes in flow and sedimentation patterns in the vicinity (one to two city blocks) of the new, widely-spaced, bridge supports. The natural evolution of Skimmer Island and other flood shoal/channel features appear to be relatively insensitive to the proposed new bridge alternatives. However, one alternative examines the effect of removing the existing bridge but leaving the stone scour protection in place. The bridge removal appears to increase flow velocities throughout the bay system, increasing the likelihood of shoal movement and shoal growth north of the location of the existing bridge.

The numerical model selected to conduct the hydrodynamic and sediment transport analysis for the US 50 Bridge alternatives was CMS-FLOW, Version 3.2 (Buttolph et al. 2006). This model is a depth-integrated representation of flow, sediment transport and morphology change and has been designed to operate at the scales needed for this project.

To validate the model, an historical bathymetry and a contemporary bathymetry were used, respectively based on navigation chart data, circa 1985, and a new survey performed in spring, 2007. Flow velocity and tidal attenuation within the bay model domains were collected in spring, 2007, and were used to verify the model's ability to simulate the measured flow velocities, flow distribution along the existing bridge, and tidal attenuation through the bays. The model was then applied to simulate the morphology change to the north and south of the existing bridge over a 15-year period (1985-2000). The driving boundary condition just offshore of Ocean City Inlet was generated by a regional tidal model of part of the Atlantic Ocean that was driven by constituents. The important observed morphology changes in the vicinity of the bridge, such as the southwesterly migration of Skimmer Island and the widening of the eastern navigation channel, did occur in the simulation.

The validated model was then used to estimate the impacts of various alternatives by using the same tidal boundary driving conditions for a 5-year period

and by using the 2007 bathymetry as an initial condition. The impacts of five alternatives were assessed. The first alternative was to continue to use the existing bridge with no new construction. The second through fourth alternatives consider a new bridge either to the north or to the south of the existing bridge, but plan to leave the existing structure in place. The fifth alternative included a new bridge and removal of the existing bridge but not the rock scour protection.

A conclusion of the historic evolution of the flood tide delta, including Skimmer Island, is that Skimmer Island is expected to migrate in a west-southwest direction at a rate of about 5-10 ft/yr. Pressure on Skimmer Island is expected to continue on its east and northeast sides from a widening and deepening east channel. Stronger flood tide currents, presumably due to the rehabilitation of the south jetty at Ocean City Inlet, have slowed and possibly stopped the southerly migration of the Island. The primary conclusion of the modeling is that the existing rock scour protection provides a primary control over the hydraulics and sedimentation processes in the area. The existing bridge pilings also play a significant role in controlling hydraulics and sedimentation. These processes would change if the rock scour protection or the existing bridge were removed. The new bridge alternatives will affect the hydraulics and sedimentation in the very local vicinity (a few city blocks) of those structures, but the far-field conditions will continue and evolve in a manner similar to the first, no-action, alternative with slight increases in current speed. The impacts seen in the model results agree with the historic processes analysis, i.e. that Skimmer Island is expected to slowly migrate to the west-southwest, as discussed above, with a continued widening and deepening on its east and northeast side.

Model findings also indicate that the new bridge piers have a very local effect on currents, primarily confined to flow acceleration between the piers and a wake region to the north and south on flood tide and ebb tide, respectively. The effects are mainly confined to a few hundred feet to the north and south of new bridge pier locations. Bridge pier alignment should be considered to minimize impacts on currents, especially near and in the navigation channel.

It is recommended that a monitoring plan be developed to continue to assess these results before, during and after a bridge is constructed because conditions change in this environment constantly change due to man-made and natural effects.

Table 5-1 presents a summary of the impacts indicated by the present study. The long term expected effects, as indicated by the tools used in this study, are illustrated in Figure 4-46, respectively.

Table 5-1. Possible Impacts Due to Alternative Bridges

Alternative	Sedimentation	Hydraulics	Shorelines	Navigation
Existing Bridge (no action)	Skimmer Island slowly migrating WSW Deposition west of west channel East channel widens Flood shoal accumulates south of bridge, driven north of bridge by ocean swell; deposition in channels south of bridge	High velocity flows continue in east channel During flood tide, high velocity flows also occur in the central flood shoal, diverging at the existing scour protection rock beneath the bridge	Slow sediment deposition along western shoreline East channel deepens along bulkheads Continued entry and reflection of ocean swell south of bridge	Continued high flows in east channel and difficulties under draw span Deposition in west channels south of bridge
4	Same as existing bridge; however, this alternative slightly reduces sediment driven north of bridge by ocean swell.	Slightly lowered currents south of the bridge and in the east and west channels Increased current south and east of Skimmer Island, in the main channel beneath the draw span, and between the new bridge supports.	Same as existing bridge.	Same as existing bridge
5	Same as Alt 4; however, this alternative further reduces sediment driven north of bridge by ocean swell; may reduce migration rate of Skimmer Island to the WSW.	Same as Alt 4, except that current south and east of Skimmer Island does not appear to increase.	Same as existing bridge	Same as existing bridge

5A	Same as Alt 4.	Same as Alt. 4.	Same as existing bridge	Same as existing bridge
5B	Skimmer Is slowly migrating WSW Deposition along western shoreline greatly increased. East channel widens Flood shoal accumulates south of bridge, driven north of bridge by ocean swell at a rate exceeding all other alternatives which may eventually merge Skimmer Island with the flood shoal, enlarging the entire shallow shoal complex. Deposition in channels south of bridge.	Increased currents south of the bridge and in the east and west channels Increased current south and east of Skimmer Island. Greatly increased current in the main channel beneath the draw span, over the remaining rock scour protection, in the east channel south of the bridge, and between the new bridge supports.	Same as existing bridge	Same as existing bridge. May be more difficult in areas west of Skimmer Island as shoaling occurs.

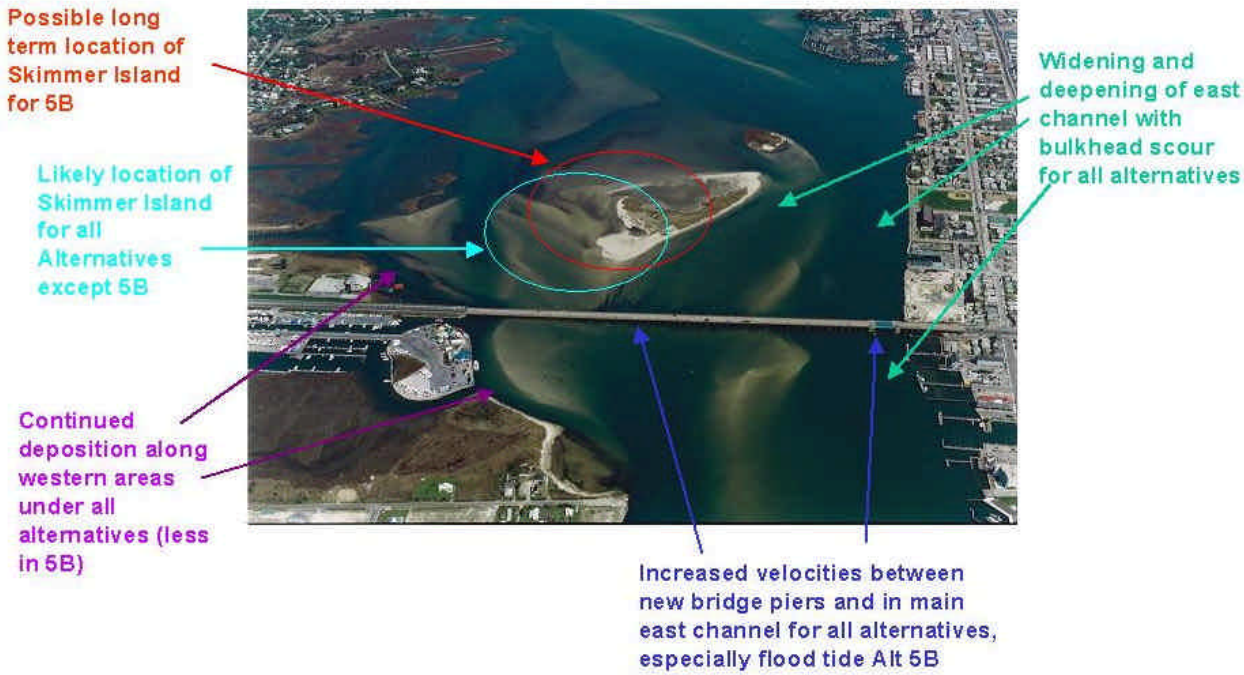

Figure 5-1. Estimated long term impacts of new bridge alternatives.

6 References

Buttolph, A. M., Reed, C. W., Kraus, N. C., Ono, N., Larson, M., Camenen, B., Hanson, H., Wamsley, T., and Zundel, A. K. 2006. *Two-Dimensional Depth-Averaged Circulation Model CMS-M2D: Version 3.0, Report 2: Sediment Transport and Morphology Change*, ERDC/CHL TR-06-9, U.S. Army Engineer Research and Development Center, Vicksburg, MS.

Camenen, B., and Larson, M. 2005. A Bedload Sediment Transport Formula for the Nearshore, *Estuarine, Coastal and Shelf Science* 63, 249-260.

Camenen, B., and Larson, M. 2006. A Suspended Load Sediment Transport Formula for the Nearshore, *Journal of Coastal Research* (in review).

Dean, R.G., Perlin, M. and Dally, W.R. 1978. *A Coastal Engineering Study of Shoaling in Ocean City Inlet,* Report to U.S. Army Corps of Engineers, Baltimore, MD.

Hanson, H., and Militello, A. 2005. *Representation of Non-Erodible (Hard) Bottom in Two-Dimensional Morphology Change Models*, Coastal and Hydraulics Engineering Technical Note ERDC/CHL CHETN-IV-63, U.S. Army Engineer Research and Development Center, Vicksburg, MS.

Maryland Department of Natural Resources 2007. *Figure showing annual walking surveys of Skimmer Island*, provided by Mr. David Brinker, Baltimore, MD.

Offshore & Coastal Technologies, Incorporated 1987. *Post Construction Bathymetric Survey and Flow Conditions Beneath the Route 50 Bridge, Ocean City, Maryland*, Submitted to the Maryland State Highway Administration, Bureau of Bridge Inspection and Remedial Engineering, Maryland Department of Transportation, Baltimore, MD.

U.S. Army Corps of Engineers, Baltimore 1998. *Ocean City, Maryland, and Vicinity Water Resources Study, Final Integrated Feasibility Report and Environmental Impact Statement, Appendix A6: Ebb and Flood Shoal Evolution*, Baltimore, MD.

Watanabe, A. 1987. 3-Dimensional Numerical Model of Beach Evolution, *Proceedings Coastal Sediments '87*, ASCE, 802-817.

Zundel, A. K. 2000. *Surface-water Modeling System Reference Manual*, Brigham Young University, Environmental Modeling Research Laboratory, Provo, UT.